

Alma Mater Studiorum – Università di Bologna

DOTTORATO DI RICERCA IN  
BIOLOGIA CELLULARE, MOLECOLARE ED INDUSTRIALE

Ciclo XXV

**Settore Concorsuale di afferenza:** 05/E2

**Settore Scientifico disciplinare:** BIO/11

Identification and functional characterization of human  
cytomegalovirus Fc binding proteins

**Presentata da:** Mirko Cortese

**Coordinatore Dottorato**

**Prof. Vincenzo Scarlato**

**Relatore**

**Prof. Vincenzo Scarlato**

**Prof. Marcello Merola**

**Esame finale anno 2013**



# **CONTENTS**

## **CHAPTER 1**

<b>INTRODUCTION</b>	<b>3</b>
1. Human Cytomegalovirus virion structure and genome organization	3
2. Envelope glycoproteins and viral replication	5
3. Pathogenesis	9
4. Immune response manipulation and evasion mechanisms	10
4.1. Complement cascade	12
4.2. Natural killer cells	12
5. Fc receptors	14
5.1. IgG and Fc gamma receptors	17
5.2. Fc receptor homologues	19
<b>PROJECT SUMMARY</b>	<b>23</b>
<b>REFERENCES</b>	<b>24</b>

## **CHAPTER 2**

<b>Dynamics of IgG binding and virus localization of HCMV Fc<math>\gamma</math> binding proteins RL11 and UL119</b>	<b>31</b>
• <b>ABSTRACT</b>	<b>32</b>
• <b>INTRODUCTION</b>	<b>33</b>
• <b>RESULTS AND DISCUSSION</b>	<b>36</b>
• <b>MATERIALS AND METHODS</b>	<b>52</b>
• <b>REFERENCES</b>	<b>59</b>

## **CHAPTER 3**

<b>Recombinant Human Cytomegalovirus (HCMV) RL13 binds human immunoglobulin G Fc</b>	<b>65</b>
• <b>ABSTRACT</b>	<b>66</b>
• <b>INTRODUCTION</b>	<b>67</b>
• <b>RESULTS</b>	<b>69</b>
• <b>DISCUSSION</b>	<b>88</b>
• <b>ACKNOWLEDGMENTS</b>	<b>96</b>
• <b>REFERENCES</b>	<b>97</b>

# INTRODUCTION

## 1. Human Cytomegalovirus virion structure and genome organization

Human Cytomegalovirus (HCMV) is a member of the  $\beta$ -herpesviridae family that includes the herpesviruses of mammals, birds and reptiles [1]. Although more recently validated by genome sequences, historically the members of the family were classified on the basis of the virion structure, composed of an envelope, tegument, capsid and an inner core containing the viral genome. The virus envelope is composed of a double host cell-derived lipid layer and contains the viral glycoproteins necessary for the cellular tropism. Compared to the other members of the family, the envelope is very irregular and generates a viral shape whose diameter reaches up to 300 nm with an average size of 230 nm diameter. Under the envelope is present an amorphous matrix referred as tegument. This compartment carries the majority of the HCMV expressed proteins plus a huge number of host species including proteins and nucleic acids. Several crucial viral functions are incorporated in the tegument including kinases, trans-activating factors and the most abundant and immunogenic protein pp65. The HCMV capsid is embedded in the tegument. The core of the capsid contains a tightly packed linear double stranded DNA genome. In line with the huge virus dimension, HCMV has the largest genome among its family with approximately 230 kb, 50% larger than HSV, despite the capsids of both viruses being roughly of the same size (110-125 nm) [1].

As for the other herpesviruses, genome organization reflects the common structure composed of unique long (UL) and unique short (US) genetic regions flanked by two sets of inverted repeats (RL, repeated long and RS, repeated short). Recombination phenomenon can occur among identical terminal and internal repeats, leading to genome isomerization. Thus, genetic material isolated from a viral population consists of equal amounts of four different genomic isomers pooled together [2].

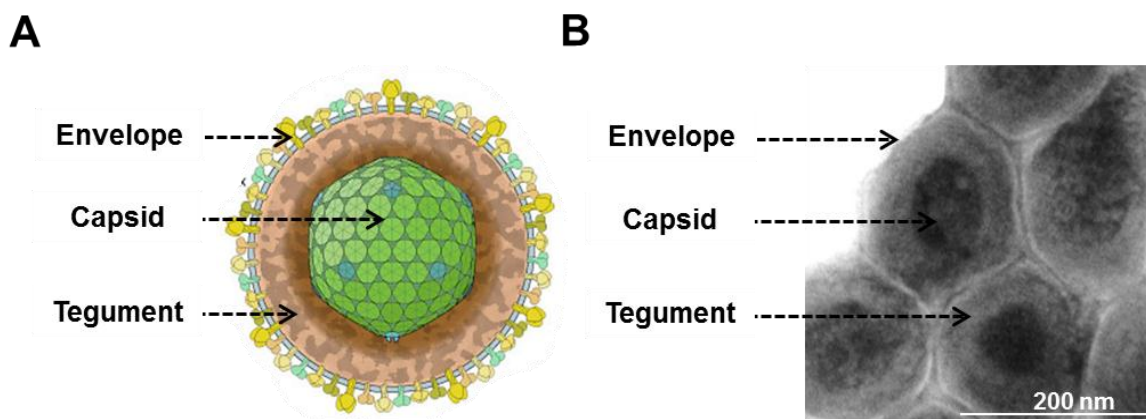


**Fig. 1:** **A.** Schematic representation of HCMV virion (modified from [http://viralzone.expasy.org/all\\_by\\_species/180.html](http://viralzone.expasy.org/all_by_species/180.html)). **B.** Negative stained purified virion preparation analyzed through electron microscopy.

While the general genomic arrangement consistent of repeated and unique sequences is conserved among HCMV strains, a major difference in the open reading frame (ORF) composition and organization can be observed among “laboratory strains” and “clinical isolates”. The latter are generally defined as viruses that underwent through none or limited passages in fibroblast cells before being clones as bacterial artificial chromosomes (BACs) and/or sequenced. On the contrary, laboratory strains indicate all the strains extensively passaged and adapted to growth in human fibroblasts. These latter have been selected for rapid replication, fast growing and high yields of produced virus. Consequently to the fibroblast adaptation severe genomic rearrangements occurred in these viruses. Both AD169 and Towne laboratory strains acquired a large deletion in a multilocus of the UL segment, concomitantly being replaced by duplicated RL region. An impaired tropism, tightly restricted to fibroblast cells only, resulted from the abrogation of several envelope glycoproteins encoded in the deleted segment. Due to these rearrangements, a difference in the coding potential can be observed between laboratory strains and clinical isolates. In particular, while the AD169, a laboratory strain prototype, is predicted to encode for 208 ORFs (including the repeated segments), the coding potential of a clinical isolate is estimated around 252 ORFs [3]. Recently, through an integrated approach that combines ribosome footprinting assays, high-resolution mass spectrometry and analysis of mutated

viruses, Stern-Ginossar and co-workers were able to identify a total of 751 translated ORFs including short peptides [4]. In spite of this huge coding potential, only a small subset of these proteins constitutes the mature virion: it has been estimated that around 50 [1,5] proteins are inserted in the virion, divided through the different compartments.

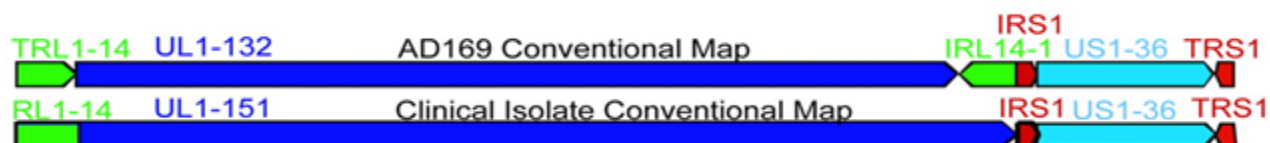


**Fig. 2: HCMV genome organization.** ORFs map of conventional laboratory strain AD169 and clinical isolate. The AD169 genome (upper) carries TRL1-14 (green arrow), UL1-132 (dark blue arrow), IRL14-1 (green arrow), IRS1 (red arrow), US1-36 (light blue arrow), and TRS1 (red arrow). In the clinical isolate RL1-14, (green arrow), UL1-151 (dark blue arrow), IRS1 (red arrow), US1-36 (light blue arrow), and TRS1 (red arrow) are present. Modified from [3].

## 2. Envelope glycoproteins and viral replication

Being the modulator of viral entry, envelope glycoproteins play a key role in HCMV pathogenesis. Of the total number of proteins composing the virion, around 20 [1,5–7] were identified as envelope associated proteins. Notably, only 8 were demonstrated as essential for virus replication *in vitro* in different cell types: glycoproteins B (gB), M (gM), N (gN), L (gL), H (gH), UL128, UL130, UL131 [8]. All these proteins act as complexes on the viral surface. gB is an homotrimeric complex mediating virus attachment and fusion, involved in the first step of heparin sulfate proteoglycans (HSPG) tethering. The most abundant envelope glycoprotein, gM, forms an heterodimeric complex associating with gN that is present on the virion only as 1:10 ratio to gM. Like gB, gM:gN complex is involved in HSPG tethering and stabilization of virus-cell contact. The complex that has been involved in the fusion event is composed by the glycoprotein gH and gL. This complex is sufficient to mediate fibroblast infection while formation of a pentameric complex through additional binding of UL128, UL130 and UL131 gene products is necessary for the infection of epithelial, endothelial,

polymorphonuclear leukocyte and dendritic cells (DC). Indeed, the attenuated tropism observed in laboratory strains can be fully explained by the mutations of the UL128-UL131 locus [3,9,10].

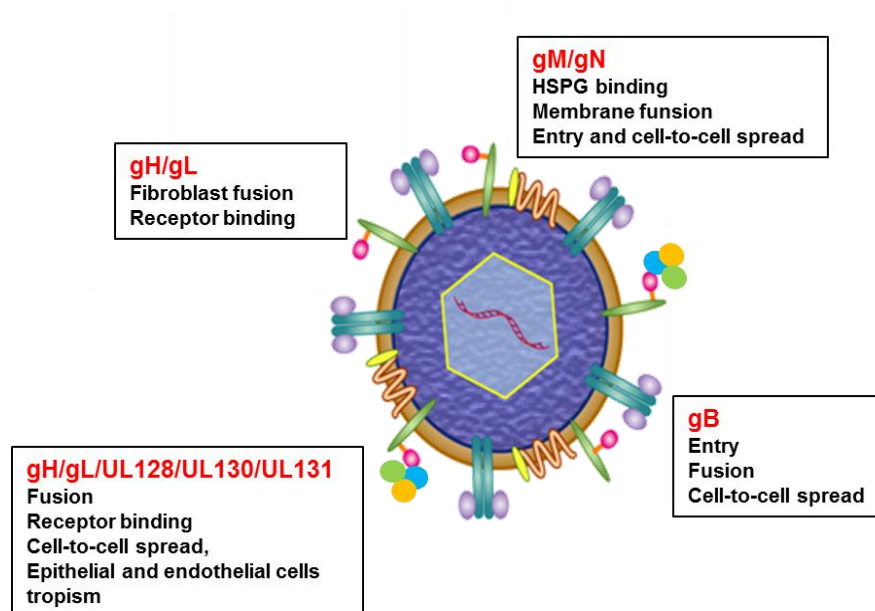


**Fig. 3:** HCMV envelope glycoprotein complexes. The proposed role of each complex is indicated in the respective box. Modified from [11].

Various works describing the HCMV entry step suggest that the virus uses distinct cellular receptors, and consequently different entry pathways, depending on the target cell. HCMV entry consists of a first low specificity - high avidity tethering step of the cell surface HSPGs mediated

by both gB and gM/gN [11,12]. The interaction with high avidity receptors has been shown to follow the first attachment step. A series of “post-attachment” receptors were proposed over the time, even if none of them completely fulfilled this role. The most accredited cellular interactors are  $\beta 1$  and, to a lesser extent,  $\beta 3$  integrins. Engagement of gB by these molecules induce receptors clustering and intracellular signaling. The entry step culminates with gH/gL mediating the fusion of viral and cellular membranes. While direct fusion at neutral pH has been observed *in vitro* in fibroblast cells [13], low pH dependent receptor-mediated endocytosis is required for viral entry in epithelial and endothelial cells [14–16]. Moreover, a recent report suggests that HCMV entry into DCs relies on macropinocytosis-like pathway in a cholesterol-dependent and pH-independent manner [17]. Interaction between gB and dendritic cell specific C-type lectin DC-SIGN (DC specific ICAM-grabbing non-integrin) has been indicated to have a prominent role in DCs infection [18].

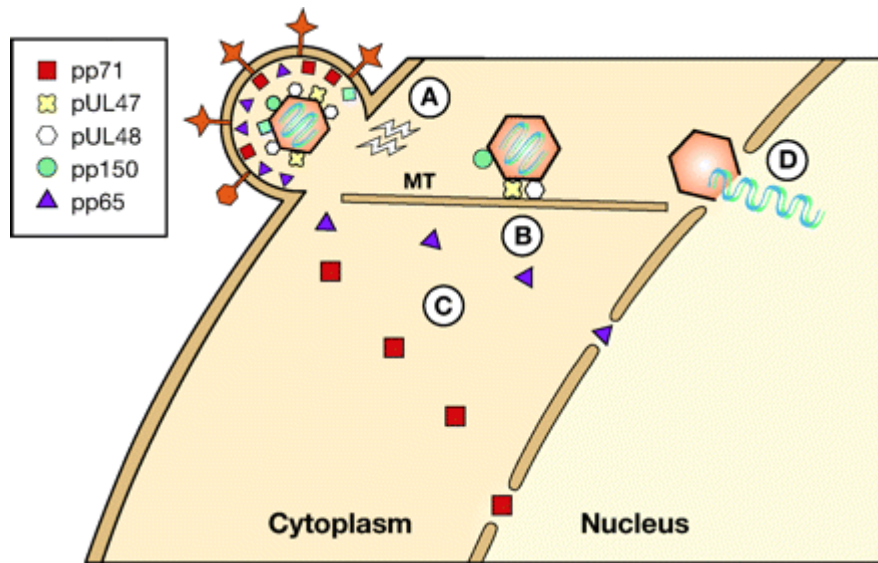


**Fig. 4: Delivery of HCMV capsid to the nucleus.** (A) HCMV capsid and associated tegument proteins are transported along the microtubules (B) toward the nucleus. A set of tegument proteins dissociate from the capsid and migrates independently to the nucleus (C). Viral DNA is released into the nucleus through the nuclear pores (D). Modified from [19].

HCMV entry is followed by the delivery of both the tegument and DNA containing capsid into the cytoplasm. Tegument proteins with regulatory function dissociate from the capsid and remain in the cytoplasm or migrate independently in the nucleus, where they modulate cellular and viral genes expression. A thick layer of tegument proteins remains tightly associated with the capsid and contributes to the delivery of the DNA to the nucleus [19]. For the efficient delivery of HCMV DNA, an intact microtubular network (MT) is essential. The MT spans from cellular periphery up to the perinuclear MT organizing center (MTOC). HCMV moves along MT branches to reach the nuclear pore complex and to inject the DNA into the nucleus [19]. Viral replicative cycle starts shortly after with the expression of immediate early (IE) genes, that can be detected as short as 4 hour post infection [20–22]. During the replicative cycle, genes expression can be divided in distinct temporal phases, defined as immediate early, early and late, that are linked together by a tightly regulated temporal cascade. A set of genes expressed with immediate early kinetic, whose transcription do not require *de novo* protein synthesis, act as global regulators of viral genes expression. Early genes protein products are responsible for DNA replication, while late genes encode for structural proteins and are transcribed following viral DNA replication [19].

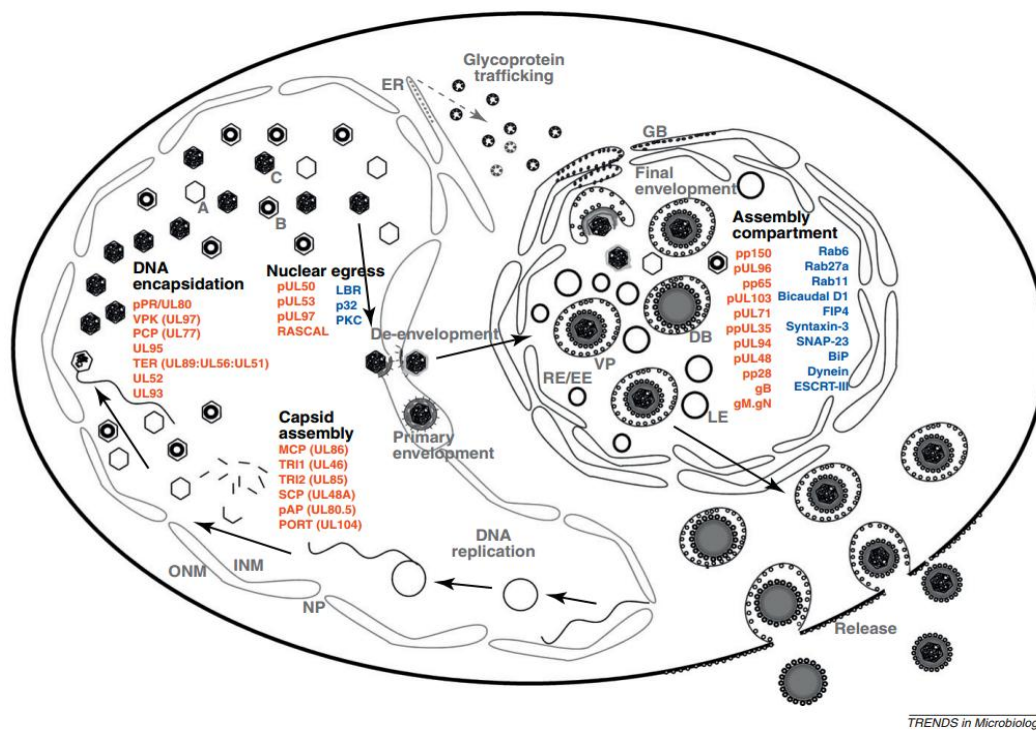


**Fig. 5: HCMV maturation.** The model illustrates the HCMV virion particles formation, maturation and budding processes. Major cellular and viral proteins involved in these processes are reported (red and blue, respectively). List of abbreviations: DB, dense body; VP, virus particle; EE/RE, early endosome/recycling endosome; LE, late endosome; GB, Golgi body; ER, endoplasmic reticulum; NP, nuclear pore; INM, inner nuclear membrane; ONM, outer nuclear membrane; A, B and C, types of nuclear capsids. From [23].

HCMV binding and entry induces a global reprogramming of the cellular activity and causes profound changes in infected cell morphology. The most evident is the formation of a large cytoplasmic juxtannuclear region defined virion assembly complex/compartament (AC), corresponding to the virus final budding site. Before being released, viral particles pass through a series of maturation steps. DNA containing capsids exit the nucleus through a successive envelopment/de-envelopment process at the nuclear membrane [23,24] and reach the cytoplasm to complete their morphogenesis. At this stage, partial tegumented nucleocapsids reach the AC to acquire the full spectrum of tegument proteins and envelope glycoproteins [25]. Viral assembly complex is organized as nested cylinders of secretory apparatus structures, surrounded by the endoplasmic reticulum (ER) network [26,27]. Golgi and trans-Golgi network membranes constitute the edge of the AC, while the inner part contains vesicles positive for both the early and recycling endosomes markers. Secondary viral envelopment

occurs when a viral particle capture a vesicle promoting its bending and fusion around the tegumented nucleocapsid [28]. Vesicles containing mature enveloped HCMV virions fuse with the cellular plasma membrane releasing the viral particles.

### **3. Pathogenesis**

Human cytomegalovirus infection is ubiquitous among adult population, ranging around 55-60% of the world population, although reaching peaks of more than 90% seroprevalence in given populations grouped according to age-gender-socioeconomic related factors [1]. Horizontal transmission can occur through exchange of bodily fluid at mucosal surfaces. Primary infection is generally asymptomatic in healthy individuals, where a strong immune response to HCMV is able to limit and contain the spread of the disease. Bland clinical symptoms and spontaneous acute infection resolution are associated to infection of immunocompetent individuals; therefore antiviral therapies are usually not indicated in these settings [1]. Nevertheless complete clearance of the virus by the organism is never achieved and lifelong lasting latency with recurrent and spontaneous viral reactivation is always observed. Viral replication and spread is brought under control by the combined action of both innate and adaptive immune responses: severe diseases, associated with HCMV infection and reactivation, occur in settings where immune response is severely suppressed (transplantations related immunosuppression) or compromised (AIDS patients). Moreover, due to the HCMV ability to cross the transplacental barrier, congenitally acquired infection can pose a severe treat to the fetus that lacks a fully functional immune system able to counteract the viral infection. Thus in the presence of an impaired or absent immune system, antiviral therapies are necessary to counteract the severe disease associated to the HCMV primary infection or reactivation. However almost all the antiviral agents actually on the market

showed a significant number of potential side effects including marrow and organ toxicity and increasing drug resistant viral strains [1].

Passive immunization using hyperimmune globulin preparations with high levels of antibodies against HCMV (CMVIG) are usually implemented as prophylactic tools to reduce the morbidity and mortality associated to HCMV infection in immunocompromised patients. For example combination of antiviral drug *gancicovir* and CMVIG proved to be effective in preventing HCMV infection in patients undergoing solid organ transplant [29]. Moreover a study suggests their effectiveness in the treatment and prevention of severe diseases associated to congenital HCMV infection [30].

Nevertheless, rather than a general prophylactic tool, the efficacy and effectiveness of CMVIG in reducing HCMV infection seems to be restricted to specific clinical cases while only modest beneficial effects were shown upon CMVIG treatment in other settings such as hematopoietic cell transplantation (HCT) and blood transfusion in premature newborns [31]. Additionally CMVIGs exhibit low potency *in vitro* [32] and must be administrated at high doses to reach the amount of neutralizing antibodies required to exert a beneficial effect. To increase the efficacy of a passive immunization therapy, a series of neutralizing monoclonal antibodies against immunodominant HCMV envelope glycoproteins were developed. For example, a highly *in vitro* neutralizing antibody against gH was isolated from the spleen of a CMV seropositive patient. The monoclonal antibody, named MSL-109 or sevirumab, was tested in phase II clinical trials as treatment for CMV-induced retinitis in AIDS patients [33]. Unfortunately the tests were stopped due to lack of efficacy [34].

#### **4. Immune response manipulation and evasion mechanisms**

Primary infection in immunocompetent individuals is accompanied by a period of viral dissemination (viremia). In this phase, virus excretion in bodily fluids, such as breast milk, blood, urine,

saliva and seminal secretions lasts from months to years depending on the host age, and is the primary cause of viral transmission. Drop and clearance of the acute infection phase correlates with the mounting of strong humoral and, more importantly, cellular adaptive immune responses. Despite the setting up of a strong response, a complete clearance of infected cells is never observed. HCMV is able to establishing lifelong latency remaining silent in myeloid lineage cells [35].

To escape from the immune system surveillance, HCMV has developed a huge arsenal of genetic functions committed to alter and modulate both innate and adaptive arms of the immune response. In particular, HCMV coevolution within its host has led to the incorporation of a repertoire of functions with strong homologies to host genes. Thus the virus is able to subvert the immune system mimicking the same strategies and mechanisms used by hosts to clear the infection. Inhibition of complement cascade and natural killer (NK) cells activation, attenuation of interferon (INF) response and disruption of antigen presentation are only few examples of the functions hijacked by virus encoded chemokines, cytokine and cellular receptors homologues [35].

**Table 1:** List of selected protein functions encoded by cytomegalovirus that interfere with adaptive and innate immune response. Modified from [35].

<b>Adaptive immune response</b>	<b>Innate immune response</b>
Inhibits MHCI and II expression ( <i>US3</i> )	Fcγ Receptor Homologs ( <i>UL119, RL11</i> )
MHC I and II degradation ( <i>US2</i> )	Interferon-Mediated Immunity ( <i>IE2, UL83</i> )
MHC I degradation ( <i>US11</i> )	Natural Killer Cells ( <i>UL18, UL142, UL141, UL40</i> )
Binds MHC I molecules ( <i>US8, US10</i> )	Cytokine Homologs ( <i>UL111</i> )
Inhibits TAP peptide transport ( <i>US6</i> )	Viral Chemokine Homologs ( <i>UL146, UL147, UL128-131</i> )
Inhibit MHC II expression ( <i>UL83</i> )	Apoptosis ( <i>UL36, UL37x1</i> )

#### **4.1. Complement cascade**

A first line of defense against viral infection resides in innate response modulators such as the complement system and natural killer mediated cytotoxicity. The complement system is composed of a multitude of serum proteins that circulate in the blood. Upon direct deposition of C3 complement molecule on invading microorganisms or infected cells surface (alternative pathway), a cascade of proteolytic events is initiated. The activation pathway usually culminates with the formation of a membrane attack complex (MAC) with the ability to lyse the bound microorganism or cell. Alternatively, complement opsonized structure can be efficiently disposed by phagocytic cells. A more efficiency complement activation is triggered by binding of complement protein C1 to the constant region (Fc) of immunoglobulin clustered by antigen binding (classical pathway). Antibodies marking surface exposed viral antigens on infected cells can trigger the classical complement pathway leading to the infected cell lysis. This mechanism is referred as antibody dependent complement mediated lysis (ADCML) [36]. Several molecules act as regulators of complement activation (RCA) controlling and assuring that the complement cascade becomes activated only when needed. Surface expression of two of these proteins, CD46 and CD55, is highly enhanced in HCMV infected cells [37]. Moreover CD55 and CD59 RCAs incorporation in the HCMV virion has also been reported [38]. These mechanisms protect both HCMV infected cells and virions from the recognition and consequently from the activation of the complement cascade.

#### **4.2. Natural killer cells**

Natural killer (NK) cells are a component of the innate immune response possessing cytotoxic activity. NK cells recognize and eliminate host damaged cells, such as virus infected cells, providing a rapid and efficient response to intracellular infections. Mechanisms regulating NK activation rely on a

fine balance between activating and inhibitory signals triggered by the binding to the target cells receptors rather than to direct recognition of the pathogen. Strong activating signals are triggered by the binding of NKG2D receptor to surface exposed MHC class I related proteins MICA and MICB. Fc portion of IgG covering the surface of a pathogen or an infected cell can be recognized by the gamma immunoglobulin Fc receptor IIIA (FcγRIIIA) CD16 present on NK cells surface leading to their activation in a mechanism called Antibody Dependent Cellular Cytotoxicity (ADCC). On the contrary, inhibitory signaling pathway arises from MHC class I recognition by different inhibitory receptors such as the Leukocyte Ig-like receptor (LIR)-1 and the CD94/NKG2 lectin-like receptors. Inhibition is achieved upon tyrosine phosphorylation of the immunoreceptor tyrosine-based inhibition motifs (ITIM) present in the cytoplasmic tails of these proteins [39–41].

Different works have demonstrated a prominent role for NK cells in controlling HCMV infections both in humans and mice [1]. As expected, HCMV has evolved numerous functions that modulate and interfere with NK cell activity [42]. The viral protein gpUL18, a MHC class I homologue, localizes on infected cells plasma membrane where it binds the NK LIR inhibitory receptor [43–45]. HCMV UL40 is able to upregulate non-classical MHC-I molecule HLA-E and to promote its efficient cell surface expression. HLA-E binds the inhibitory receptor CD94/NKG2A and the overall effect of its upregulation during HCMV infection is thought to protect the infected cells through NK cells inhibition [46]. Finally, the two protein products of the UL142 and UL16 genes downregulate the surface exposition of the NK activating receptor ligands MICA and MICB retaining them intracellularly in the ER or Golgi apparatus [47–51].

## 5. Fc receptors

Fc receptors (FcR) are cellular surface exposed proteins present on almost every kind of immune cell and on some epithelial, endothelial and hepatocytic cells. Fc receptors are involved in the process of antigen recognition but, unlike the B and T cell receptors (BCR and TCR, respectively) they do not directly bind the antigen: instead the Fc receptor ligands are the constant region of immunoglobulins. Each Ig class has one or more dedicated Fc receptors and they are named according to the type of bound Ig: Fc $\alpha$ R, Fc $\gamma$ R, Fc $\delta$ R, Fc $\mu$ R and Fc $\epsilon$ R bind respectively Ig of the A, G, D, M and E class.

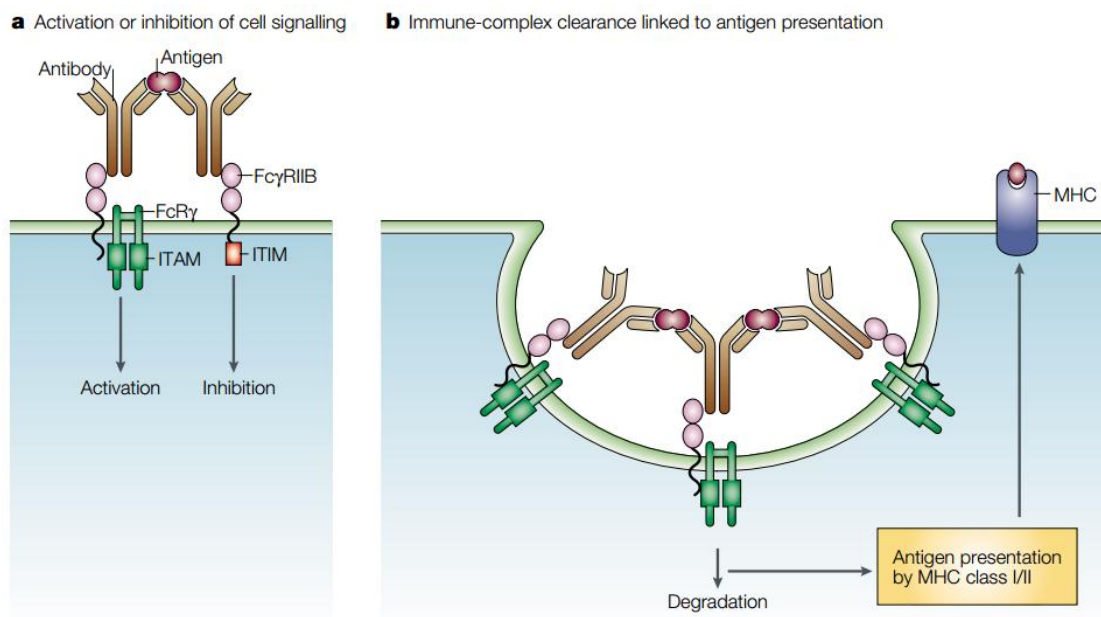
The Fc receptors belong to the immunoglobulin superfamily (IgSF) and possess at least one immunoglobulin domain. The only exception is the Fc $\epsilon$ RII receptor that belongs to the lectin family and possesses a C-type Lectin Domain (CLTD). Two layers of  $\beta$ -sheets composed from seven to nine antiparallel  $\beta$ -strands connected by a loop compose the immunoglobulin fold common to all the members of the Ig superfamily [52].

Fc receptor functions can be divided in three main categories: regulation of immune-cell responses through their activation or inhibition; antigen-antibodies immunocomplexes (IC) uptake; immunoglobulin transport and stabilization.

Regulation of immune cells functions can be initiated through the recruitment of surface FcRs by antigen bound Igs. Depending on the kind of FcRs recruited and on the type of cell, activatory or inhibitory stimuli can be triggered. Many different downstream effects can result from the signaling cascade including up- or down- modulation of cellular proliferation, phagocytosis, degranulation, cytokine production. Most FcRs do not possess intrinsic signaling motifs thus they must associated with other proteins able to mediate the signals transduction. The Immunoreceptor Tyrosine-based Activatory or Inhibitory Motifs (ITAM and ITIM, respectively) are regulatory motifs that are present in

the cytoplasmic tails of the receptor or in the associated units and regulate the signaling cascade. Receptor engagement induces a phosphorylation event on the tyrosine present in both motifs that culminates with the activation, in the case of ITAM triggered signaling, or in the inhibition, in the case of ITIM signaling, of the cell functions [52].

Another important function mediated by the FcRs is the immune complexes internalization. FcRs mediate ICs endocytosis and delivery into lysosomes for degradation. Proteolytically cleaved antigen-derived peptides can then be loaded and presented on MHC class I and II molecules [52].

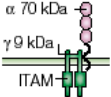
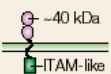
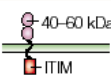
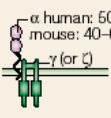
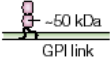
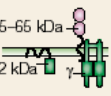
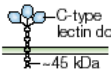
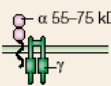
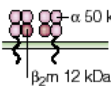
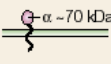
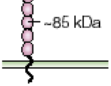
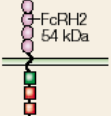


**Fig. 6: Principal functions of Fc receptors.** **a:** Fc receptors modulate positive or negative cellular signaling upon IC binding. Activation can lead to cellular proliferation, phagocytosis, degranulation and is mediated by the ITAM motif present in the FcR associated  $\gamma$ -chain. By contrast, an inhibitory signaling cascade can be initiated through engagement of the ITIM motif possessing Fc $\gamma$ RIIB. **b:** FcR can mediate both IC and Ig-coated pathogens phagocytosis. The internalization process can lead to the clearance of the pathogen/IC and to MHC class I and class II antigen-presentation of the resulting antigenic peptides. From [52].

Finally, some specialized Fc receptors have different functions based on the organism development stage: for example neonatal Fc receptor (FcRn) is essential for the transfer of passive humoral immunity from the mother to the fetus through transportation of maternal IgG across the placenta.

Similarly, the polymeric Ig receptor, pIgR, is present on polarized epithelia and it is responsible for polymeric IgA and IgM transcytosis [52].

**Table 2:** Fc receptors: structure, Fc affinity and expression profiles. From [52].

Receptor	Structure and apparent $M_r$	Affinity for immunoglobulin	Human	Expression
FcγRIA (CD64)	 α 70 kDa γ 9 kDa ITAM	$10^7$ – $10^8$ $M^{-1}$ to IgG2a>>3,1,2b	$10^7$ – $10^8$ $M^{-1}$ to IgG1≈3>4>>2	Macrophage, monocyte, neutrophil, eosinophil, DC
FcγRIIA (CD32)	 ~40 kDa ITAM-like	NF	$<10^7$ $M^{-1}$ to IgG3≈1,2>>4	Macrophage, neutrophil, eosinophil, platelet, DC, LC
FcγRIIB (CD32)	 40–60 kDa ITIM	$<10^7$ $M^{-1}$ to IgG1,2a,2b>>3 $3 \times 10^5$ $M^{-1}$ to IgE	$<10^7$ $M^{-1}$ to IgG3≈1>4>2	B cell, mast cell, basophil, macrophage, eosinophil, neutrophil, DC, LC
FcγRIIA (CD16)	 α human: 50–80 kDa mouse: 40–60 kDa γ (or C)	$<10^7$ $M^{-1}$ to IgG1,2a,2b>>3 $5 \times 10^5$ $M^{-1}$ to IgE	$2 \times 10^7$ $M^{-1}$ to IgG1,3>>2,4	Macrophage, monocyte, NK cell, mast cell, eosinophil, DC, LC, neutrophil (mouse)
FcγRIIB (CD16)	 ~50 kDa GPI link	NF	$<10^7$ $M^{-1}$ to IgG1,3>>2,4	Neutrophil, eosinophil
FcεRI	 α 45–65 kDa β 32 kDa γ	$>10^{10}$ $M^{-1}$ to IgE	$>10^{10}$ $M^{-1}$ to IgE	Mast cell, basophil, eosinophil, LC (human), DC (human)
FcεRII (CD23)	 C-type lectin domain α ~45 kDa	$10^6$ $M^{-1}$ to IgE	$10^6$ $M^{-1}$ to IgE	Ubiquitous, platelet
FcαRI (CD89)	 α 55–75 kDa γ	NF	$2 \times 10^7$ $M^{-1}$ to IgA1, IgA2	Macrophage, neutrophil, eosinophil
FcRn	 α 50 kDa β <sub>2</sub> m 12 kDa	$10^6$ $M^{-1}$ to rat IgG2a>2b,1,2c	$2 \times 10^6$ $M^{-1}$ to IgG	Placenta, small intestine, monocyte, DC
Fcα/μR	 α ~70 kDa	ND	$10^6$ $M^{-1}$ to IgM, IgA	B cell, macrophage
Poly-IgR	 ~85 kDa	High, but ND	High, but ND	Epithelium, liver, small intestine, lung
FcRH1–5*	 FcRH2 54 kDa	ND	ND	B cell

β<sub>2</sub>m, β<sub>2</sub>–microglobulin; DC, dendritic cell; FcRH, Fc-receptor homologue; FcRn, neonatal Fc receptor; GPI, glycosylphosphatidylinositol; Ig, immunoglobulin; LC, Langerhans cell; Mr, relative molecular mass; ND, not determined; NF, not found in mice; NK, natural killer; poly-IgR, polymeric immunoglobulin receptor.

## 5.1. IgG and Fc gamma receptors

IgG is the most abundant and most versatile immunoglobulin isotype. It is present in almost all extracellular fluids and in blood where it constitutes up to 75% of total serum Ig. In human, IgGs are divided in 4 distinct subgroups designed IgG1, IgG2, IgG3 and IgG4 that despite having around 95% amino acidic identity, show remarkable differences in terms of biological and physicochemical properties and relative abundance. IgG are monomeric glycoproteins composed of two identical longer polypeptides called heavy chains (H) linked by disulfide bonds to two identical shorter light chains (L). Disulfide bonds keep together the two heavy chains and form an “hinge region” responsible for the protein flexibility. Each chain is composed of structured immunoglobulin domains: four Ig domains ( $C_{H1}$ ,  $C_{H2}$ ,  $C_{H3}$  and  $V_H$ ) are present in the heavy chain and two domains ( $C_L$  and  $V_L$ ) in the light chain. IgG fragmentation through papain protease generates two identical Fab (Fragment antigen binding) fragments and one Fc (Fragment crystallisable).  $V_H$  and  $V_L$  variable regions of the heavy and light chains constitute the immunoglobulin antigen binding site. IgGs have a prominent role as effectors of the adaptive response by protecting the organism against extracellular pathogens through binding and neutralization or complement activation and lysis. Moreover IgG can engage the  $Fc\gamma R$ s present on almost all kind of innate immune system cells activating a plethora of cellular responses that concur in the pathogen clearing. Thus  $Fc\gamma R$  interaction with IgG bridges the cellular and humoral immune responses.

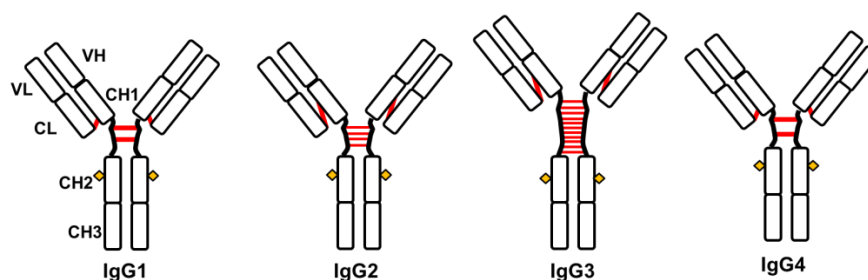


**Fig. 7: Human IgG subclasses.** Igs domains are indicated as: VL, variable light; CH, variable heavy; CH, constant heavy; CL, constant light. Red line, disulfide bond; rhombus, N-linked glycosylation

In human Fc $\gamma$ R are divided in: Fc $\gamma$ RI (CD64), Fc $\gamma$ RII (CD32) composed of three isoforms A, B and C, and Fc $\gamma$ RIII (CD16) divided in isoforms A and B. All of them are single pass membrane spanning proteins, with the exception of glycosyl-phosphatidylinositol (GPI)-linked membrane anchored Fc $\gamma$ RIIIB [53,54]. Like other FcRs, Fc $\gamma$ Rs are usually protein complexes composed of an IgG Fc binding  $\alpha$ -chain associated to different signaling transducing homodimeric proteins called  $\gamma$ ,  $\beta$  or  $\zeta$  chains, which contain the ITAM motif in their cytoplasmic tail. The only exception is the Fc $\gamma$ RIIIB that do not induce downstream signaling, and the Fc $\gamma$ RII class, that is able to transduce the signal independently from the association with accessory proteins. While ITAM motif is present in the Fc $\gamma$ RIIA C-terminus, the Fc $\gamma$ RIIB is the only known ITIM containing FcR.

Fc $\gamma$ RI is the only high affinity receptor and is able to bind monomeric IgG with an affinity  $10^8$ - $10^9$  M<sup>-1</sup>, while all the others receptors show 100-1000 lower affinity. Thus, Fc $\gamma$ RI is completely saturated with the ligand, but is unable to mediate signaling until antigen binding induces receptors clusterization. By contrast, indiscriminate activation of pro-inflammatory response by circulating monomeric IgG is prevented by the low affinity of the majority of Fc $\gamma$ R. For these receptors, ICs binding induces receptors cross-linking allowing for the initiation of the signaling pathways. Moreover the binding stoichiometry of 1:1 receptor-ligand prevents accidental receptor activation [54].

In response to a viral infection, Fc $\gamma$ Rs and specific IgGs together are able to put in place a coordinated series of cellular responses that involve both the innate and the adaptive arms of the immune system.

Antibodies coated virions or infected cells can be readily recognized by cytotoxic cells through their Fc $\gamma$ Rs, leading to a strong Antibody Dependent Cellular Cytotoxicity response. Thus, the Fc $\gamma$ R

present on the innate branch cells, such as NK and macrophages, can link the specificity of the humoral adaptive response to the potent effector function of the innate response.

## 5.2. Fc receptor homologues

Among the mechanisms used by pathogens to escape the immune system response, the acquisition of FcR homologues function seems to be highly diffuse. While the host cells use the FcR as a mean to sense and dispose of antibodies marked intruders, pathogens have developed similar functions in order to counteract immune system recognition. *Staphylococcus aureus*, a Gram positive bacterium, covers its membrane with the Fc binding protein A that captures and fixes immunoglobulins in the wrong orientation on the bacterium surface, disguising it and impairing its identification [55]. Fc binding proteins are highly conserved among the human herpesviruses: genes coding for FcR homologue functions were found almost in all genomes of the herpesviridae family suggesting a prominent role for these functions in pathogen survival [56].

Most of the viral FcRs (vFcR) recognize and bind the constant region of IgG probably impairing and inhibiting host effector function. Different mechanisms of action were proposed depending on the localization of the vFcR. Disguising mechanisms, similar to those observed for *S. aureus* protein A, can be put in place by vFcR present on the virions while circulating antibodies clearing can start from vFcR exposed on infected cells membrane. While the latter can inhibit the ADCC of the infected cells, the former can contribute to counteract the neutralization activity of antibodies bound to their target on the viral surface. The blockage of the free Fc portion can avoid the recognition of the viral particles and the activation of mechanisms such as the complement cascade or phagocytosis processes. This mechanism, named antibody bipolar bridging, has been described for Herpes Simplex Virus (HSV) heterodimeric FcR gE:gI.

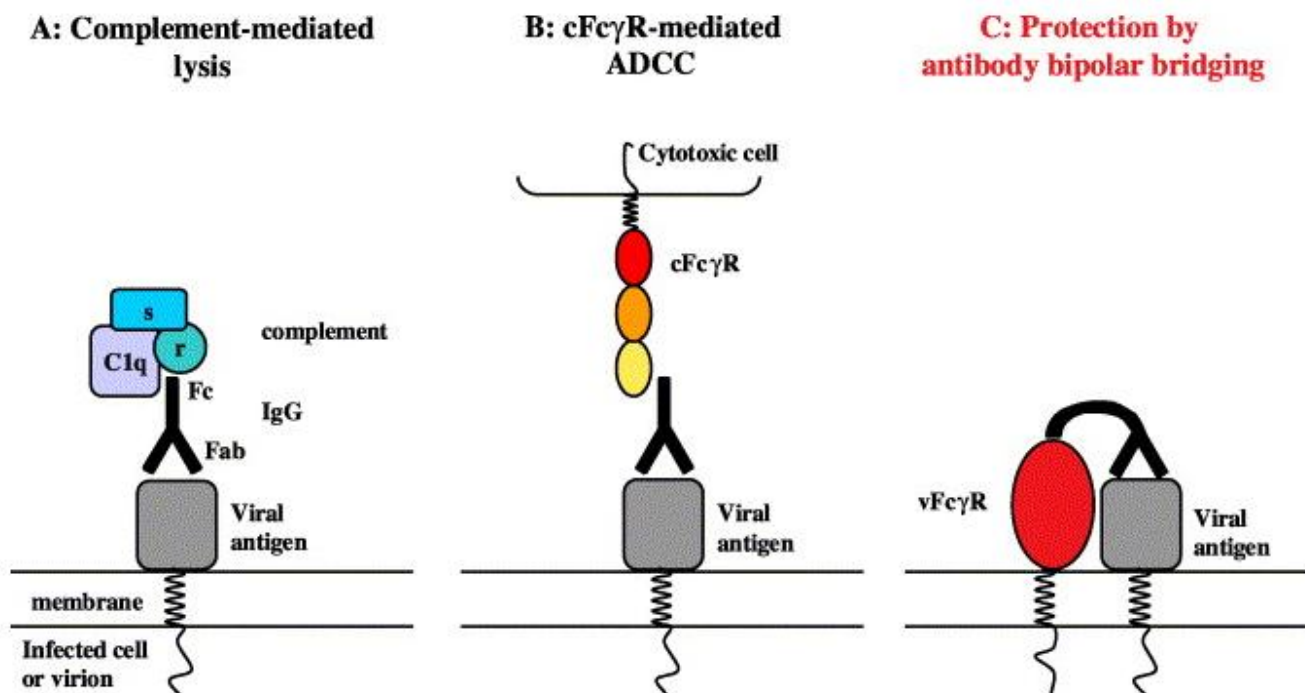


**Fig. 8: Herpesviral FcγRs mediated mechanism of protection against antiviral IgG.** The Fc portion of human IgG bound to viral antigen on infected cell surface or on virus particle can recruit complement proteins (A) or host FcγRs (B). The former mechanism culminates with the complement-mediated lysis (ADCML) of the infected cells/viral particle. Recruitment of host FcγRs present on the surface of cytotoxic effector cells results in the antibody-dependent cellular cytotoxicity (ADCC). (C) Viral FcγR impairs both mechanisms through the blockage of the Fc portion of the IgG. This mechanism of antibody bipolar bridging protects the virus particle or infected cell from recognition and destruction. From [56].

Moreover, several reports underline the importance of the vFcγR endocytic activity of HSV, Pseudorabies Virus (PrV) and Varicella Zoster Virus (VZV) in the contest of the infected cells [57–60]. For example gE:gI vFcγR complex in PrV infected monocytes internalizes antibodies-viral antigens complexes from the cell surface preventing the ADCML of the infected cell [61].

HCMV is known to encode for two different FcγRs: glycoprotein gp68, encoded from the UL118-119 locus, and gp34, encoded from the RL11 locus [62,63]. Both gp68 and gp34 are type I membrane proteins with a predicted IgSF domain and extensive glycosylation and localize on the membrane of transfected cells. gp68 is a 347 amino acid long protein generated through a splicing event between the UL119 and UL118 open reading frames (ORFs). It is predicted to possess up to 12 potential N-linked

and several O-linked glycosylation sites. *In silico* alignment showed that the IgSF domain of gp68 displays a high degree of similarity to the third IgSF domain of cellular Fc $\gamma$ RI. Moreover an almost consensus ITIM motif (WSYKRL<sub>328</sub>) is present in gp68 cytoplasmic tail. Studies conducted on the purified ectodomain showed that gp68 binds Fc $\gamma$  with a 2:1 stoichiometry. Thus a single IgG can crosslink two molecules of gp68 allowing receptor clusterization in the absence of antigen binding. Surface plasmon resonance studies demonstrated a high affinity between gp68 and Fc $\gamma$  with a  $K_D$  in the nanomolar range. Furthermore the binding remained stable at acidic pH, a major difference from the previously characterized gE:gI- Fc $\gamma$  complex that dissociate at pH lower than neutrality [64].

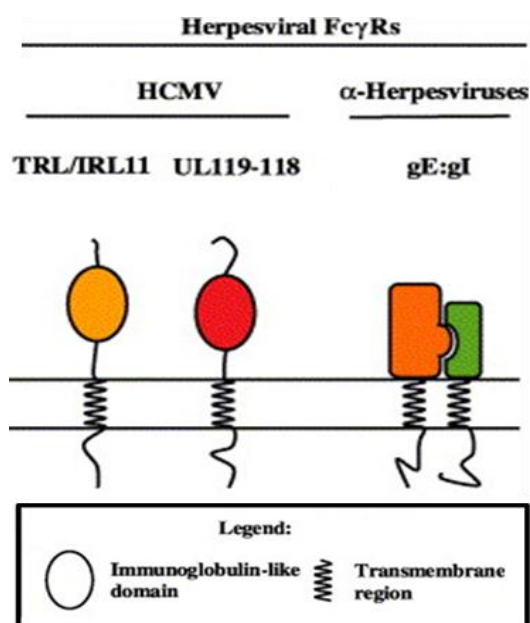


**Fig. 9:** Herpesviral Fc $\gamma$  receptors. Modified from [56].

Less experimental information is available for RL11 gene product gp34. It consists of 234 amino acids and possesses only N-linked glycosylations on three predicted sites. Multiple alignments showed the presence of determinants that are conserved in the Fc binding region of host Fc $\gamma$ IIIcRs. The cytoplasmic tail contains a predicted dileucine internalization motif (DXXXLL<sub>226</sub>) that could indicate a propensity of the protein to enter the endocytic route upon Fc $\gamma$  binding. Differential binding propensity to the IgG subclasses for gp68 and gp34 are still unknown, but

the different reported affinities for IgG from various species suggest a diverse mechanism of binding for the two proteins. In particular, both gp68 and gp34 were able to bind to the same levels IgG1, IgG2, IgG3 and IgG4 while only gp34 showed affinity for non-human IgG binding both rabbit and rat IgGs [62]. Moreover the HCMV FcRs seem to be diverse from HSV gE:gI not only for what concern pH requirement but also in terms of binding sites. In fact, while gE:gI binding site to the Fc fragment

competes with protein A, HCMV vFcγRs bound to the Fc can be immunoprecipitated with the *S. aureus* Fc binding protein. Overall the structural and topological similarities between HCMV FcγR and the Fc binding proteins coded by other herpesviruses may indicate a mechanism of action similar for these classes of proteins [56]. Nevertheless some distinctive features can evidence a mode of action that do not reside in the mechanisms previously described, suggesting a diverse and peculiar role for the HCMV FcγR in the contest of viral infection.

**Project summary**

Human cytomegalovirus (HCMV) employs many different mechanisms to escape and subvert the host immune system surveillance. Among these different mechanisms the role of human IgG Fc receptors (Fc $\gamma$ R) in HCMV pathogenesis is still unclear. In mammals, Fc $\gamma$ Rs are expressed on the surface of all haematopoietic cells and have a multifaceted role in regulating the activity of antibodies to generate a well-balanced immune response. Viral proteins with Fc $\gamma$  binding ability are highly diffuse among herpesviruses. They interfere with the host receptors functions in order to counteract immune system recognition. So far, two human HCMV Fc $\gamma$  binding proteins have been described: UL119 and RL11. This work was aimed to the identification and characterization of HCMV Fc $\gamma$  binding proteins. The study is divided in two parts: first the characterization of UL119 and RL11; second the identification and characterization of novel HCMV Fc $\gamma$  binding proteins. Regarding the first part, we demonstrated that both UL119 and RL11 internalize Fc $\gamma$  fragments from transfected cells surface through a clathrin dependent pathway. In infected cells both proteins were found in the viral assembly complex and on virions surface as envelope associated glycoproteins. Moreover, internalized Fc $\gamma$  in infected cells do not undergo lysosomal degradation but rather traffic in early endosomes up to the viral assembly complex. Regarding the second part, we were able to identify two novels Fc $\gamma$  binding protein coded by CMV: RL12 and RL13. The latter was also further characterized as recombinant protein in terms of cellular localization, Fc binding site and IgG internalization ability. Finally binding specificity of both RL12 and RL13 seems to be confined to human IgG1 and IgG2. Taken together, these data show that HCMV codes for up to 4 Fc $\gamma$ R and that they could have a double role both on virus and on infected cells.

**REFERENCES**

1. Mocarski ES, Shenk T, Pass RF (2007) Cytomegaloviruses. In: Knipe D.M. HPMed, editors. Fields virology. Lippincott Williams & Wilkins. pp. 2701-2772.
2. Murphy E, Shenk T (2008) Human cytomegalovirus genome. *Curr Top Microbiol Immunol* 325: 1-19.
3. Murphy E, Yu D, Grimwood J, Schmutz J, Dickson M, Jarvis MA, Hahn G, Nelson JA, Myers RM, Shenk TE (2003) Coding potential of laboratory and clinical strains of human cytomegalovirus. *Proc Natl Acad Sci U S A* 100: 14976-14981. 10.1073/pnas.2136652100 [doi];2136652100 [pii].
4. Stern-Ginossar N, Weisburd B, Michalski A, Le VT, Hein MY, Huang SX, Ma M, Shen B, Qian SB, Hengel H, Mann M, Ingolia NT, Weissman JS (2012) Decoding human cytomegalovirus. *Science* 338: 1088-1093. 338/6110/1088 [pii];10.1126/science.1227919 [doi].
5. Varnum SM, Streblov DN, Monroe ME, Smith P, Auberry KJ, Pasa-Tolic L, Wang D, Camp DG, Rodland K, Wiley S, Britt W, Shenk T, Smith RD, Nelson JA (2004) Identification of proteins in human cytomegalovirus (HCMV) particles: the HCMV proteome. *J Virol* 78: 10960-10966. 10.1128/JVI.78.20.10960-10966.2004 [doi];78/20/10960 [pii].
6. Stanton RJ, Baluchova K, Dargan DJ, Cunningham C, Sheehy O, Seirafian S, McSharry BP, Neale ML, Davies JA, Tomasec P, Davison AJ, Wilkinson GW (2010) Reconstruction of the complete human cytomegalovirus genome in a BAC reveals RL13 to be a potent inhibitor of replication. *J Clin Invest* 120: 3191-3208. 42955 [pii];10.1172/JCI42955 [doi].
7. Shikhagaie M, Merce-Maldonado E, Isern E, Muntasell A, Alba MM, Lopez-Botet M, Hengel H, Angulo A (2012) The human cytomegalovirus-specific UL1 gene encodes a late-phase glycoprotein incorporated in the virion envelope. *J Virol* 86: 4091-4101. JVI.06291-11 [pii];10.1128/JVI.06291-11 [doi].
8. Isaacson MK, Juckem LK, Compton T (2008) Virus entry and innate immune activation. *Curr Top Microbiol Immunol* 325: 85-100.
9. Hahn G, Revello MG, Patrone M, Percivalle E, Campanini G, Sarasini A, Wagner M, Gallina A, Milanesi G, Koszinowski U, Baldanti F, Gerna G (2004) Human cytomegalovirus UL131-128 genes are indispensable for virus growth in endothelial cells and virus transfer to leukocytes. *J Virol* 78: 10023-10033. 10.1128/JVI.78.18.10023-10033.2004 [doi];78/18/10023 [pii].
10. Wang D, Shenk T (2005) Human cytomegalovirus UL131 open reading frame is required for epithelial cell tropism. *J Virol* 79: 10330-10338. 79/16/10330 [pii];10.1128/JVI.79.16.10330-10338.2005 [doi].
11. Compton T (2004) Receptors and immune sensors: the complex entry path of human cytomegalovirus. *Trends Cell Biol* 14: 5-8. S0962892403002721 [pii].
12. Isaacson MK, Juckem LK, Compton T (2008) Virus entry and innate immune activation. *Curr Top Microbiol Immunol* 325: 85-100.

13. Compton T, Nepomuceno RR, Nowlin DM (1992) Human cytomegalovirus penetrates host cells by pH-independent fusion at the cell surface. *Virology* 191: 387-395.
14. Bodaghi B, Slobbe-van Drunen ME, Topilko A, Perret E, Vossen RC, van Dam-Mieras MC, Zipeto D, Virelizier JL, LeHoang P, Bruggeman CA, Michelson S (1999) Entry of human cytomegalovirus into retinal pigment epithelial and endothelial cells by endocytosis. *Invest Ophthalmol Vis Sci* 40: 2598-2607.
15. Ryckman BJ, Jarvis MA, Drummond DD, Nelson JA, Johnson DC (2006) Human cytomegalovirus entry into epithelial and endothelial cells depends on genes UL128 to UL150 and occurs by endocytosis and low-pH fusion. *J Virol* 80: 710-722. 80/2/710 [pii];10.1128/JVI.80.2.710-722.2006 [doi].
16. Wang D, Yu QC, Schroer J, Murphy E, Shenk T (2007) Human cytomegalovirus uses two distinct pathways to enter retinal pigmented epithelial cells. *Proc Natl Acad Sci U S A* 104: 20037-20042. 0709704104 [pii];10.1073/pnas.0709704104 [doi].
17. Haspot F, Lavault A, Sinzger C, Laib SK, Stierhof YD, Pilet P, Bressolette-Bodin C, Halary F (2012) Human cytomegalovirus entry into dendritic cells occurs via a macropinocytosis-like pathway in a pH-independent and cholesterol-dependent manner. *PLoS One* 7: e34795. 10.1371/journal.pone.0034795 [doi];PONE-D-11-14831 [pii].
18. Halary F, Amara A, Lortat-Jacob H, Messerle M, Delaunay T, Houles C, Fieschi F, Arenzana-Seisdedos F, Moreau JF, Dechanet-Merville J (2002) Human cytomegalovirus binding to DC-SIGN is required for dendritic cell infection and target cell trans-infection. *Immunity* 17: 653-664. S1074761302004478 [pii].
19. Kalejta RF (2008) Tegument proteins of human cytomegalovirus. *Microbiol Mol Biol Rev* 72: 249-65, table. 72/2/249 [pii];10.1128/MMBR.00040-07 [doi].
20. Weston K (1988) An enhancer element in the short unique region of human cytomegalovirus regulates the production of a group of abundant immediate early transcripts. *Virology* 162: 406-416.
21. Chee MS, Bankier AT, Beck S, Bohni R, Brown CM, Cerny R, Horsnell T, Hutchison CA, III, Kouzarides T, Martignetti JA, . (1990) Analysis of the protein-coding content of the sequence of human cytomegalovirus strain AD169. *Curr Top Microbiol Immunol* 154: 125-169.
22. Stasiak PC, Mocarski ES (1992) Transactivation of the cytomegalovirus ICP36 gene promoter requires the alpha gene product TRS1 in addition to IE1 and IE2. *J Virol* 66: 1050-1058.
23. Tandon R, Mocarski ES (2012) Viral and host control of cytomegalovirus maturation. *Trends Microbiol* 20: 392-401. S0966-842X(12)00081-9 [pii];10.1016/j.tim.2012.04.008 [doi].
24. Buser C, Walther P, Mertens T, Michel D (2007) Cytomegalovirus primary envelopment occurs at large infoldings of the inner nuclear membrane. *J Virol* 81: 3042-3048. JVI.01564-06 [pii];10.1128/JVI.01564-06 [doi].
25. Sanchez V, Greis KD, Sztul E, Britt WJ (2000) Accumulation of virion tegument and envelope proteins in a stable cytoplasmic compartment during human cytomegalovirus replication: characterization of a potential site of virus assembly. *J Virol* 74: 975-986.

26. Das S, Vasanji A, Pellett PE (2007) Three-dimensional structure of the human cytomegalovirus cytoplasmic virion assembly complex includes a reoriented secretory apparatus. *J Virol* 81: 11861-11869. JVI.01077-07 [pii];10.1128/JVI.01077-07 [doi].
27. Das S, Pellett PE (2011) Spatial relationships between markers for secretory and endosomal machinery in human cytomegalovirus-infected cells versus those in uninfected cells. *J Virol* 85: 5864-5879. JVI.00155-11 [pii];10.1128/JVI.00155-11 [doi].
28. Schauflinger M, Villinger C, Mertens T, Walther P, von EJ (2013) Analysis of human cytomegalovirus secondary envelopment by advanced electron microscopy. *Cell Microbiol* 15: 305-314. 10.1111/cmi.12077 [doi].
29. Zamora MR, Nicolls MR, Hodges TN, Marquesen J, Astor T, Grazia T, Weill D (2004) Following universal prophylaxis with intravenous ganciclovir and cytomegalovirus immune globulin, valganciclovir is safe and effective for prevention of CMV infection following lung transplantation. *Am J Transplant* 4: 1635-1642. 10.1111/j.1600-6143.2004.00571.x [doi];AJT571 [pii].
30. Nigro G, Adler SP, La TR, Best AM (2005) Passive immunization during pregnancy for congenital cytomegalovirus infection. *N Engl J Med* 353: 1350-1362. 353/13/1350 [pii];10.1056/NEJMoa043337 [doi].
31. Snyderman DR, Werner BG, Meissner HC, Cheeseman SH, Schwab J, Bednarek F, Kennedy JL, Jr., Herschel M, Magno A, Levin MJ, . (1995) Use of cytomegalovirus immunoglobulin in multiply transfused premature neonates. *Pediatr Infect Dis J* 14: 34-40.
32. Roy DM, Grundy JE (1992) Evaluation of neutralizing antibody titers against human cytomegalovirus in intravenous gamma globulin preparations. *Transplantation* 54: 1109-1110.
33. Borucki MJ, Spritzler J, Asmuth DM, Gnann J, Hirsch MS, Nokta M, Aweeka F, Nadler PI, Sattler F, Alston B, Nevin TT, Owens S, Waterman K, Hubbard L, Caliendo A, Pollard RB (2004) A phase II, double-masked, randomized, placebo-controlled evaluation of a human monoclonal anti-Cytomegalovirus antibody (MSL-109) in combination with standard therapy versus standard therapy alone in the treatment of AIDS patients with Cytomegalovirus retinitis. *Antiviral Res* 64: 103-111. S0166-3542(04)00131-7 [pii];10.1016/j.antiviral.2004.06.012 [doi].
34. Jabs DA, Gilpin AM, Min YI, Erice A, Kempen JH, Quinn TC (2002) HIV and cytomegalovirus viral load and clinical outcomes in AIDS and cytomegalovirus retinitis patients: Monoclonal Antibody Cytomegalovirus Retinitis Trial. *AIDS* 16: 877-887.
35. Miller-Kittrell M, Sparer TE (2009) Feeling manipulated: cytomegalovirus immune manipulation. *Virol J* 6: 4. 1743-422X-6-4 [pii];10.1186/1743-422X-6-4 [doi].
36. Rus H, Cudrici C, Niculescu F (2005) The role of the complement system in innate immunity. *Immunologic Research* 33: 103-112.
37. Spiller OB, Morgan BP, Tufaro F, Devine DV (1996) Altered expression of host-encoded complement regulators on human cytomegalovirus-infected cells. *Eur J Immunol* 26: 1532-1538. 10.1002/eji.1830260719 [doi].

38. Spear GT, Lurain NS, Parker CJ, Ghassemi M, Payne GH, Saifuddin M (1995) Host cell-derived complement control proteins CD55 and CD59 are incorporated into the virions of two unrelated enveloped viruses. Human T cell leukemia/lymphoma virus type I (HTLV-I) and human cytomegalovirus (HCMV). *J Immunol* 155: 4376-4381.
39. Lanier LL (2005) NK cell recognition. *Annu Rev Immunol* 23: 225-274. 10.1146/annurev.immunol.23.021704.115526 [doi].
40. Bryceson YT, Long EO (2008) Line of attack: NK cell specificity and integration of signals. *Curr Opin Immunol* 20: 344-352. S0952-7915(08)00030-7 [pii];10.1016/j.coi.2008.03.005 [doi].
41. Burshtyn DN, Lam AS, Weston M, Gupta N, Warmerdam PA, Long EO (1999) Conserved residues amino-terminal of cytoplasmic tyrosines contribute to the SHP-1-mediated inhibitory function of killer cell Ig-like receptors. *J Immunol* 162: 897-902.
42. Wilkinson GW, Tomasec P, Stanton RJ, Armstrong M, Prod'homme V, Aicheler R, McSharry BP, Rickards CR, Cochrane D, Llewellyn-Lacey S, Wang EC, Griffin CA, Davison AJ (2008) Modulation of natural killer cells by human cytomegalovirus. *J Clin Virol* 41: 206-212. S1386-6532(07)00376-9 [pii];10.1016/j.jcv.2007.10.027 [doi].
43. Prod'homme V, Griffin C, Aicheler RJ, Wang EC, McSharry BP, Rickards CR, Stanton RJ, Borysiewicz LK, Lopez-Botet M, Wilkinson GW, Tomasec P (2007) The human cytomegalovirus MHC class I homolog UL18 inhibits LIR-1+ but activates LIR-1- NK cells. *J Immunol* 178: 4473-4481. 178/7/4473 [pii].
44. Wagner CS, Riise GC, Bergstrom T, Karre K, Carbone E, Berg L (2007) Increased expression of leukocyte Ig-like receptor-1 and activating role of UL18 in the response to cytomegalovirus infection. *J Immunol* 178: 3536-3543. 178/6/3536 [pii].
45. Wagner CS, Ljunggren HG, Achour A (2008) Immune modulation by the human cytomegalovirus-encoded molecule UL18, a mystery yet to be solved. *J Immunol* 180: 19-24. 180/1/19 [pii].
46. Prod'homme V, Tomasec P, Cunningham C, Lemberg MK, Stanton RJ, McSharry BP, Wang EC, Cuff S, Martoglio B, Davison AJ, Braud VM, Wilkinson GW (2012) Human cytomegalovirus UL40 signal peptide regulates cell surface expression of the NK cell ligands HLA-E and gpUL18. *J Immunol* 188: 2794-2804. jimmunol.1102068 [pii];10.4049/jimmunol.1102068 [doi].
47. Wills MR, Ashiru O, Reeves MB, Okecha G, Trowsdale J, Tomasec P, Wilkinson GW, Sinclair J, Sissons JG (2005) Human cytomegalovirus encodes an MHC class I-like molecule (UL142) that functions to inhibit NK cell lysis. *J Immunol* 175: 7457-7465. 175/11/7457 [pii].
48. Ashiru O, Bennett NJ, Boyle LH, Thomas M, Trowsdale J, Wills MR (2009) NKG2D ligand MICA is retained in the cis-Golgi apparatus by human cytomegalovirus protein UL142. *J Virol* 83: 12345-12354. JVI.01175-09 [pii];10.1128/JVI.01175-09 [doi].
49. Cosman D, Mullberg J, Sutherland CL, Chin W, Armitage R, Fanslow W, Kubin M, Chalupny NJ (2001) ULBPs, novel MHC class I-related molecules, bind to CMV glycoprotein UL16 and stimulate NK cytotoxicity through the NKG2D receptor. *Immunity* 14: 123-133. S1074-7613(01)00095-4 [pii].

50. Chalupny NJ, Rein-Weston A, Dosch S, Cosman D (2006) Down-regulation of the NKG2D ligand MICA by the human cytomegalovirus glycoprotein UL142. *Biochem Biophys Res Commun* 346: 175-181. S0006-291X(06)01149-1 [pii];10.1016/j.bbrc.2006.05.092 [doi].
51. Dunn C, Chalupny NJ, Sutherland CL, Dosch S, Sivakumar PV, Johnson DC, Cosman D (2003) Human cytomegalovirus glycoprotein UL16 causes intracellular sequestration of NKG2D ligands, protecting against natural killer cell cytotoxicity. *J Exp Med* 197: 1427-1439. 10.1084/jem.20022059 [doi];jem.20022059 [pii].
52. Takai T (2002) Roles of Fc receptors in autoimmunity. *Nat Rev Immunol* 2: 580-592. 10.1038/nri856 [doi];nri856 [pii].
53. Nimmerjahn F, Ravetch JV (2007) Fc-receptors as regulators of immunity. *Adv Immunol* 96: 179-204. S0065-2776(07)96005-8 [pii];10.1016/S0065-2776(07)96005-8 [doi].
54. Nimmerjahn F, Ravetch JV (2008) Fcgamma receptors as regulators of immune responses. *Nat Rev Immunol* 8: 34-47. nri2206 [pii];10.1038/nri2206 [doi].
55. Foster TJ (2005) Immune evasion by staphylococci. *Nat Rev Microbiol* 3: 948-958. nrmicro1289 [pii];10.1038/nrmicro1289 [doi].
56. Budt M, Reinhard H, Bigl A, Hengel H (2004) Herpesviral Fcgamma receptors: culprits attenuating antiviral IgG? *Int Immunopharmacol* 4: 1135-1148. 10.1016/j.intimp.2004.05.020 [doi];S1567-5769(04)00176-6 [pii].
57. Tirabassi RS, Enquist LW (1999) Mutation of the YXXL endocytosis motif in the cytoplasmic tail of pseudorabies virus gE. *J Virol* 73: 2717-2728.
58. Tirabassi RS, Enquist LW (1998) Role of envelope protein gE endocytosis in the pseudorabies virus life cycle. *J Virol* 72: 4571-4579.
59. Lubinski JM, Lazear HM, Awasthi S, Wang F, Friedman HM (2011) The herpes simplex virus 1 IgG fc receptor blocks antibody-mediated complement activation and antibody-dependent cellular cytotoxicity in vivo. *J Virol* 85: 3239-3249. JVI.02509-10 [pii];10.1128/JVI.02509-10 [doi].
60. Olson JK, Grose C (1997) Endocytosis and recycling of varicella-zoster virus Fc receptor glycoprotein gE: internalization mediated by a YXXL motif in the cytoplasmic tail. *J Virol* 71: 4042-4054.
61. Van de Walle GR, Favoreel HW, Nauwynck HJ, Pensaert MB (2003) Antibody-induced internalization of viral glycoproteins and gE-gI Fc receptor activity protect pseudorabies virus-infected monocytes from efficient complement-mediated lysis. *J Gen Virol* 84: 939-948.
62. Atalay R, Zimmermann A, Wagner M, Borst E, Benz C, Messerle M, Hengel H (2002) Identification and expression of human cytomegalovirus transcription units coding for two distinct Fcgamma receptor homologs. *J Virol* 76: 8596-8608.
63. Lilley BN, Ploegh HL, Tirabassi RS (2001) Human cytomegalovirus open reading frame TRL11/IRL11 encodes an immunoglobulin G Fc-binding protein. *J Virol* 75: 11218-11221. 10.1128/JVI.75.22.11218-11221.2001 [doi].

64. Sprague ER, Reinhard H, Cheung EJ, Farley AH, Trujillo RD, Hengel H, Bjorkman PJ (2008) The human cytomegalovirus Fc receptor gp68 binds the Fc CH2-CH3 interface of immunoglobulin G. *J Virol* 82: 3490-3499. JVI.01476-07 [pii];10.1128/JVI.01476-07 [doi].



## **Dynamics of IgG binding and virus localization of HCMV Fcγ binding proteins RL11 and UL119**

**Mirko Cortese<sup>1</sup>, Stefano Calò<sup>1</sup>, Luca Bruno<sup>1</sup>, Tobias Kessler<sup>2</sup>, Anders Lilja<sup>3</sup> and Marcello Merola<sup>1,4,\*</sup>.**

<sup>1</sup>) Novartis Vaccines and Diagnostics, Via Fiorentina 1, 53100 Siena, Italy

<sup>2</sup>) Sandoz GmbH, Sandoz Development Center Austria, Biochemiestrasse 10, A-6250 Kundl, Austria.

<sup>3</sup>) Novartis Vaccines and Diagnostics, 45 Sidney Street, Cambridge, MA 02139, USA.

<sup>4</sup>) Department of Structural and Functional Biology, University of Naples “Federico II”, Via Cinthia 21, 80126 Naples, Italy

Keywords: viral Fc binding proteins, UL119, RL11, HCMV, IgG internalization.

\* Corresponding author. Mailing address: Marcello Merola, Ph.D. [marcello.merola@novartis.com](mailto:marcello.merola@novartis.com) [m.merola@unina.it](mailto:m.merola@unina.it)

**ABSTRACT**

Human cytomegaloviruses (HCMVs) employ many different mechanisms to escape and subvert the host immune system expressing proteins that mimic MHC class I molecules, chemokines and human IgG Fc receptors (FcRs). Among these different mechanisms the role of FcRs in HCMV pathogenesis is still unclear. We focused our attention on the characterization of HCMV Fc binding proteins UL119 and RL11. In particular, we demonstrated that both proteins are able to bind human Fc fragments on the surface of transfected cells. This event triggers the internalization of the receptor-ligand complex trafficking from the cellular membrane to endosomes through a clathrin dependent pathway. Intriguingly, internalized IgG do not reach the lysosomal compartment, but remain localized in Rab5 positive vesicles. Moreover, we demonstrated that both proteins are found in infected cells assembly complex and are present on the surface of the virions as envelope associated glycoproteins. Finally, we analyzed the Fcγ internalization activity of infected cells demonstrating that internalized immunoglobulins do not undergo lysosomal degradation but rather traffic in early endosomes EEA1 positive vesicles up to the viral assembly complex. Taken together, these data suggest that HCMV FcR could have a double role both on virus and on infected cells.

## INTRODUCTION

Infection by Human cytomegalovirus (HCMV) occurs in the majority of population. Following primary infection, which generally remains asymptomatic, the virus establishes a lifelong latent infection persisting in precursor of dendritic and myeloid cells [1,2]. Reactivation requires immunosuppressive conditions and is associated to a variety of diseases [3]. Among *herpesviridae*, HCMV owns the largest genome and carries several gene products able to counteract host immune-response. Such immune-modulatory proteins span from MHC class I and receptor homologues to chemokine-like and Fc receptor-mimicking molecules [4].

Human Fc receptors (hFcRs) are present on the cell surface of most cells of myeloid and lymphoid origin and represent the connection between cell-mediated and humoral immune-response [5]. Immune cells benefit of these plasma membrane molecules as sensor of antigens or immune complexes in the extracellular environment. Following ligand engagement, they trigger the appropriate responses to infection. Several herpesviruses code for proteins able to bind the constant region of immunoglobulin known as viral Fc receptors (vFcRs), most of them recognize the constant fragment of IgG (Fc $\gamma$ ) and potentially interfere with the host Fc receptors [6,7]. IgG production in response to viral infection is a crucial step in activating host effector functions, including neutralization/phagocytosis processes and antibody-dependent cellular cytotoxicity (ADCC) [8]. Nonetheless, passive transfer of anti-HCMV IgG has been shown to limit viral infection and used as therapeutic agent to cure acute cytomegalovirus infection in human patients [9,10]. Basically three putative mechanisms of action have been envisioned for vFcRs: a) recruiting antibodies on the viral particles to facilitate cells internalization, b) counteract neutralizing antibodies via a mechanism known as “antibody bipolar bridging” [11–14] and c) clearing circulating IgG by capturing them on the surface of infected cells with consequent internalization and

lysosome targeting of the antibody [15]. The first and second hypothesis assume their localization on the viral particle, the third requires solely their expression in infected cells. Despite several indications favoring one or the other among these hypotheses, the functional role of vFcRs has never been fully elucidated. Furthermore, other herpesviral Fc $\gamma$  binding proteins, such the HSV-1 gE, the murine CMV m138 and the varicella-zoster virus (VZV) gE, are known to play crucial roles in *in vivo* infection independently of their antibody binding ability [16–20].

HCMV encodes four proteins possessing Fc $\gamma$  ability [21–23] All of them are glycosylated type I membrane proteins with a predicted Ig-like domain and localize on cell surface when expressed in isolation. The gene products RL11, known also as gp34, and UL119, indicated as gp68, was found expressed at the cell surface based on flow cytometry analysis of Fc binding to unpermeabilized cells transduced with adenoviruses expressing gp34 or gp68 [22]. Flow cytometry analysis was also used to assess RL12 and RL13 plasma membrane localization and Fc binding ability in transfected cells [21]. The presence on purified viral particles has so far been reported for UL119 and RL13 [24,25]. Binding specificity versus human IgG subclasses differs among these proteins. RL11 and UL119 bind all human IgGs whereas RL12 and RL13 do not bind IgG3 and IgG4 [21,22].

Irrespective of whether they have to be inserted into the viral particles or escort IgG to degradation, herpesviral Fc $\gamma$  binding proteins need to be targeted to the plasma membrane and then enter the endocytic pathway. Among the HCMV Fc $\gamma$  binding proteins, only RL13 has been reported to be able to internalize following Fc binding at plasma membrane [21]. Endocytosis of Fc $\gamma$  binding protein has been well documented for the analogous functions carried by VZV, pseudorabies virus (PrV) and HSV-1. The VZV gE protein undergoes clathrin-dependent endocytosis mediated by a tyrosine-based motif of its cytoplasmic tail [26]. Postendocytotic events include recycling to the plasma membrane or TGN

sorting mediated by an acidic cluster [31]. Internalization of VZV gE is enhanced upon association with the escort protein gI, a glycoprotein deprived of Fc $\gamma$  binding activity but possessing independent internalization and trafficking motifs [27,28]. Correct targeting of gE:gI complex to TGN is crucial for the formation of the viral particle [29]. For PrV, gE is responsible for the ligand-independent internalization of gE:gI since gI alone is unable to undergo endocytosis [30]. The gE:gI complex expressed by HSV contains several internalization motifs on their cytoplasmic tails. Such as its VZV counterpart, the HSV gE C-terminal includes a tyrosin-containing motif crucial for TGN sorting of the gE:gI complex, an event that also drives correct targeting of viral particles [31–33]. However, gE:gI complex from HSV displays an Fc $\gamma$  binding-independent crucial function in cell-to-cell spreading of the virus and requires primary TGN accumulation followed by redistribution to cell junction [34].

In this report we investigate the HCMV Fc $\gamma$  binding proteins UL119 and RL11, demonstrating that both proteins are able to internalize human IgG. We characterized this ability in terms of internalization pathway and intracellular route of the ligand. We also define the localization of UL119 and RL11 in infected cells and on purified HCMV virions, demonstrating that both proteins associate with the viral envelope. Finally we started to define the IgG internalization ability in HCMV infected cells.

## RESULTS AND DISCUSSION

### *Expression, glycosylation and intracellular localization of TR UL119 and RL11*

Immunoglobulin internalization mediated by viral Fc $\gamma$  receptors (vFc $\gamma$ R) has been reported for different herpesviruses. Endocytotic activity of Cytomegalovirus Fc binding proteins UL119 and RL11 was proposed by Atalay *et. al.* [22], based on the observation that both proteins were targeted to degradation in endolysosomal compartments, but never experimentally addressed. Internalization upon cell surface IgG binding was supported also by the presence of endocytic motifs in the C-terminal tail of both proteins (YxxL and DXXXLL motifs for UL119 and RL11, respectively [22]). We decided to characterize expression, localization and IgG internalization ability of UL119 and RL11 starting from the analysis of the recombinant protein transiently expressed in cell cultures.

The sequences for both genes were derived from clinical CMV strain TR and cloned as codon optimized genes in the mammalian expression vector pcDNA3.1-mycHis. The expressed proteins included C-terminal double tag that was used for the detection. Western blot analysis in transiently expressing HEK293T cells showed the presence of two species for both UL119 and RL11 proteins with a molecular mass of approximately 120 kDa and 98 kDa for the former and 48 kDa and 40 kDa for the latter (Fig. 1A, first lane left and right panels, respectively). TR UL119 is a 345 residue protein with a calculated MW of 38.72 kDa that possesses 12 consensus Asn for N-linked glycosylation plus 26 O-linked carbohydrate acceptor Thr or Ser, thus with a high potential to be post-translational modified by glycosylation. Furthermore, our products include additional 3 kDa due to the presence of the myc and His tags. Digestion with endoglycosidase H reduced the molecular mass of both UL119 species to 102 kDa and 40 kDa, respectively (Fig. 1A, second lane, left panel). PNGase F treatment of UL119 further reduced the molecular mass of both species to about 55 and 38 kDa for the slower and faster migrating

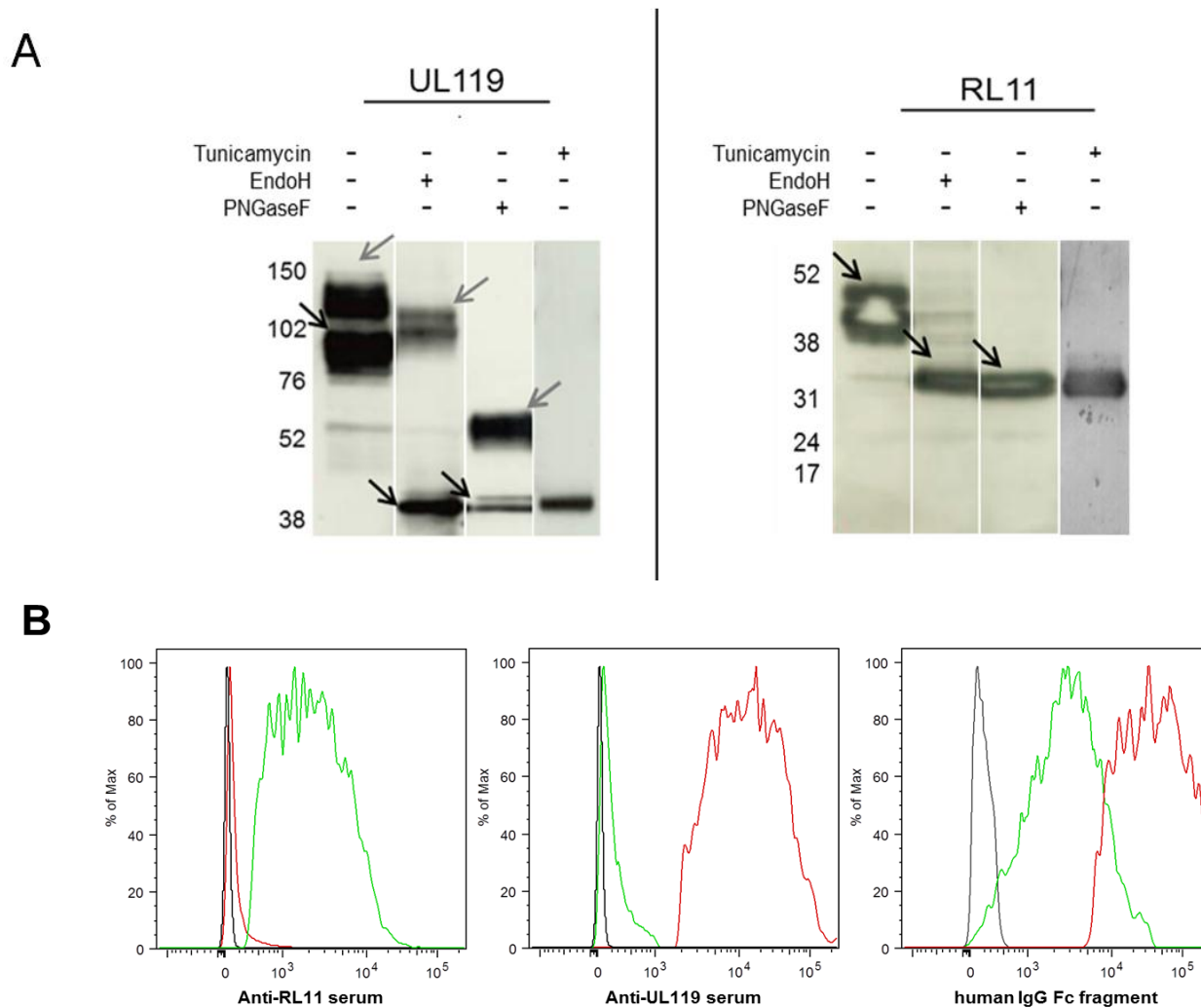
band respectively (Fig. 1A, third lane, left panel). This pattern suggests that the slower migrating UL119 form includes O-linked glycosylation. Treatment with tunicamycin, an ER N-linked glycosylation inhibitor, of UL119 resulted in a band of 38 kDa, confirming the complete deglycosylation of the EndoH sensitive band (Fig. 1A, fourth lane, left panel). The RL11 protein carried by the TR strain is 234 residues long with a calculated molecular weight of about 26.7 kDa. On its sequence, 4 Asn and 2 Thr acceptors of N- and O-linked glycan respectively are predicted. Treatment with either EndoH, PNGase F or with tunicamycin lead to the appearance of a single band at 32 kDa (Fig. 1A, second, third and fourth lanes, right panel) suggesting that this species is not subject to heavy Golgi modification and does not receive O-linked carbohydrates. Although the analysis shown has been performed in HEK293T cells, identical results were obtained with proteins expressed in epithelial ARPE-19 cells (data not shown).

The analysis of glycosidase digestion suggested that, as single gene transfection, UL119 is present in two main post-translational modified species, the faster migrating likely localized at early steps of the secretory pathway while the slower migrating species represent a post-Golgi product. RL11 showed a simpler glycosylation pathway only as non-complex N-linked glycans.

To assess the plasma membrane localization of UL119 and RL11, cytofluorimetric analysis on transiently transfected cells was performed. HEK293T cells expressing YFP-tagged proteins were stained 24 h post transfection with mouse sera against RL11 and UL119 (Fig. 1B, left and central panels, respectively). In both cases, a signal higher than control was registered confirming UL119 and RL11 surface localization in our system. Surface exposed proteins were also correctly folded as confirmed by their ability to bind fluorescent Fc $\gamma$  in non-permeabilized cells (Fig. 1B, right panel). These experiments demonstrated that in our system both proteins are able to reach the plasma membrane and to assume a full functional conformation.

In figure 2 is shown the intracellular localization of RL11 and UL119 performed by confocal microscopy in ARPE-19 human epithelial cells. Similar results, however, were obtained with human derived fibroblastoid cell line MRC-5 (not shown). Transiently transfected cells, expressing YFP-tagged UL119 and RL11, were fixed, permeabilized and stained with different markers of the secretory apparatus. At steady state, total intracellular pool of both UL119 and RL11 is revealed by the YFP (green in Fig. 2) and is mainly constituted from vesicles co-localizing with markers of the early endosomes such as EEA1 and Rab5 (Fig. 2, middle and lower panels). In these conditions, we did not find significant co-localization with lamp1, a marker of the lysosomal compartment (not shown). These results suggested that UL119 and RL11 undergo endocytosis from the plasma membrane to early endosomes in transfected cells, but questioned a targeting to degradation pathway. The human IgG Fc binding ability of UL119 and RL11 is displayed in the upper panel of Fig. 2. Most of the intracellular fraction of both proteins was able to bind human immunoglobulin as showed by the co-localization with a fluorophore conjugated human IgG Fc fragment (Fc, Fig. 2, upper panel). However, for both proteins a minor fraction did not bind the Fc $\gamma$ , perhaps immature proteins entering the initial steps of the secretory pathway.

Taken together, these data indicate the transport of these two Fc $\gamma$ -binding proteins to plasma membrane followed by internalization and long lasting into vesicles with marker of early endosomes.

**Fig. 1:**

**A. Deglycosylation profiles of UL119 and RL11.** Western blot of UL119 and RL11 proteins transiently expressed from HEK293T. Size of the native forms or after treatment with Endoglycosidase H, PNGaseF and Tunicamycin are shown. Endoglycosidase H sensitive and resistant isoforms are indicated (black and gray arrows, respectively).

**B. Membrane localization and Fc $\gamma$  binding ability of UL119 and RL11** Cytofluorimetric analysis of HEK293T expressing RL11-YFP (green lines) and UL119-YFP (red lines). Cells were stained with either anti-RL11 or anti-UL119 mouse anti-sera (left and central panels, respectively) or with a fluorophore conjugated human IgG Fc fragment (right panel). Signals retrieved from YFP positive cells were compared to empty vector transfected control cells. Each histogram represents  $1 \times 10^4$  cells.

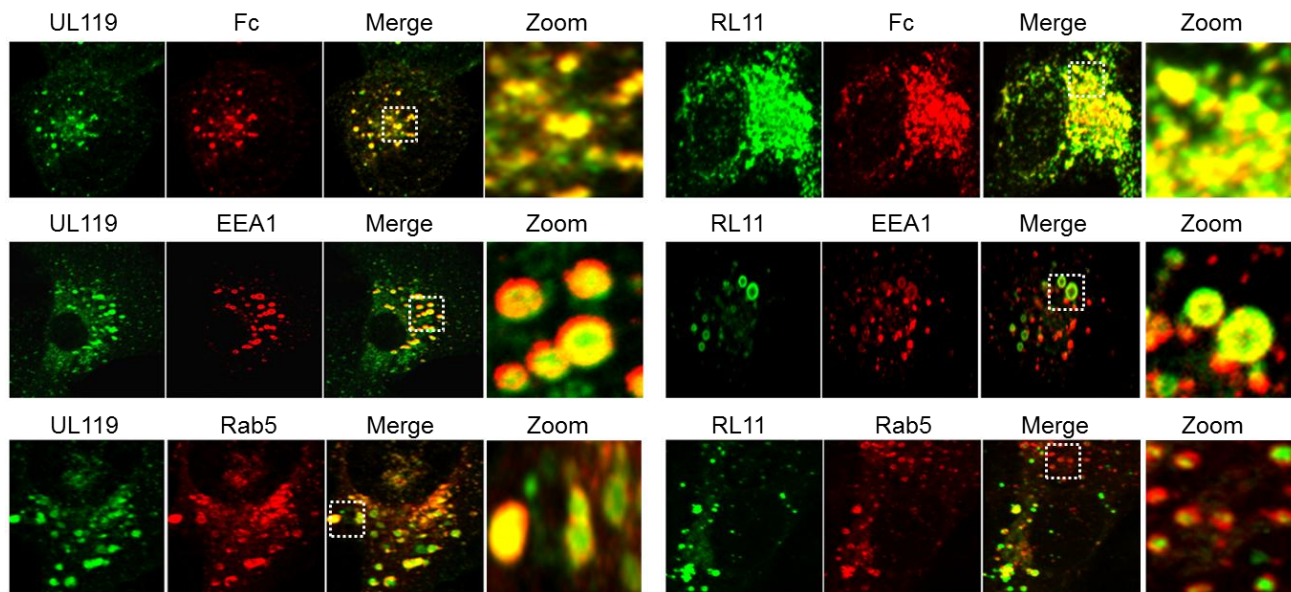


**Fig. 2: UL119 and RL11 localized with markers of endocytic pathway.** ARPE-19 grown on glass coverslips were transfected with vectors coding for C-terminus YFP fused UL119 and RL11 proteins (green color, left and right panels, respectively). Cells were fixed, permeabilized and stained with human IgG Fc fragment (Fc, red color on top) and with markers of the early endosomes (EEA1 and Rab5 middle and bottom panels, respectively) before being analyzed through confocal microscopy. Merge panels show the superimposition between green and red colors. The boxed regions in the merged images are magnified.

***Immunoglobulin Fc fragment internalization ability of recombinant UL119 and RL11***

Having defined the presence on the plasma membrane of UL119 and RL11 in transfected cells, we sought to investigate ability of these two proteins to internalize upon binding of the Fc $\gamma$  fragment. ARPE-19 cells transiently expressing C-terminus YFP-tagged UL119 and RL11 were incubated on ice with fluorescently labelled Fc $\gamma$ . Incubation was protracted for 30 min, then the excess of fluorescent probe was washed out while cells were either fixed (time 0) or incubated in complete medium for 30 min at 37°C to allow for internalization. Cells were then fixed and submitted to confocal microscopy analysis (Fig. 3). As expected, cells that were not switched at 37°C showed a marked membrane staining due to the binding on the plasma membrane of the Fc $\gamma$  fragment. This result was similar for both UL119 and RL11 transfected cells (Fig. 3 upper rows, left and right panels, respectively). Re-establishment of membrane trafficking after temperature switching allowed endocytosis of the human Fc $\gamma$  from the plasma membrane and both proteins and Fc $\gamma$  completely co-localized into intracellular vesicles (Fig. 3, bottom panels). Kinetic of the internalization process was followed over the time through live microscopy on UL119-YFP expressing cells (Fig. 4). Small vesicles containing Fc $\gamma$  signal can be seen as short as 4 min after immunoglobulin G fragment addition to the culture medium (Fig. 4, white arrow upper right panels). Fc $\gamma$  accumulated inside endosomes, whose dimension increased, in spite of a decrease in number, during the time course (white arrows in left zoomed panels and data not shown). Furthermore, the overnight live imaging revealed only a slight decrease of Fc $\gamma$  signal bound to the fluorescent UL119, suggesting that the endosomes were not targeted to lysosomes (data not shown). These observations assessed that both recombinant UL119 and RL11 were able to internalize human IgG Fc fragment from the plasma membrane and are consistent with the lack of lysosomal delivery of the cargo.

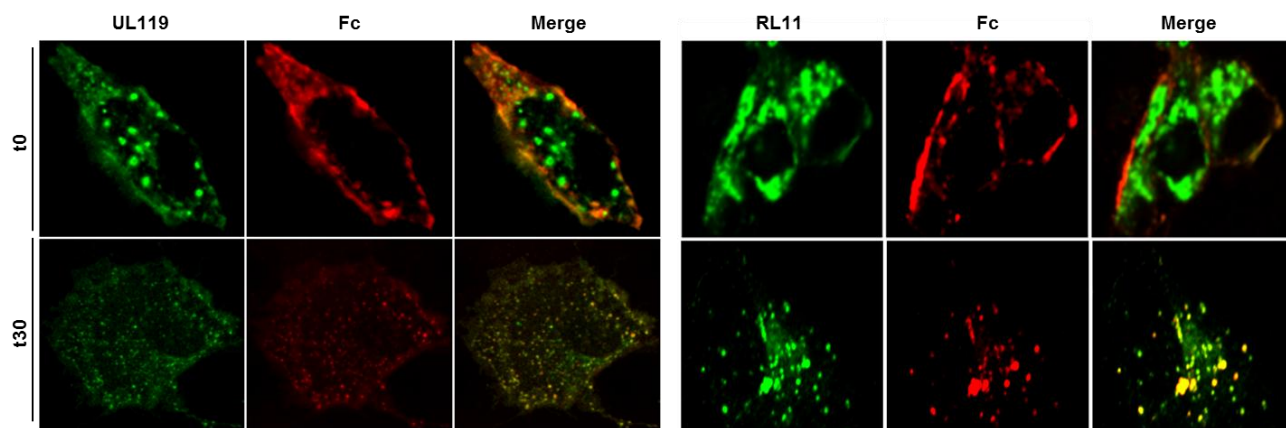


**Fig. 3: UL119 and RL11 internalized human IgG Fc fragment in transfected cells.** ARPE-19 cells grown on glass coverslips were transfected with plasmids expressing C-terminally YFP fused UL119 and RL11 proteins (green color, left and right panels, respectively). 48 h post transfection, 649 Dylight conjugated human IgG Fc fragment (Fc, red color) was added for 30 min on ice. Cells were washed and either fixed (t0) or shifted at 37°C for 30 min prior fixation (t30) to allow for internalization.

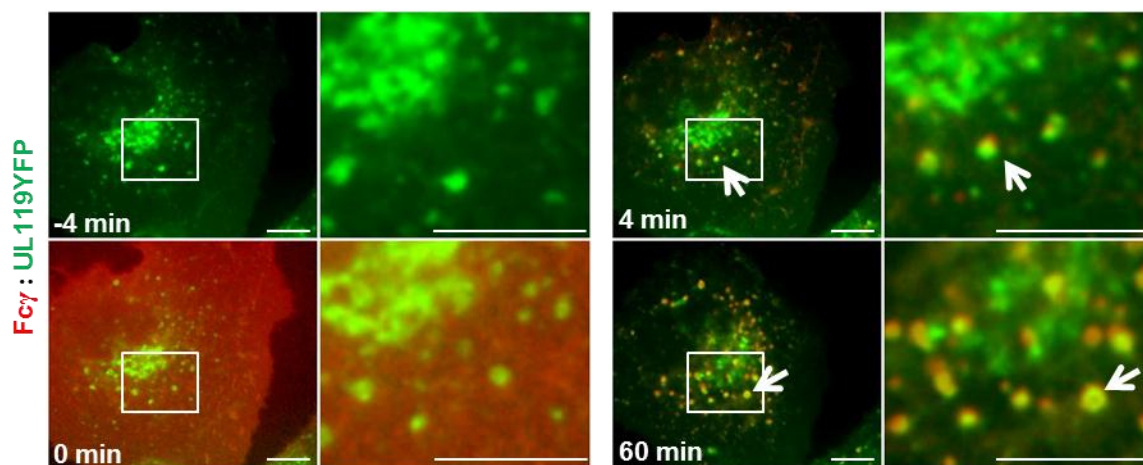


**Fig. 4: UL119 Fc $\gamma$  live-microscopy internalization assay.** UL119-YFP (green color) expressing ARPE-19 were imaged live during Fc $\gamma$  (red color) uptake from culture medium. One frame per minute was taken. Scale bar 10  $\mu$ m. Images enclosed in white boxes are showed in the zoomed panels. Co-localization between UL119 and Fc $\gamma$  signals is shown in yellow.

### ***Internalization of Fc $\gamma$ by UL119 and RL11 is clathrin dependent***

Receptor mediated endocytosis of small IC and soluble IgG by cFc $\gamma$  is dependent on both clathrin and dynamin [35,36]. Clathrin dependent endocytosis relies on the interaction with a small set of adaptor proteins and a huge number of accessory proteins, which regulate different aspects of the endocytosis [37]. Overexpression of the C-terminus, containing the clathrin binding domain, of adaptor protein AP180 (AP180-C), leads to the redistribution of clathrin and the complete inhibition of clathrin mediated endocytosis [38]. To define whether the internalization pathway of the two CMV Fc $\gamma$  binding proteins UL119 and RL11, follows the above mentioned mechanism, a vector expressing the AP180-C was used. Internalization of Fc $\gamma$  was assayed on ARPE-19 cells transiently co-expressing UL119 or RL11 with AP180-C. Results of the assay are showed in figure 5. When clathrin endocytosis was abrogated, Fc $\gamma$  was observed only at the plasma membrane of UL119 and RL11 positive cells (Fig. 5, top panel of A and B, respectively). On the contrary, distinct punctate signals were present at the same time in control cells expressing the CMV proteins alone (Fig. 5A-B, bottom panel). Same pattern was observed for transferrin, whose transport depends on clathrin internalization (Fig. 5C), confirming the inhibitory activity of AP180-C protein in our system. These experiments showed that Fc $\gamma$  fragment internalization pathway by UL119 and RL11 relied on clathrin-coated pits formation.

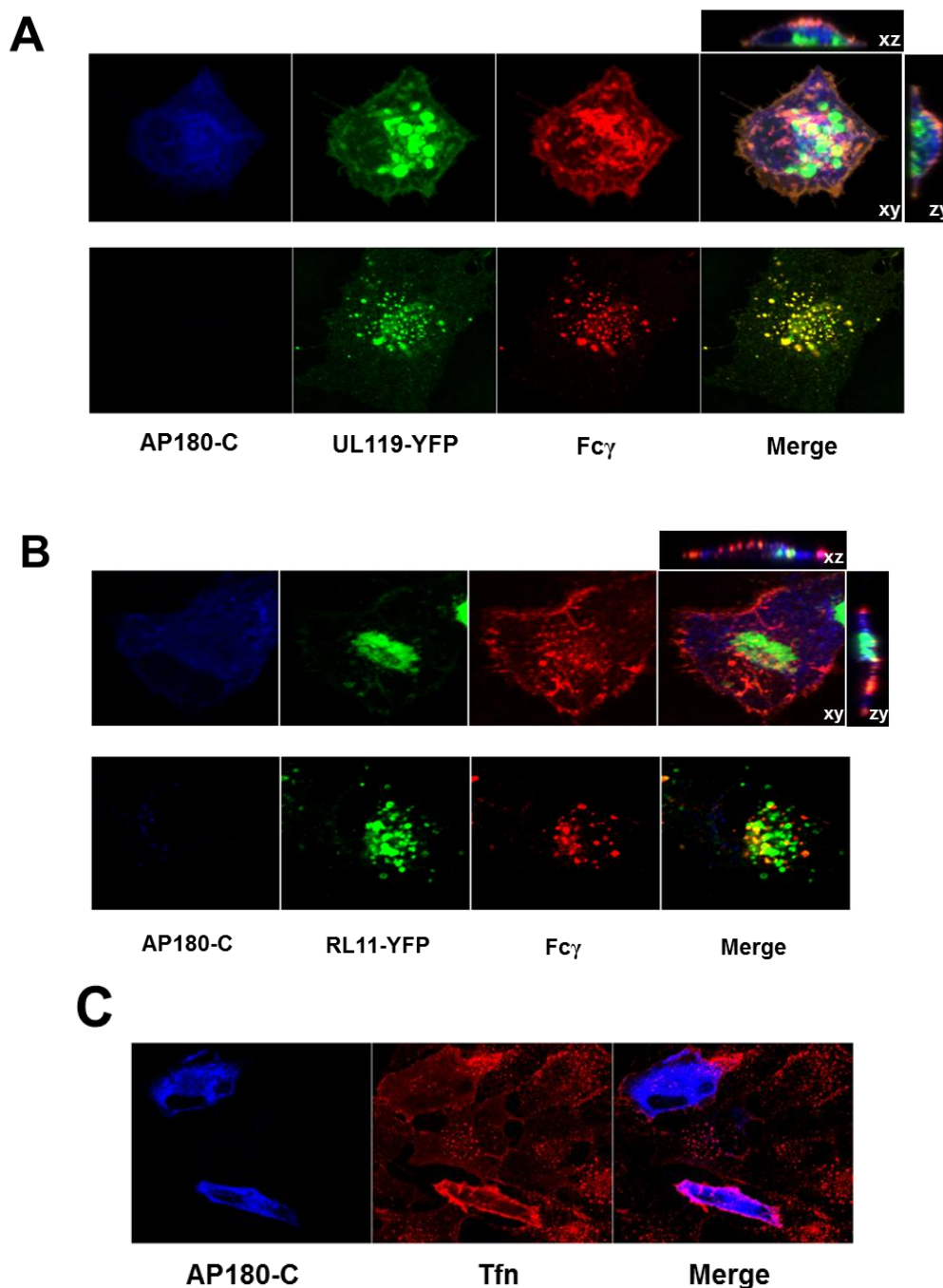


**Fig. 5: Overexpression of dominant-negative mutant of AP180 inhibited UL119 Fcγ endocytosis.** ARPE-19 were transiently transfected with UL119-YFP or RL11-YFP alone (lower panels of A and B, respectively) or in combination with myc-tagged AP180 (A and B, top panels). At 48 h post transfection, cells were allowed to internalize 549 Dylight conjugated human IgG Fc fragment for 30 min at 37 °C (A-B, red color). For transferrin uptake (C), cells were serum starved for 1 h at 37 °C, and then incubated with 50 μg/ml 568 Alexa fluor conjugated transferrin (Tfn, red color) in DMEM without serum at 37 °C for 30 min. At the end of endocytosis, cells were cooled to 4°C quickly, washed and fixed. Endocytosis was analyzed by confocal laser-scanning microscope.

***UL119 and RL11 localize in the viral assembly complex and associate with the virion envelope.***

The IgG Fc $\gamma$  internalization ability and endocytic trafficking of UL119 and RL11 suggested their potential involvement in antiviral IgG removal from the surface of infected cells. However, lack of co-localization with endolysosomal markers argue against a possible lysosomotropic function. This could be explained considering the system under analysis that is the transient transfection of single proteins. Additional protein functions could be needed to alter the intracellular transport. The strong remodeling of the secretory apparatus in CMV infected cells and the huge number of viral proteins expressed during the course of the infection could affect and modify the observed vFc $\gamma$  endocytosis mechanism [39–41]. To this aim, we decided to analyze the UL119 and RL11 Fc $\gamma$  internalization ability in the context of the CMV infection. First we defined the intracellular distribution of both proteins in CMV infected human foreskin fibroblast (HFF). TB40E strain, harboring GFP sequence in frame with the gene coding for the viral tegument protein pp150 [42], was used for the first experiment (Fig. 6, upper panel). Cells seeded on glass coverslips were infected for 5 days before being fixed, permeabilized and stained using specific anti-sera developed in mouse against UL119 and RL11. As reported in literature [43], accumulation of pp150 in a large cytoplasmic perinuclear inclusion, compatible with the viral assembly complex (AC), was observed. Signals retrieved from UL119 and RL11 anti-sera concentrated to the same intracellular structure, co-localizing with pp150 tegument protein (Fig. 6, upper green and merge panels, respectively). To further confirm the presence of UL119 and RL11 in the assembly complex, staining of glycoprotein gL (a virion envelope glycoprotein encoded by gene UL115) and trans-Golgi network (TGN46 marker) was performed on cells infected with CMV TR strains coding for tagged version of both viral Fc $\gamma$  proteins. The Flag and HA epitopes were used to track UL119 and RL11 expression, respectively. Both proteins co-localized with gL glycoprotein and partially with the trans-Golgi marker. The latter also surrounded the sites of UL119 and RL11 accumulation, consistent

with the reported reorientation of trans-Golgi compartment at the outer edge of the assembly complex [44].

The observation that UL119 and RL11 localized at the virion assembly site suggested their potential inclusion in the virion envelope as surface exposed glycoproteins. To test this hypothesis virions were purified from infected HFF and subjected to detergent fractionation in order to separate envelope embedded proteins from tegument and capsids ones. Results from these studies are shown in figure 7. Both UL119 and RL11 co-purified with envelope glycoprotein B (gB) in the envelope fraction (E). No co-elution of UL119 and RL11 in the tegument/capsid fraction, defined by the presence of tegument protein pp65, was observed (Tc lane). The UL119 presence on purified virus was already reported in literature by Varnum and co-authors [25]. Through a mass spectrometry analysis of purified virions they were able to detect peptides derived from proteolytic digestion of UL119. However the approach could not provide any information regarding the localization of the protein. Our analysis revealed and defined the presence of both Fc $\gamma$  binding proteins as envelope associated proteins. Recently, our group identified two novel Fc $\gamma$  binding proteins, RL12 and RL13 [21]. The latter has been reported as envelope associated protein by Stanton and co-workers [24]. The fact that almost all the HCMV Fc $\gamma$  binding proteins identified so far are exposed on the envelope can imply an important role for these functions. For example, the antibody bipolar bridging mechanism, described for HSV Fc $\gamma$  binding proteins gE-gI [45], can be activated on the HCMV surface by exposed proteins with Fc $\gamma$  binding ability, allowing the virus to escape immune system recognition.

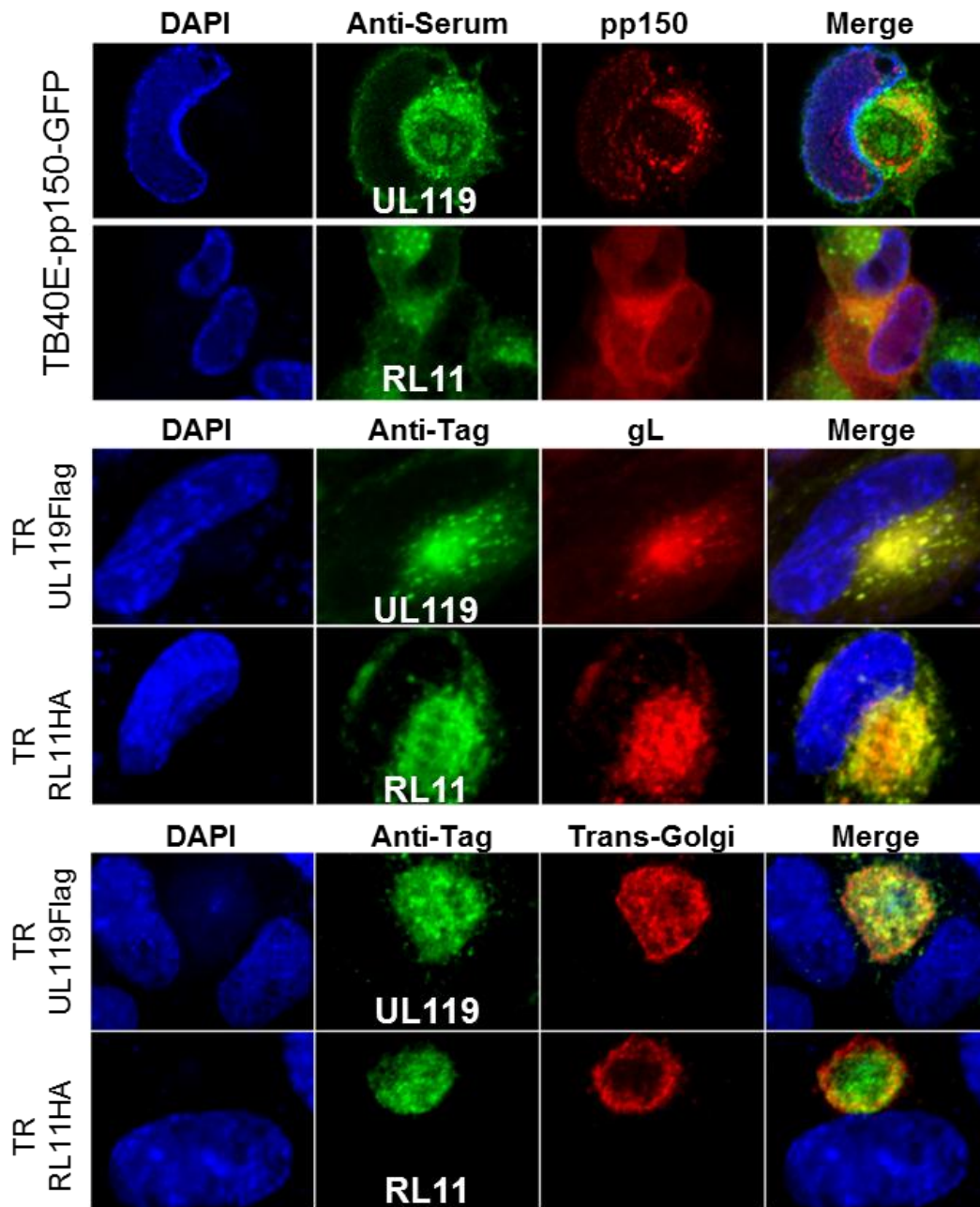


**Fig. 6: UL119 and RL11 localized within the viral assembly complex in HCMV infected cells.** HFF cells were infected with TB40E-pp150-EGFP (upper panels), TR-UL119Flag and TR-RL11HA (middle and bottom panels, top and bottom rows, respectively). 5 d.p.i. cells were fixed, permeabilized and stained. UL119 and RL11 (green color) were detected either with mouse anti-sera or with anti-tag antibodies. Tegument protein pp150, envelope glycoprotein gL and trans-Golgi network protein TGN46 were either expressed in fusion with GFP or stained with antibodies (red color). Z-stacks were collected with a confocal microscope. Representative Z-stack projections of each sample are shown.

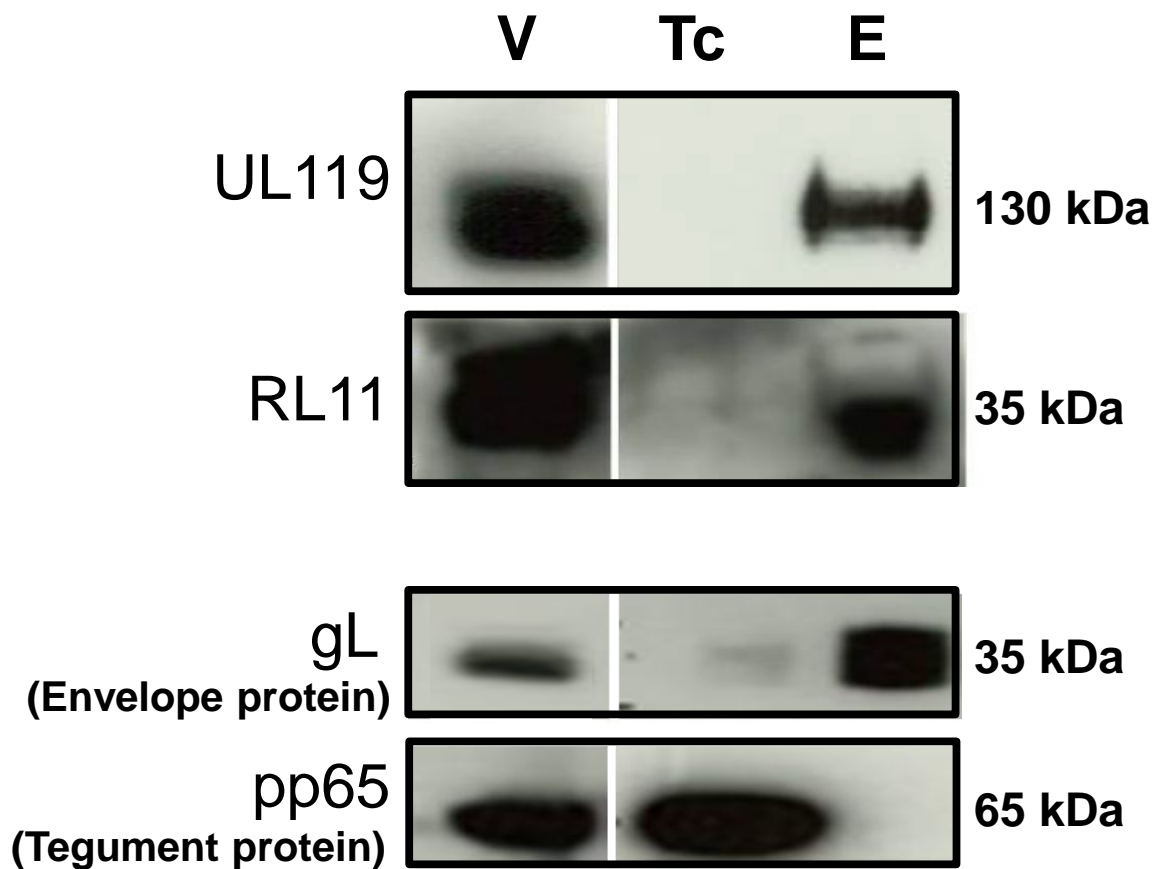


**Fig. 7: UL119 and RL11 are CMV envelope glycoproteins.** Analysis of UL119 and RL11 in TB40E-pp150-GFP virions purified from 5 days infected HFF cells. Complete virions (V), tegument/capsid fraction (Tc) and envelope fraction (E) were probed for the antigens indicated.

### **Internalized human IgGs do not undergo lysosomal degradation in infected cells**

Uptake of both human IgG and Fc $\gamma$  fragment in infected cells was first reported in 1976 by Keller and co-authors [46]. However the fate of human IgG upon internalization has not been defined yet. We decided to investigate the route of Fc $\gamma$  internalization and the role of viral Fc $\gamma$  binding proteins in the context of productive infection. For these studies, wild type TR and a mutated TR strain encoding for YFP version of UL119 were used. HFF infected for 5 days with CMV TR strains were incubated with labeled Fc $\gamma$  fragments for 60 min on ice. Cells were then washed and temperature was raised to 37°C to allow for internalization. At different times after temperature switching, cells were fixed and stained for markers of the endocytic machinery. A strong colocalization between Fc $\gamma$  fragment and the vFc $\gamma$  binding proteins (Fig. 8, green and magenta colors, respectively) was found throughout all time points. At 30 min, Fc $\gamma$  was present in early endosomes and was retained within early endosomes up to the latest time of observation (Fig. 8, first and second rows, fourth and sixth panels). Moreover, Fc $\gamma$  positive vesicles did not fuse with lysosomes as suggested by lack of co-localization with lysosomal marker Lamp1 after 120 min from the internalization start (Fig. 8, third row, red color in fourth and sixth panels).

While no direct evidences are yet available, the lack of co-localization with lysosomal markers, the retention in EEA1 positive vesicles and the accumulation in the viral assembly complex site allow us to speculate for a possible insertion of human Fc $\gamma$  fragment in the budding virions. Indeed the insertion of human immunoglobulins in the HCMV virion upon budding from infected cells has been reported [47]. Manley and co-authors [47] demonstrated that HCMV virus produced in presence of sub-neutralizing doses of anti gH human monoclonal antibody MSL-109 gain antibody resistance through IgG internalization and virion cloaking. Nevertheless in the same paper, two observations argue against our

model. First the phenomenon seems to be specific for the MSL-109, because no insertion of IgGs in the virion was observed when the human anti-gB neutralizing antibody ITC88 was tested. Second, resistant virus genetically abrogates the UL119 and the RL13 functions. Thus, the fate of internalized human IgG by infected cells still need to be fully addressed. This understanding could be crucial in order to gain better insight into potential mechanism used by the virus to escape immune system response and allow a better design of antiviral therapies.

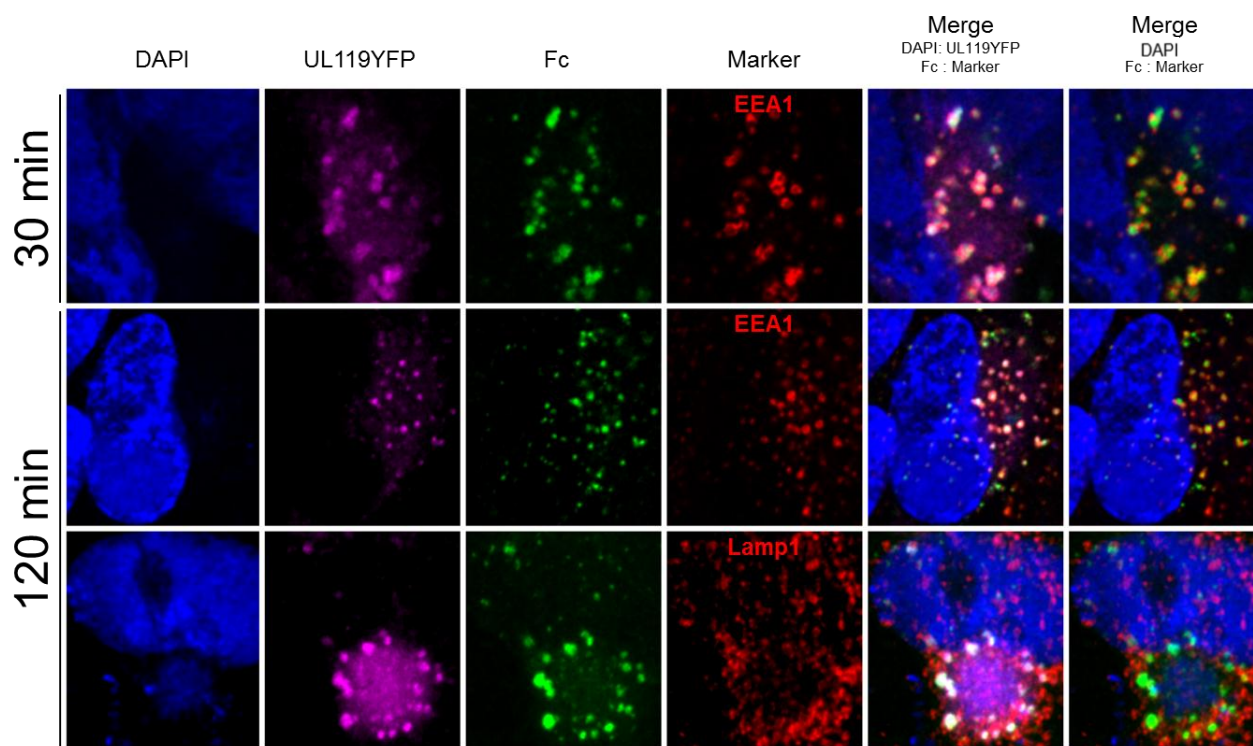


**Fig. 8: Endocytosed human Fc fragment is retained in the early endosomes.** HFF were infected with TR-UL119YFP. 5 d.p.i. cells were incubated with 647 Dylight conjugated human IgG Fc fragment on ice for 60 min before being washed and shifted to 37°C to allow for internalization. At the indicated time points, cells were fixed and stained with antibodies against early endosomes and/or lysosomes (red color, EEA1 and Lamp1, respectively). Images were collected through confocal microscopy. Z-stack projections of representative pictures are shown. Superimposition of signals from human Fc (Fc, green color), cellular markers and with or without UL119YFP (magenta color), are shown in the merge panels (fifth and sixth columns, respectively).

## MATERIALS AND METHODS

### *Cells, plasmids and antibodies*

ARPE-19, MRC-5, HFF and HEK293T cell lines were purchased from ATCC (catalogue numbers CRL-2302, CCL-171, CRL-2429 and CRL-11268, respectively) and cultured according to the supplier's instructions. DMEM high glucose and DMEM:F12 media (Gibco, Invitrogen) were supplemented with 10% fetal calf serum (FCS) and penicillin streptomycin glutamine (Gibco, Invitrogen). Lipofectamine 2000 (Invitrogen) was used to transfect HEK293T cells, while Fugene 6 (Roche) and Nucleofector kit V (Amaxa) were used to transfect ARPE-19 cells as suggested by manufacturer. Human codon-optimized UL119 and RL11 genes, from HCMV TR strain, were synthesized by Geneart and cloned in plasmid pcDNA3.1(-)/myc-His C (Invitrogen) in frame with C-terminal myc and six histidine tag sequences. Fluorescent fusion proteins were obtained by subcloning the genes of interest upstream of the EYFP sequence in pEYFP-N1 vector (Clontech). Primary antibodies used in this work were: anti-His\_C-term (Invitrogen), anti-PDI (Invitrogen), anti-HA (Invitrogen), anti-Rab5 (Santa Cruz), anti-Rab11 (Santa Cruz), anti-Rab7 (Santa Cruz), anti-lamp1 (Santa Cruz), anti-GM130 (Abcam), anti-TGN46 (AbD Serotec), anti-EEA1 (Abcam). All primary antibodies were produced in mouse. Mouse anti-sera recognizing UL119 and RL11 were developed in house. Briefly, His-tagged peptides encompassing the amino acid regions 107-254 of UL119 and 111-180 of RL11 from TR strain were produced in *E. coli* and purified through metal ion affinity chromatography. Purified peptides were used to immunize mice. Secondary antibodies used in this study were: Alexa Fluor F(ab)<sub>2</sub> fragment of 488-, 568-, and 647-conjugated goat anti-mouse (Invitrogen) and HRP-conjugated secondary antibodies from Perkin Elmer. Chrompure DyLight 649-, 549-conjugated human Fc fragments were purchased from Jackson ImmunoResearch.

### ***Glycosidase and tunicamycin treatments***

For deglycosylation treatments, 20 µg of protein extract was incubated either with 2.5 µl of Endoglycosidase H (Endo Hf, NEB) or 2.5 µl peptide-N-glycosidase F (PNGaseF, NEB) or buffer only for 3 h at 37°C according to the manufacturer's protocol. Samples were analyzed by Western immunoblotting.

For tunicamycin treatments, HEK293T cells were incubated for 24 h with 2 µg/ml of tunicamycin A (Sigma) and then subjected to lysis with RIPA lysis buffer (SIGMA) supplemented with protease inhibitors (Roche).

### ***Flow cytometry***

To define the proteins plasma membrane localization, HEK293T cells transiently expressing UL119, RL11 and empty vector were harvested with trypsin 48 h post transfection and subjected to staining with mouse anti-serum. Briefly, cells were incubated 30 min at RT with Live&Dead Aqua (Invitrogen) diluted 1:400 in PBS, washed twice and incubated with for 30 min with blocking buffer (PBS with 5% FBS). Mouse anti-sera, diluted 1:100 in blocking buffer, were added for 60 min on ice. Cells were washed 3 times in PBS and then incubated with Alexa Fluor F(ab)<sub>2</sub> fluorophore conjugate secondary antibodies for 30 min on ice. Cells were washed thrice in PBS before being analyzed. When intracellular staining was required, cells were permeabilized with Cytotfix/Cytoperm kit (BD) and perm/wash buffer was used in all subsequently steps. For cells expressing the myc tagged proteins, anti-myc-FITC antibody (Invitrogen) was used at 1:500 dilution. Binding of the Fc portion of the

human IgGs (Fc $\gamma$ ) was assessed using DyLight 649 conjugated human IgG Fc fragment (Jackson ImmunoResearch) at different dilutions (50  $\mu$ g/ml, 10  $\mu$ g/ml and 5  $\mu$ g/ml).

A total of  $10^4$  cells were analyzed for each histogram using a FACSCanto II (Becton Dickinson).

### ***Confocal microscopy analysis***

Cells expressing the proteins of interest were grown on glass coverslips or glass chamberslides. For intracellular staining, cells were fixed 48 h post transfection with 3.7% paraformaldehyde and permeabilized with 0.1 % Triton X-100 (Sigma). For membrane staining, the permeabilization step was omitted and fixation was performed after staining with primary and secondary antibodies for 60 min on ice. In both cases, cells were incubated in blocking buffer (PBS + 5% FBS) for 30 min before antibody staining. Antibodies were always diluted in blocking buffer.

For human Fc $\gamma$  internalization, cells transiently expressing YFP- tagged UL119, RL11 or YFP only (control) were plated on glass coverslips 24 h post transfection. 24 h later, cells were washed in cold PBS and incubated at 4°C with 20  $\mu$ g/ml of DyLight 649-conjugated human Fc $\gamma$  for 60 min. After extensive washes, temperature was switched to 37°C to allow for internalization. When required, cells were fixed, permeabilized and stained before mounting.

For intracellular localization and internalization analyses in infected cells, HFF were seeded on glass coverslips and infected for 5 days with HCMV. Staining and internalization protocols were then performed as described above. When applicable, 5% non-immune human serum was added to blocking buffer in order to reduce non-specific signal.

The intracellular locations of antibody-tagged or fluorescent fusion proteins were examined under laser illumination in a Zeiss LMS 710 confocal microscope and images were captured using ZEN software (Carl Zeiss). Live microscopy experiments were performed with a Zeiss Axio Observer widefield fluorescence microscope.

### ***HCMV virions purification and virion proteins fractionation***

Mature HCMV virions were separated from dense bodies (DB) and noninfectious enveloped particles (NIEPs) through a positive density/negative viscosity step-gradient centrifugation as described previously (Talbot et al). Briefly, medium from infected cells was collected when 100% cytopathic effect was observed and subjected to 3500 rpm centrifugation for 20 min at 16°C. Supernatant was transferred to polycarbonate tubes underlied with 20% sucrose and centrifuged for 60 min at 23000 rpm in a Beckman SW32Ti rotor. Pelleted virus was resuspended in 1 ml PBS and 2 ml of 4 different solutions containing decreasing concentration of sucrose and increasing concentration of glycerol tartarate were layered underneath. Tubes were centrifuged at 42000 rpm for 60 min at 10°C in a Beckman SW28Ti rotor. Band containing mature virions was collected through a syringe, resuspended in PBS, centrifuged for 60 min at 23000 rpm in a Beckman SW32Ti rotor and the pellet containing virus was resuspended in PBS. Quality of the purification was assessed through negative staining electron microscopy (EM) analysis. To separate envelope from capsid and tegument proteins, purified virions were mixed 1:1 with envelope extraction buffer (1% NP-40 and 4% Sodium Deoxycholate) and incubated on ice for 30 min with occasional vortexing. Soluble fraction was collected through max speed centrifugation in a benchtop centrifuge for 30 min at 4°C. The insoluble pellet was washed twice in PBS before being solubilized in SDS-PAGE sample buffer. For each extraction, a total of 4

confluent T175 cm<sup>2</sup> flasks of HFF cells were infected. Virus was purified as described above and 10% was mixed with SDS-PAGE loading buffer while the rest was subjected to proteins extraction.

### ***Construction and generation of TR-RL11HA, TR-UL119Flag, TR-RL11HA/UL119Flag and TR-UL119YFP***

Markerless two-step RED-GAM BAC mutagenesis was used to generate recombinant viruses harboring tagged version of RL11 and UL119 genes in their genome [48]. Briefly, kanamycin resistance cassette, flanked by I-SceI restriction enzyme cleavage site, was PCR amplified from pEP-KanS shuttle vector. The primers used contained homologous regions to allow the integration of the amplicon in the region of interest of the BAC DNA through lambda Red recombinases induction. Combination of I-SceI cleavage with a second Red recombination event removed the resistance gene leaving only the new sequences of interest. The primers used to generate the mutated HCMV strains were (Table 1, supplemental material): for TR-RL11HA, RL11HAFw and RL11HARv on pEP-KanS plasmid as template; for TR-UL119Flag, UL119FlagFw and UL119FlagRv on pEP-KanS plasmid as template; for TR-UL119YFP, UL119YFPFw and UL119YFPRv on pEYFP-KanS plasmid as template. Recombination events were performed with *E. coli* GS1783 strain containing a BAC clone of the HCMV TR strain. The *E. coli* strain contains also the lambda Red system and the I-SceI genes under the control of heat shock- inducible and arabinose-inducible promoters, respectively. The desired mutations were confirmed by sequencing and integrity of the whole recombinant HCMV genomes was checked through restriction analysis.

To construct the pEYFP-KanS shuttle vector, a BclI restriction enzyme site was inserted in the pEYFP-N1 plasmid by Quickchange site directed mutagenesis (Stratagene) as suggested by the

manufacturer with primers YFPmutBclIFw and Rv (Table 1, supplemental material). Methylation of the restriction site was abrogated inserting the mutated pEYFP-N1 plasmid in the Inv110 *E. coli* strain. Unmethylated plasmid DNA was collected and linearized with BclI. A kanamycin gene with an adjoining I-SceI site and a region homologue to the YFP gene was amplified from the pEP-KanS plasmid with primers YFPKanS Fw and Rv (Table 1). pEYFP-KanS shuttle vector was obtained inserting the antibiotic cassette in the linearized plasmid.

To reconstitute the virus, MRC-5 cells from a confluent T175 cm<sup>2</sup> were trypsin detached, mixed with 10 µl fresh prepared BAC DNA (around 3 µg) and 1 µg of pCMVKm2-pp71 plasmid and electroporated in 4 mm cuvette at 250 V and 950 µF. Supernatant containing virus was collected from infected cells when cytopathic effects were >90%. For all following infection experiments, human foreskin fibroblast (HFF) cells were used.

**Table 1:** Oligonucleotides used in this study.

<b>Name</b>	<b>Sequence</b>
RL11HA Fw	GGATACGGAACCTTTGTTGTTGACGGTGGACGGAGATTTGGAATACCCTTACGACGTGCCTGACTACGCCAGGATGACGACGATAAGTAGGG
RL11HA Rv	TGTCGGTACGTAAGGTTGTTGCGTCTTTGACGGTTGACGCGCATCTTTTAGGGCTAGTCAGGCACGTCGTAAGGGTATTCCAAATCTCCGTCCA CCGTCACAACCAATTAACCAATTCTGATTAG
YFPkanS Fw	ATATGATCACATGGTCCTGCTGGAGTTCGTGACCGCCGCCGGGATCACTCTCGGCATGGGATAAGTAGGGATAACAGGGT
YFPkanS Rv	ATATGATCACAACCAATTAACCAATTCTGATTAG
UL119YFP Fw	AGGAGCCCCTTGAGGAAAAGAAACACCCGGTGCCCTACTTCAAGCAGTGGCGGGATCCACCGGTCGCCACC
UL119YFP Rv	AAGTCAGCGAAATAAAGACAACACAGCAGCCACTCCTCTCGTCTCGGGCCTTACTTGTACAGCTCGTCCATG
YFPmutBclI Fw	CAACGAGAAGCGTGATCACATGGTC
YFPmutBclI Rv	GACCATGTGATCACGCTTCTCGTTG

## REFERENCES

1. Mocarski E.S., Shenk T, Pass RF (2007) Cytomegaloviruses. In: Knipe D.M. HPMed, editors. Fields virology. Lippincott Williams & Wilkins. pp. 2701-2772.
2. Hahn G, Jores R, Mocarski ES (1998) Cytomegalovirus remains latent in a common precursor of dendritic and myeloid cells. *Proc Natl Acad Sci U S A* 95: 3937-3942.
3. Britt W (2008) Manifestations of human cytomegalovirus infection: proposed mechanisms of acute and chronic disease. *Current topics in microbiology and immunology* 325: 417-470.
4. Engel P, Angulo A (2012) Viral immunomodulatory proteins: usurping host genes as a survival strategy. *Adv Exp Med Biol* 738: 256-276. 10.1007/978-1-4614-1680-7\_15 [doi].
5. Nimmerjahn F, Ravetch JV (2008) Fcγ receptors as regulators of immune responses. *Nat Rev Immunol* 8: 34-47. nri2206 [pii];10.1038/nri2206 [doi].
6. Hook LM, Friedman HM (2007) Subversion of innate and adaptive immunity: immune evasion from antibody and complement. NBK47404 [bookaccession].
7. Tortorella D, Gewurz BE, Furman MH, Schust DJ, Ploegh HL (2000) Viral subversion of the immune system. *Annu Rev Immunol* 18: 861-926. 18/1/861 [pii];10.1146/annurev.immunol.18.1.861 [doi].
8. Nimmerjahn F, Ravetch JV (2008) Analyzing antibody-Fc-receptor interactions. *Methods Mol Biol* 415: 151-162. 10.1007/978-1-59745-570-1\_9 [doi].
9. Sawyer LA (2000) Antibodies for the prevention and treatment of viral diseases. *Antiviral Res* 47: 57-77. S0166-3542(00)00111-X [pii].
10. Snyderman DR, Falagas ME, Avery R, Perlino C, Ruthazer R, Freeman R, Rohrer R, Fairchild R, O'Rourke E, Hibberd P, Werner BG (2001) Use of combination cytomegalovirus immune globulin plus ganciclovir for prophylaxis in CMV-seronegative liver transplant recipients of a CMV-seropositive donor organ: a multicenter, open-label study. *Transplant Proc* 33: 2571-2575. S0041134501021017 [pii].
11. Lubinski JM, Lazear HM, Awasthi S, Wang F, Friedman HM (2011) The herpes simplex virus 1 IgG Fc receptor blocks antibody-mediated complement activation and antibody-dependent cellular cytotoxicity in vivo. *J Virol* 85: 3239-3249. JVI.02509-10 [pii];10.1128/JVI.02509-10 [doi].
12. Sprague ER, Wang C, Baker D, Bjorkman PJ (2006) Crystal structure of the HSV-1 Fc receptor bound to Fc reveals a mechanism for antibody bipolar bridging. *PLoS Biol* 4: e148. 06-PLBI-RA-0034R1 [pii];10.1371/journal.pbio.0040148 [doi].
13. Frank I, Friedman HM (1989) A novel function of the herpes simplex virus type 1 Fc receptor: participation in bipolar bridging of antiviral immunoglobulin G. *J Virol* 63: 4479-4488.
14. Van Vliet KE, De Graaf-Miltenburg LA, Verhoef J, Van Strijp JA (1992) Direct evidence for antibody bipolar bridging on herpes simplex virus-infected cells. *Immunology* 77: 109-115.

15. Sprague ER, Martin WL, Bjorkman PJ (2004) pH dependence and stoichiometry of binding to the Fc region of IgG by the herpes simplex virus Fc receptor gE-gI. *J Biol Chem* 279: 14184-14193. 10.1074/jbc.M313281200 [doi];M313281200 [pii].
16. Zerboni L, Berarducci B, Rajamani J, Jones CD, Zehnder JL, Arvin A (2011) Varicella-zoster virus glycoprotein E is a critical determinant of virulence in the SCID mouse-human model of neuropathogenesis. *J Virol* 85: 98-111. JVI.01902-10 [pii];10.1128/JVI.01902-10 [doi].
17. Polcicova K, Goldsmith K, Rainish BL, Wisner TW, Johnson DC (2005) The extracellular domain of herpes simplex virus gE is indispensable for efficient cell-to-cell spread: evidence for gE/gI receptors. *J Virol* 79: 11990-12001. 79/18/11990 [pii];10.1128/JVI.79.18.11990-12001.2005 [doi].
18. Moffat J, Mo C, Cheng JJ, Sommer M, Zerboni L, Stamatis S, Arvin AM (2004) Functions of the C-terminal domain of varicella-zoster virus glycoprotein E in viral replication in vitro and skin and T-cell tropism in vivo. *J Virol* 78: 12406-12415. 78/22/12406 [pii];10.1128/JVI.78.22.12406-12415.2004 [doi].
19. Wang F, Tang W, McGraw HM, Bennett J, Enquist LW, Friedman HM (2005) Herpes simplex virus type 1 glycoprotein e is required for axonal localization of capsid, tegument, and membrane glycoproteins. *J Virol* 79: 13362-13372. 79/21/13362 [pii];10.1128/JVI.79.21.13362-13372.2005 [doi].
20. Arapovic J, Lenac RT, Reddy AB, Krmpotic A, Jonjic S (2009) Promiscuity of MCMV immunoevasin of NKG2D: m138/fcr-1 down-modulates RAE-1epsilon in addition to MULT-1 and H60. *Mol Immunol* 47: 114-122. S0161-5890(09)00074-1 [pii];10.1016/j.molimm.2009.02.010 [doi].
21. Cortese M, Calo S, D'Aurizio R, Lilja A, Pacchiani N, Merola M (2012) Recombinant Human Cytomegalovirus (HCMV) RL13 Binds Human Immunoglobulin G Fc. *PLoS One* 7: e50166. 10.1371/journal.pone.0050166 [doi];PONE-D-12-25729 [pii].
22. Atalay R, Zimmermann A, Wagner M, Borst E, Benz C, Messerle M, Hengel H (2002) Identification and expression of human cytomegalovirus transcription units coding for two distinct Fc gamma receptor homologs. *J Virol* 76: 8596-8608.
23. Lilley BN, Ploegh HL, Tirabassi RS (2001) Human cytomegalovirus open reading frame TRL11/IRL11 encodes an immunoglobulin G Fc-binding protein. *J Virol* 75: 11218-11221. 10.1128/JVI.75.22.11218-11221.2001 [doi].
24. Stanton RJ, Baluchova K, Dargan DJ, Cunningham C, Sheehy O, Seirafian S, McSharry BP, Neale ML, Davies JA, Tomasec P, Davison AJ, Wilkinson GW (2010) Reconstruction of the complete human cytomegalovirus genome in a BAC reveals RL13 to be a potent inhibitor of replication. *J Clin Invest* 120: 3191-3208. 42955 [pii];10.1172/JCI42955 [doi].
25. Varnum SM, Strelbow DN, Monroe ME, Smith P, Auberry KJ, Pasa-Tolic L, Wang D, Camp DG, Rodland K, Wiley S, Britt W, Shenk T, Smith RD, Nelson JA (2004) Identification of proteins in human cytomegalovirus (HCMV) particles: the HCMV proteome. *J Virol* 78: 10960-10966. 10.1128/JVI.78.20.10960-10966.2004 [doi];78/20/10960 [pii].
26. Olson JK, Bishop GA, Grose C (1997) Varicella-zoster virus Fc receptor gE glycoprotein: serine/threonine and tyrosine phosphorylation of monomeric and dimeric forms. *J Virol* 71: 110-119.
27. Olson JK, Grose C (1998) Complex formation facilitates endocytosis of the varicella-zoster virus gE:gI Fc receptor. *J Virol* 72: 1542-1551.

28. Wang ZH, Gershon MD, Lungu O, Zhu Z, Gershon AA (2000) Trafficking of varicella-zoster virus glycoprotein gI: T(338)-dependent retention in the trans-Golgi network, secretion, and mannose 6-phosphate-inhibitable uptake of the ectodomain. *J Virol* 74: 6600-6613.
29. Wang ZH, Gershon MD, Lungu O, Zhu Z, Mallory S, Arvin AM, Gershon AA (2001) Essential role played by the C-terminal domain of glycoprotein I in envelopment of varicella-zoster virus in the trans-Golgi network: interactions of glycoproteins with tegument. *J Virol* 75: 323-340. 10.1128/JVI.75.1.323-340.2001 [doi].
30. Tirabassi RS, Enquist LW (1998) Role of envelope protein gE endocytosis in the pseudorabies virus life cycle. *J Virol* 72: 4571-4579.
31. Alconada A, Bauer U, Sodeik B, Hoflack B (1999) Intracellular traffic of herpes simplex virus glycoprotein gE: characterization of the sorting signals required for its trans-Golgi network localization. *J Virol* 73: 377-387.
32. Olson JK, Grose C (1997) Endocytosis and recycling of varicella-zoster virus Fc receptor glycoprotein gE: internalization mediated by a YXXL motif in the cytoplasmic tail. *J Virol* 71: 4042-4054.
33. Wisner T, Brunetti C, Dingwell K, Johnson DC (2000) The extracellular domain of herpes simplex virus gE is sufficient for accumulation at cell junctions but not for cell-to-cell spread. *J Virol* 74: 2278-2287.
34. Farnsworth A, Johnson DC (2006) Herpes simplex virus gE/gI must accumulate in the trans-Golgi network at early times and then redistribute to cell junctions to promote cell-cell spread. *J Virol* 80: 3167-3179. 80/7/3167 [pii];10.1128/JVI.80.7.3167-3179.2006 [doi].
35. Mukherjee S, Ghosh RN, Maxfield FR (1997) Endocytosis. *Physiol Rev* 77: 759-803.
36. Tse SM, Furuya W, Gold E, Schreiber AD, Sandvig K, Inman RD, Grinstein S (2003) Differential role of actin, clathrin, and dynamin in Fc gamma receptor-mediated endocytosis and phagocytosis. *J Biol Chem* 278: 3331-3338. 10.1074/jbc.M207966200 [doi];M207966200 [pii].
37. McMahon HT, Boucrot E (2011) Molecular mechanism and physiological functions of clathrin-mediated endocytosis. *Nat Rev Mol Cell Biol* 12: 517-533. nrm3151 [pii];10.1038/nrm3151 [doi].
38. Ford MG, Pearse BM, Higgins MK, Vallis Y, Owen DJ, Gibson A, Hopkins CR, Evans PR, McMahon HT (2001) Simultaneous binding of PtdIns(4,5)P2 and clathrin by AP180 in the nucleation of clathrin lattices on membranes. *Science* 291: 1051-1055. 10.1126/science.291.5506.1051 [doi];291/5506/1051 [pii].
39. Das S, Vasanji A, Pellett PE (2007) Three-dimensional structure of the human cytomegalovirus cytoplasmic virion assembly complex includes a reoriented secretory apparatus. *J Virol* 81: 11861-11869. JVI.01077-07 [pii];10.1128/JVI.01077-07 [doi].
40. Murphy E, Shenk T (2008) Human cytomegalovirus genome. *Current topics in microbiology and immunology* 325: 1-19.
41. Murphy E, Rigoutsos I, Shibuya T, Shenk TE (2003) Reevaluation of human cytomegalovirus coding potential. *Proc Natl Acad Sci U S A* 100: 13585-13590. 10.1073/pnas.1735466100 [doi];1735466100 [pii].

42. Sampaio KL, Cavignac Y, Stierhof YD, Sinzger C (2005) Human cytomegalovirus labeled with green fluorescent protein for live analysis of intracellular particle movements. *J Virol* 79: 2754-2767. 79/5/2754 [pii];10.1128/JVI.79.5.2754-2767.2005 [doi].
43. Sanchez V, Greis KD, Sztul E, Britt WJ (2000) Accumulation of virion tegument and envelope proteins in a stable cytoplasmic compartment during human cytomegalovirus replication: characterization of a potential site of virus assembly. *J Virol* 74: 975-986.
44. Das S, Vasanji A, Pellett PE (2007) Three-dimensional structure of the human cytomegalovirus cytoplasmic virion assembly complex includes a reoriented secretory apparatus. *J Virol* 81: 11861-11869. JVI.01077-07 [pii];10.1128/JVI.01077-07 [doi].
45. Favoreel HW, Van MG, Van de Walle GR, Ficinska J, Nauwynck HJ (2006) Herpesvirus interference with virus-specific antibodies: bridging antibodies, internalizing antibodies, and hiding from antibodies. *Vet Microbiol* 113: 257-263. S0378-1135(05)00374-3 [pii];10.1016/j.vetmic.2005.11.003 [doi].
46. Keller R, Peitchel R, Goldman JN, Goldman M (1976) An IgG-Fc receptor induced in cytomegalovirus-infected human fibroblasts. *J Immunol* 116: 772-777.
47. Manley K, Anderson J, Yang F, Szustakowski J, Oakeley EJ, Compton T, Feire AL (2011) Human cytomegalovirus escapes a naturally occurring neutralizing antibody by incorporating it into assembling virions. *Cell Host Microbe* 10: 197-209. S1931-3128(11)00253-8 [pii];10.1016/j.chom.2011.07.010 [doi].
48. Tischer BK, von EJ, Kaufer B, Osterrieder N (2006) Two-step red-mediated recombination for versatile high-efficiency markerless DNA manipulation in *Escherichia coli*. *Biotechniques* 40: 191-197. 000112096 [pii].





## **Recombinant Human Cytomegalovirus (HCMV) RL13 binds human immunoglobulin G Fc**

**Mirko Cortese<sup>1</sup>, Stefano Calò<sup>1</sup>, Romina D'Aurizio<sup>1</sup>, Anders Lilja<sup>2</sup>, Nicola Pacchiani<sup>1</sup> and Marcello Merola<sup>1,3,\*</sup>.**

<sup>1</sup>) Novartis Vaccines and Diagnostics, Via Fiorentina 1, 53100 Siena, Italy

<sup>2</sup>) Novartis Vaccines and Diagnostics, 45 Sidney Street, Cambridge, MA 02139, USA.

<sup>3</sup>) Department of Structural and Functional Biology, University of Naples “Federico II”, Via Cinthia 21, 80126 Naples, Italy

Keywords: viral Fc binding proteins, RL13, HCMV, RL12

\* Corresponding author. Mailing address: Marcello Merola, Ph.D. [marcello.merola@novartis.com](mailto:marcello.merola@novartis.com) [m.merola@unina.it](mailto:m.merola@unina.it)

**ABSTRACT**

The human cytomegalovirus (HCMV) protein RL13 has recently been described to be present in all primary isolates but rapidly mutated in culture adapted viruses. Although these data suggest a crucial role for this gene product in HCMV primary infection, no function has so far been assigned to this protein. Working with RL13 expressed in isolation in transfected human epithelial cells, we demonstrated that recombinant RL13 from the clinical HCMV isolates TR and Merlin have selective human immunoglobulin (Ig)-binding properties towards IgG1 and IgG2 subtypes. An additional Fc binding protein, RL12, was also identified as an IgG1 and IgG2 binding protein but not further characterized. The glycoprotein RL13 trafficked to the plasma membrane where it bound and internalized exogenous IgG or its constant fragment (Fc $\gamma$ ). Analysis of RL13 ectodomain mutants suggested that the RL13 Ig-like domain is responsible for the Fc binding activity. Ligand-dependent internalization relied on a YxxL endocytic motif located in the C-terminal tail of RL13. Additionally, we showed that the tyrosine residue could be replaced by phenylalanine but not by alanine, indicating that the internalization signal was independent from phosphorylation events. In sum, RL13 binds human IgG and may contribute to HCMV immune evasion in the infected host, but this function does not readily explain the instability of the RL13 gene during viral propagation in cultured cells.

## INTRODUCTION

Human cytomegalovirus (HCMV) infection is common and, although typically subclinical in the healthy population, it can cause severe disease in congenitally infected infants and in individuals with suppressed immunity [1]. In immunocompetent individuals, infection is controlled by both cellular and humoral immune responses, defenses that are weakened in immunocompromised patients leading to infection of several tissues and a vast range of cell types [2].

Characterization and use of clinical and low passage isolates of cultured HCMV strains have led to a reconsideration of the viral coding potential and suggested the presence of new unidentified functions (reviewed in [3]). Comparative sequencing analysis of unpassaged clinical isolates versus cell culture adapted viruses allowed a more refined identification of the genetic changes corresponding to functions that are lost in *in vitro* cultures. This is the case of RL13 and UL128 gene products, both possessing a suppressive phenotype on tissue culture adapted viruses [4,5]. For RL13 in particular, Stanton *et al.* recently reported rapidly emerging genetic mutations following a few passages of BAC-derived Merlin strain virus in cultures of human cells of different origins [6]. These authors, using an elegant BAC system of conditional gene repression during virus propagation, were able to show that virus with reconstructed wild type RL13 repressed cell culture growth while the emerging deletion mutants allowed the virus to adapt to cell culture growth [6]. Providing that a functional RL13 gene appears to be carried by all sequenced clinical isolates, the authors hypothesized that this protein is critical for productive HCMV replication *in vivo*, perhaps increasing the repertoire of HCMV cell tropism [6].

HCMV has evolved a number of different ways to evade the immune system, often employing seemingly redundant factors and mechanisms to maintain the lifelong infection of the host [7]. Limitation of the host antibodies and complement activities through the expression of viral proteins

able to bind the constant region of immunoglobulin G (Fc $\gamma$ ) is a mechanism common to several herpesviruses [8,9]. These viral proteins interfere with the host receptors for the Fc portion (Fc $\gamma$ Rs) of immunoglobulin G (IgG), expressed on the surface of all cell types in the innate and adaptive parts of the immune system [10].

Fc $\gamma$ Rs are a complex family of proteins with several distinct classes and subclasses that function at the interface of the adaptive and innate immune systems [10]. They sense immune complexes in the extracellular environment and regulate signaling cascades in effector cells, which may contribute significantly to balancing pro- and anti-inflammatory responses to infection. HCMV expresses two proteins of 34 and 68 kDa that bind the Fc region of IgGs [11–13]. gp34 is encoded in clinical isolates by RL11 and in laboratory isolates by the duplicate genes TRL11 and IRL11 [12,14]. gp68 is translated from the spliced mRNA encoded by UL119 and UL118 [11] and has been detected in preparations of purified virions [15]. Both gp34 and gp68 are glycosylated type I membrane proteins predicted to form immunoglobulin supergene family (IgSF)-like domains [11]. They bind all classes of human IgG with approximately equal affinity, whereas gp34 also binds rabbit IgG and, to a lesser extent, rat IgG1.

In this report we identified two additional Fc $\gamma$  binding activities encoded by the HCMV genome, RL12 and RL13, and characterized this property of recombinant RL13 from the TR and Merlin strains of HCMV. We demonstrated that RL13 transfected into cultured human epithelial and fibroblast cells binds and internalizes the Fc portion of human IgGs.

## RESULTS

### *Fc $\gamma$ binding ability of selected members of the RL11 family*

RL11 was the first identified Fc $\gamma$  binding protein of HCMV [12] and is hypothesized to function through its Ig-like domain [11]. Using RL11 as positive control, we sought to test if RL10, RL12 and RL13 were also able to bind human IgGs. We included gB (UL55) as a negative control. HEK293T cells were transfected with expression plasmids for myc-His tagged gB, RL10, RL11, RL12, RL13. 48 h after transfection, flow cytometry analysis was performed with DyLight 649-conjugated human Fc $\gamma$  and FITC-conjugated anti-myc. Permeabilized (Fig. 1A) and non-permeabilized (Fig. 1B) FITC-positive cells were tested for ability to bind human Fc $\gamma$ . RL11, RL12 and RL13 bind the Fc portion of human IgG while RL10 and gB are comparable to negative control (Fig. 1A and 1B). It appears that a large fraction of the Fc $\gamma$ -binding activity of RL13 (brown trace) is surface exposed, whereas a large fraction of RL11 and RL12 (blue and green trace, respectively) is not (Fig. 1A and 1B). Expression of the different proteins was equal as demonstrated by comparable percentage of FITC positive populations and their mean fluorescence intensity (data not shown). Taken together, these data suggested that RL12 and RL13 are two previously unidentified human Fc $\gamma$  binding proteins encoded by HCMV.

RL11 has been shown to bind all different subclasses of human IgGs [11]. To assess if RL12 and RL13 differentially recognized human IgG subclasses, flow cytometry on permeabilized HEK293T cells expressing RL11, RL12, or RL13 was performed using individual human IgG subclasses as probes. Cells expressing RL11 bind all IgG subclasses whereas cells expressing RL13 appear to specifically bind IgG1 and IgG2 (Fig. 1C).

These data and similar analysis of RL12 binding to human Ig isotypes and binding of RL12 and RL13 to Igs from different species are summarized in Table 1. Although the finding that RL12 binds Fc $\gamma$  was novel, we focused the rest of this report on RL13.

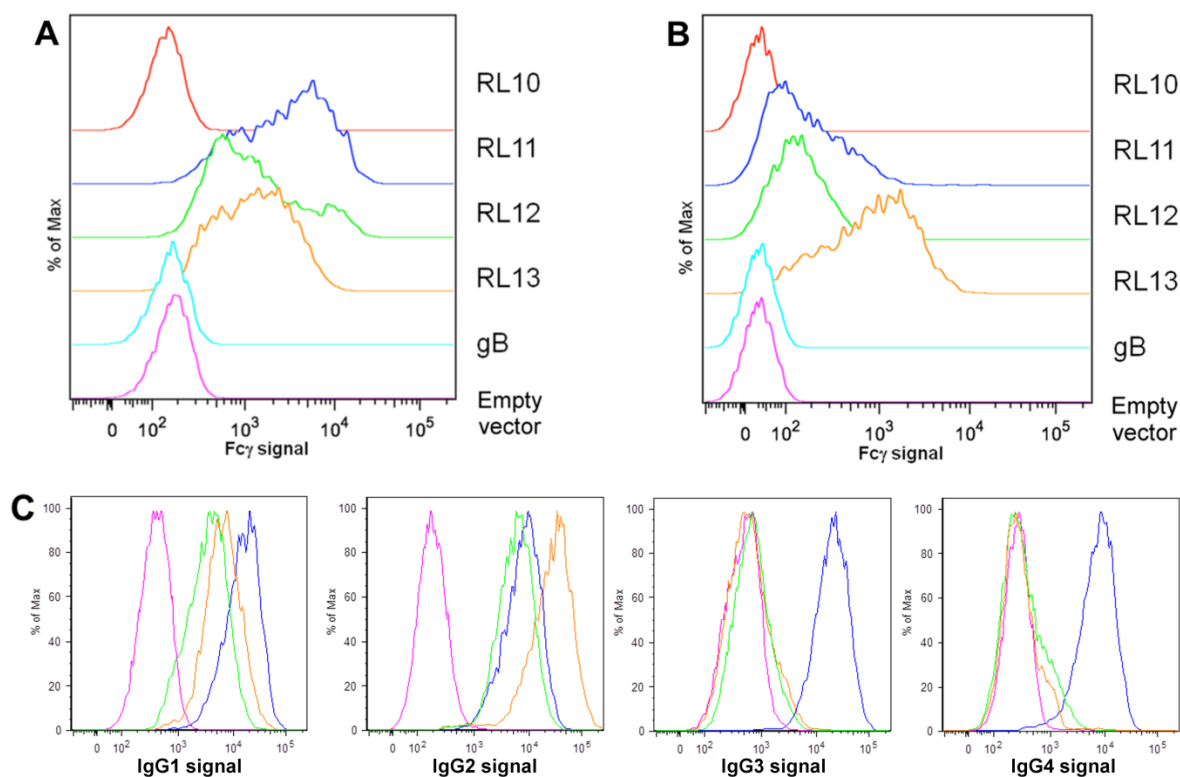


**Figure 1: FACS analysis of Fc $\gamma$  and IgG binding.**

**A:** Binding of Fc $\gamma$  to RL13 in permeabilized cells. HEK293T cells transfected with empty vector or expression vectors for myc-tagged gB, RL10, RL11, RL12 or RL13 were fixed, permeabilized and stained using FITC-conjugated anti-myc and 25  $\mu$ g/ml DyLight 649-conjugated human IgG Fc fragment (Fc $\gamma$ ). FITC positive cells were compared to mock transfected cells for their ability to bind Fc $\gamma$ .

**B:** Binding of Fc $\gamma$  to surface-exposed RL13. HEK293T cells transfected with empty vector or expression vectors for myc-tagged gB, RL10, RL11, RL12 or RL13 were first stained at 4°C with DyLight 649-conjugated human IgG Fc fragment (25  $\mu$ g/ml). Excess of probe was removed by washing in PBS and then cells were fixed and stained with FITC-conjugated anti-myc. FITC positive cells were compared to mock transfected cells for their ability to bind Fc $\gamma$ .

**C:** Binding specificity of RL10-RL13 towards different human immunoglobulin subclasses. HEK293T cells were transiently transfected with myc-tagged RL11 (blue), RL12 (green), RL13 (brown) or with empty vector (magenta). Cells were fixed, permeabilized and stained with FITC-conjugated anti-myc together with 10  $\mu$ g/ml of human Ig of the different subclasses. Alexa fluor 647-conjugated goat anti-human was used as secondary antibody. FITC positive cells were compared to mock transfected cells for their ability to bind Fc $\gamma$ .

Species	Ig subtype	Ig binding by		
		RL11	RL12	RL13
Human	IgG1	++	+	+
Human	IgG2	++	++	+++
Human	IgG3	++	-	-
Human	IgG4	++	-	-
Human	IgM	-	-	-
Human	IgA	-	-	-
Human	IgE	-	-	-
Rabbit	IgG	+	++	++
Mouse	IgG	-	-	-
Rat	IgG	-	-	-
Goat	IgG	-	-	-

**Table 1: Ig-binding specificity of Fc-binding proteins RL11, RL12 and RL13.**

HEK293T cells were transfected with expression plasmids encoding a tagged version of RL11, RL12, and RL13 genes, stained with the indicated immunoglobulins, and analyzed by flow cytometry. +/++/+++ indicates efficiency of Fc-binding observed as mean fluorescent intensity; – indicates no binding.

***Amino acid residues 109 to 218 of TR strain RL13 are necessary for Fc $\gamma$  binding***

The RL13 protein possesses strong topology similarities with the previously characterized HCMV Fc $\gamma$  binding proteins coded by the RL11 and UL119 genes (gp34 and gp68 respectively) [11]. HCMV RL13 is a member of the RL11 multigene family [16] encoding a characteristic domain, known as RL11D or CR1 [17]. RL13 from HCMV strain TR has the typical features of a type I membrane glycoprotein (Fig. 2A): a 20 amino acids (aa) long signal peptide, a transmembrane domain in the 248-268 aa region, and a predicted cytoplasmic tail of 26 aa in accordance with previous studies [6]. Further analysis suggests the likely presence of 11 N-linked glycosylation sites (pos. 21, 32, 37, 41, 90, 108, 120, 167, 201, 208, 215 aa) and 22 O-linked glycosylation sites along the sequence, all restricted to the N-terminal region between residues 40 and 89. gp34 and gp68 contain a DxxxLL dileucine consensus motif for internalization and a potential I/V/L/SxYxxL intracytoplasmic immunoreceptor tyrosine based-like inhibition motif, respectively [11,12]. Similarly, we noted the presence of a tyrosine-based motif (YxxL) for intracellular targeting of transmembrane proteins [18] in the C-terminal cytoplasmic domain of the RL13 sequence (Fig. 2A). A search for conserved patterns in the TR RL13 ectodomain revealed an immunoglobulin (Ig)-like domain (Fig. 2A) identified as SM00409 (IG) in the SMART family classification (106-205 aa, with an HMMSmart E-value of 6.16e-04) [19]. A multiple sequence alignment generated from 15 different HCMV strains reported a very high conservation along the entire domain except 3 short regions predicted to form loops (Fig. 2B). All 15 sequence variants contain an immunoglobulin domain identified as SMART SM00409 or Interpro IPR013783 (E-values ranging from 9.9e-07 to 3.4e-04 and from 4.70E-07 to 6.10E-04, respectively). The secondary structure predictions suggested a propensity of the identified TR RL13 Ig-like domain to form a series of 8 beta-strands (Fig. 2B).

To investigate the involvement of the Ig-like domain in the Fc $\gamma$  binding ability, we produced 4 different mutants of the RL13 ectodomain (Fig. 2C): RL13 $\Delta$ NT, lacking 76 residues (aa 24-99) from the N-terminal region predicted to contain the O-linked glycosylation sites; RL13 $\Delta$ E1, lacking 29 (aa 218-246) residues between the Ig-like domain and the transmembrane region; RL13 $\Delta$ E2 (aa 159-246), with the same deletion as above plus 57 residues of the C-terminus of the Ig-like domain; and RL13 $\Delta$ Ig, lacking the entire Ig-like domain (aa 109-218). The mutant proteins were transiently expressed fused to myc and His tags in HEK293T cells with comparable expression levels as judged by flow cytometry analysis using anti-myc antibody (data not shown).

Fc $\gamma$  binding ability was assayed by flow cytometry of myc-expressing permeabilized cells after staining with different concentrations of DyLight 649-conjugated Fc $\gamma$  (Fig. 3A, only 12.5  $\mu$ g/ml concentration is shown). Quantification of the results is reported as percentage of Fc $\gamma$  stained cells in each sample compared to wild type RL13 (Fig. 3B). Values from RL13 $\Delta$ NT were comparable to the wild type RL13, while a substantial reduction was observed in the RL13 $\Delta$ E1 and RL13 $\Delta$ E2 samples. Deletion of the Ig-like domain carried by the RL13 $\Delta$ Ig (RL13 $\Delta$ E1 and RL13 $\Delta$ E2) mutants completely abolished specific Fc $\gamma$  binding since the number of positive cells was comparable to negative controls, cells expressing RL10 or transfected with empty vector (Fig. 3A-B).

These data indicated that the Fc $\gamma$  binding activity of RL13 maps to amino acids 109-218. Removal of the region located between the Ig-like domain and the transmembrane domain severely impaired Fc $\gamma$  binding but did not completely abrogate it. This observation suggests that this region could be important for the stability of the binding and/or the correct protein fold.

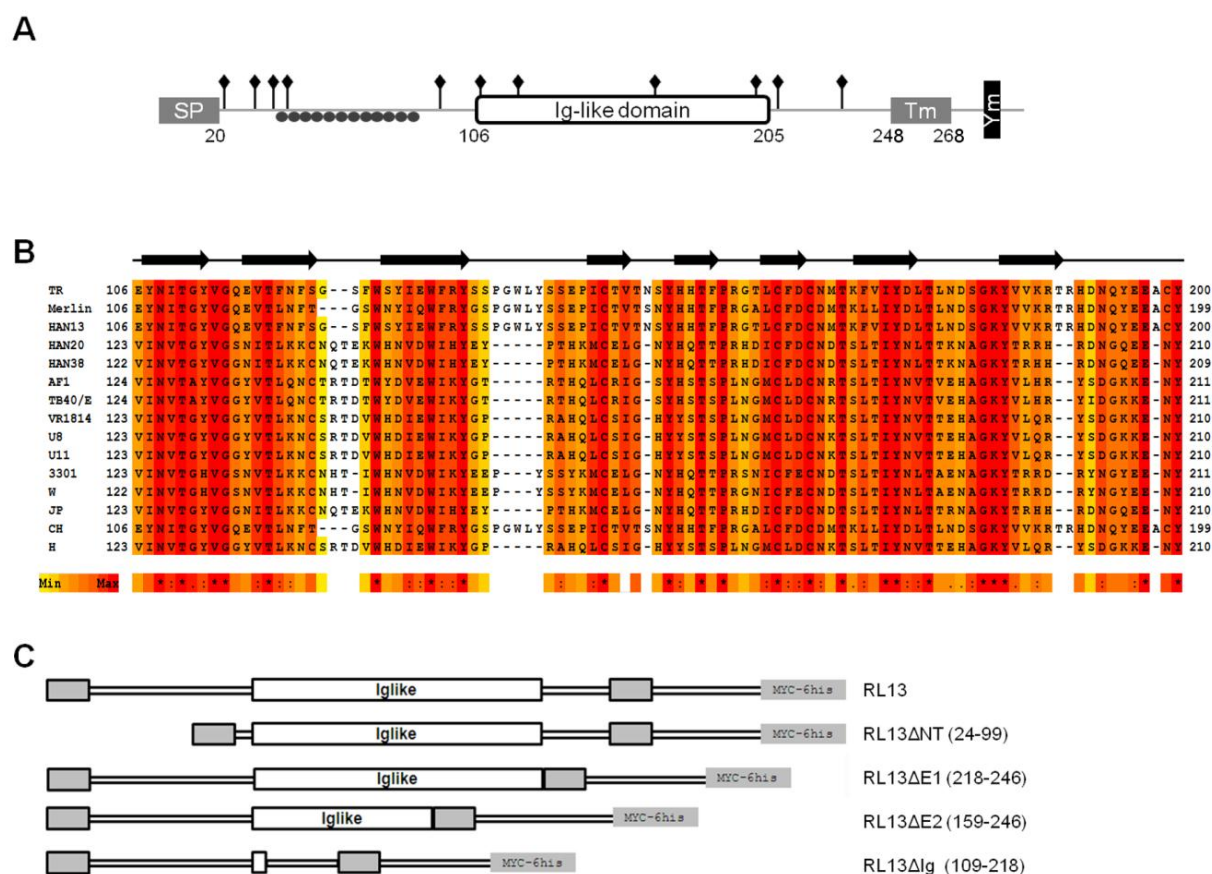


**Figure 2: Predicted structure of the RL13 protein and schematic representation of TR RL13 ectodomain mutants.**

**A:** Schematic representation of the HCMV TR RL13 full length protein. The signal peptide at the N-terminus (SP), the Ig-like domain, the transmembrane domain (Tm), the tyrosine-based motif YxxL (Ym) sorting signal, 11 potential N-linked glycosylation sites (diamonds), and the O-linked glycosylation region (closed circles) are indicated.

**B:** Multiple sequence alignment of the predicted RL13 Ig-like domain from the indicated strains of HCMV. The residues are colored according to the conservation level (red for higher conservation). Asterisks (\*) below the alignments represent conserved amino acid in all sequences; colons (:) represent residues with similar physicochemical properties; dots (.) semi-conserved residues. The black arrows represent the positions of predicted  $\beta$  strands along the sequence.

**C:** Graphic representation of TR RL13 and the ectodomain mutants used in this study. The amino-terminal signal peptide, the carboxy-terminal transmembrane (gray boxes) and the Ig-like domain (white box) are indicated.

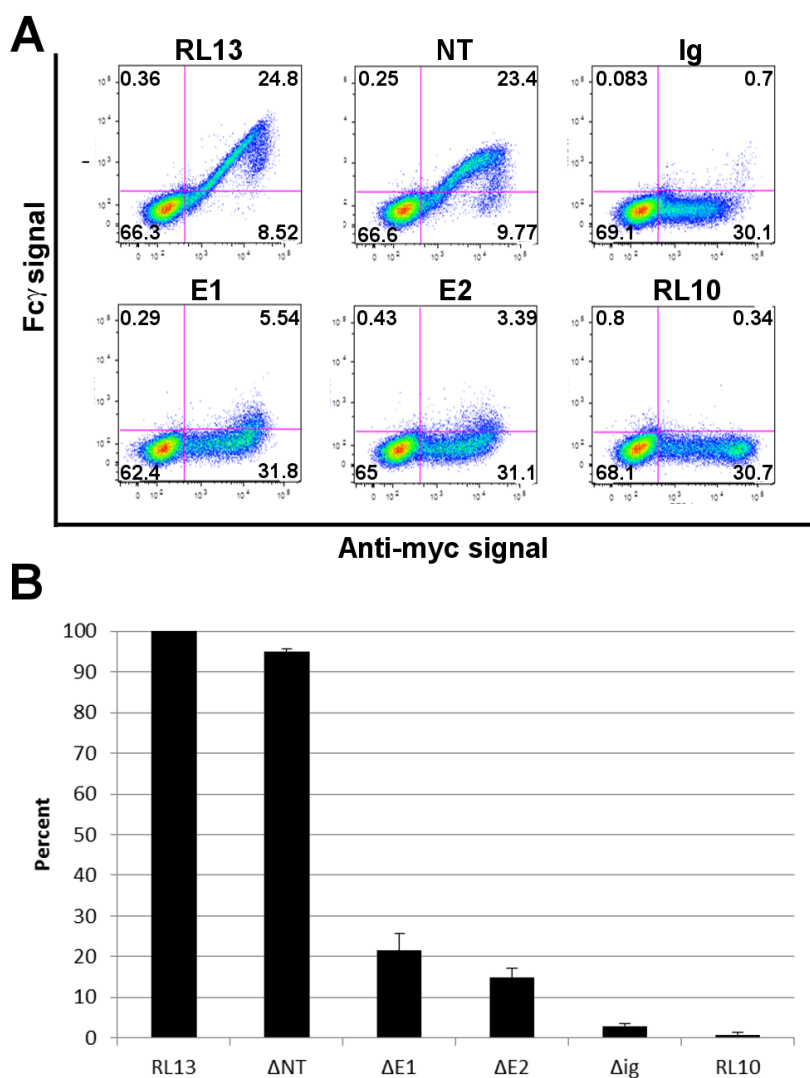


**Figure 3: Fc $\gamma$ -binding by RL13 ectodomain mutants.**

**A: Cytofluorometric analysis of Fc $\gamma$  binding by RL13 ectodomain mutants.** HEK293T cells transfected with the indicated constructs were permeabilized and stained with DyLight 649-conjugated human IgG Fc fragment (Fc $\gamma$ , 12.5  $\mu$ g/ml) and Alexa Fluor 488-conjugated mouse anti-myc. Signals from 10,000 myc-positive cells are shown in each graph. The percentage of cells in each quadrant is indicated.

**B: Quantitative analysis of the FACS data.** Each histogram shows the percentage of Fc $\gamma$  positive cells relative to the RL13 wild type positive population (RL13). Values and error bars represent the mean and range of three independent experiments.

### ***Subcellular localization of RL13 in transfected cells***

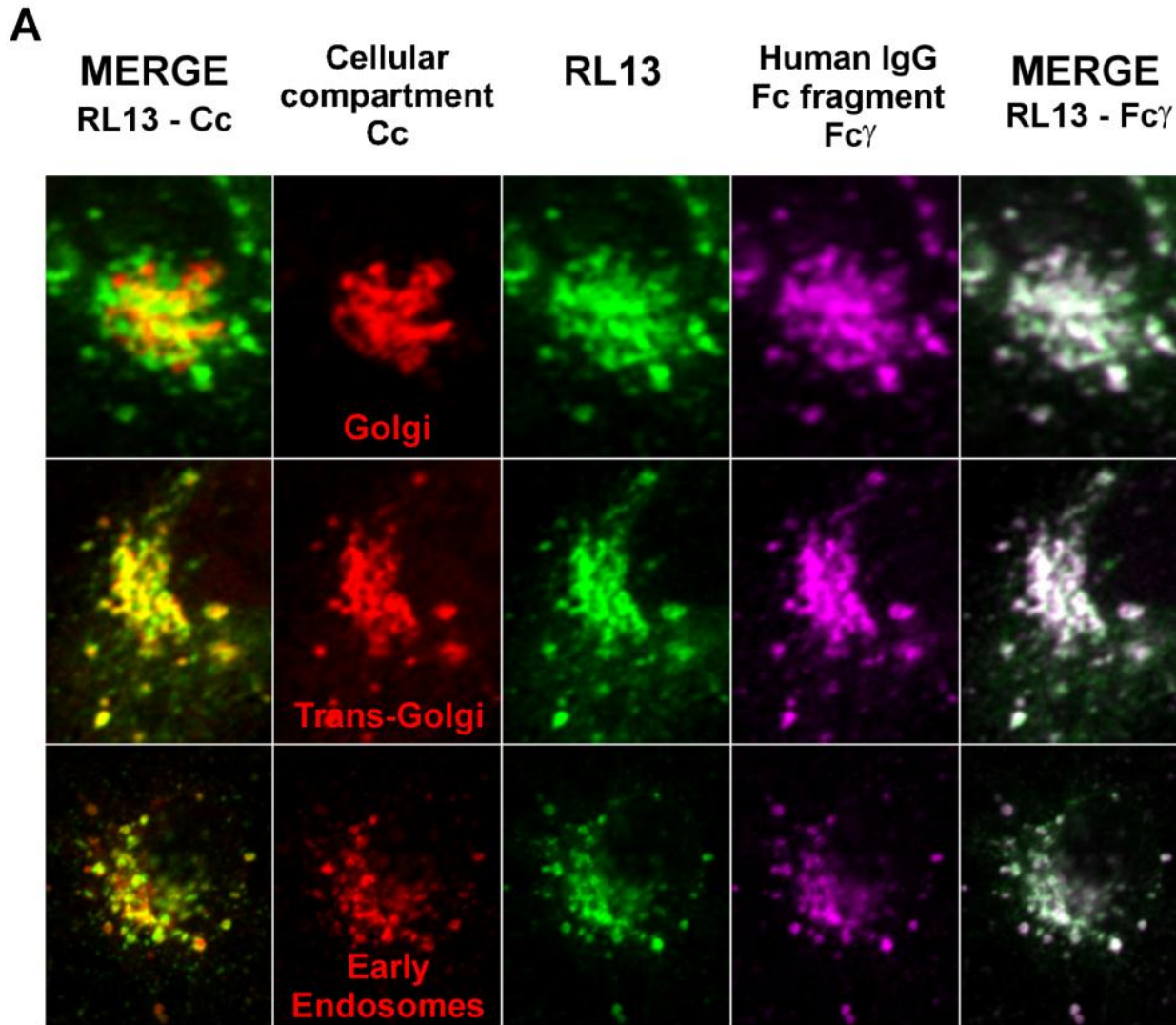
Stanton *et al.* recently reported that adenovirus-expressed RL13 transits through the Golgi and traffics mainly to Rab5-positive cytoplasmic vesicles [6]. We sought to verify the intracellular localization of RL13 expressed transiently in human cells. Confocal microscopy images were collected from epithelial (ARPE-19) and fibroblast (MRC-5) cells transfected with two different constructs, the previously described myc-His tagged construct and a second construct coding for RL13 with a C-terminal YFP-tag. Since sub-cellular localization of RL13 with different tags was identical in both cell types (data not shown), only representative data obtained in ARPE-19 human epithelial cells with RL13-YFP are shown.

48 h after transfection, cells were fixed, permeabilized and stained with different markers of cellular compartments and with fluorophore-conjugated Fc $\gamma$ . The confocal microscopy analysis of these samples is shown in Fig. 4A. RL13 co-localized to a limited extent with Golgi markers and EEA1-positive endosomes and more extensively with markers of the trans-Golgi network (TGN) (Fig. 4A, left panels). Fc $\gamma$  co-localized extensively with RL13 (Fig. 4A, far right panels), although a population of RL13 that does not bind to the Fc of human IgGs was consistently observed (Fig. 4A, green color in far right panels). Although it is tempting to speculate that this pool represents an immature ER population, also suggested by the shape of the RL13 distribution, we have been unable to find any co-localization of RL13 with the ER marker PDI (not shown).

The presence of RL13 on the surface of both HEK293T and ARPE-19 cells was further verified by the use of a mouse monoclonal antibody (mAb 5H3/B10) directed against the ectodomain portion of RL13. Analysis by flow cytometry was performed on transiently transfected non-permeabilized HEK293T cells (Fig. 4B). A clear increase in fluorescence was obtained on RL13 expressing cells stained with mAb 5H3/B10 compared to mock transfected cells or isotype control. Confocal

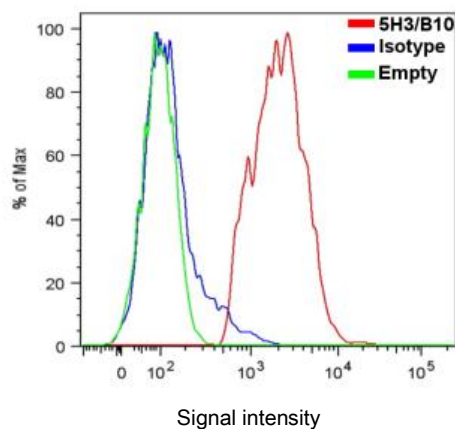
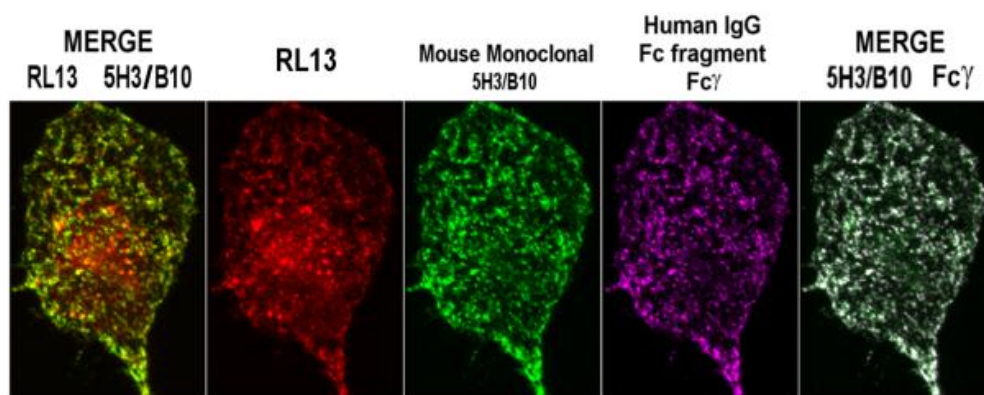
microscopy analysis of non-permeabilized RL13 expressing ARPE-19 cells stained with both Fc $\gamma$  and 5H3/B10 revealed a strong accumulation of RL13 on plasma membrane clusters (Fig. 4C) that extensively overlapped with Fc $\gamma$  signals (Fig. 4C, white color in right merge panel).

These observations are consistent with RL13 trafficking through the secretory pathway and recycling from the plasma membrane, although other possible explanations for this pattern have not been excluded.



**Figure 4: Localization of RL13 in transfected cells.**

**A: Co-localization of RL13 with organelle markers and Fc $\gamma$  in ARPE-19 cells.** ARPE-19 epithelial cells were transfected with RL13-YFP fusion protein (green color, central column) and treated for confocal analysis 48 h later. Cells were fixed, permeabilized and stained with antibodies against either GM130, TGN46 or EEA1 intracellular markers (red color, second column) and with 20  $\mu\text{g/ml}$  of DyLight 649-conjugated human IgG Fc fragment (magenta color, fourth column). The merged panels on the far left show co-localization between RL13 and, from top to bottom, markers of Golgi (GM130), trans-Golgi (TGN46) and early endosomes (EEA1) respectively (co-localization in yellow). The merged panels on the far right show co-localization of Fc $\gamma$  with RL13 (co-localization in white).

**B****C**

**B: Flow cytometry analysis of RL13 surface-expression.** HEK293T cells were transiently transfected with vector coding for YFP (green line) or RL13-YFP fusion protein (red and blue lines). Cells were allowed to recover for 48 h and then surface-exposed RL13 was stained either with 5  $\mu\text{g}/\text{ml}$  of mouse monoclonal antibody directed against RL13 ectodomain (clone 5H3/B10, red and green lines) or isotype control at the same concentration (isotype, blue line) on ice. Alexa fluor 647 conjugated goat anti-mouse was used as secondary antibody. YFP positive cells were compared to empty vector transfected cells for their ability to bind 5H3/B10 antibody.

**C: Immunofluorescence analysis of RL13 surface expression on ARPE-19 cells.** ARPE-19 cells expressing RL13-YFP fusion protein (red color) were stained on ice with 12.5  $\mu\text{g}/\text{ml}$  of 5H3/B10 monoclonal antibody (green color) and 20  $\mu\text{g}/\text{ml}$  of DyLight 649-conjugated human IgG Fc fragment (magenta color) without permeabilization. Merge panels show co-localization between 5H3/B10 and either RL13-YFP or Fc $\gamma$  signals (yellow color in the far left panel and white color in the far right panel, respectively).

### ***Internalization of RL13-Fc $\gamma$ complex***

The presence of an internalization motif in the C-terminal tail, together with the intracellular localization data in Fig. 4, suggested that RL13 could traffic to the cell surface where it may bind and internalize extracellular IgGs. To test this hypothesis, we performed a short time-course characterization of the internalization of YFP-tagged RL13 in transfected ARPE-19 cells. Cells were initially placed on ice to reduce lateral diffusion of membrane proteins and block potential internalization of the ligand. Fluorescently labelled Fc $\gamma$  was added and allowed to bind for 30 min on ice. Following extensive washing of the Fc $\gamma$  excess and fixation of the cells, fluorescence analysis at time 0 showed that RL13 partially co-localized with Fc $\gamma$  on the surface of transfected cells (Fig. 5A). Restoring the internalization processes at 37°C induced the uptake of the RL13- Fc $\gamma$  complex, the majority of which accumulated mostly in large ring-shaped structures after 30 min (Fig. 5B). These RL13-Fc $\gamma$  structures persisted 90 min after the shift to 37°C and stained positive for the early endosome marker Rab5 (Fig. 5C).

These data demonstrate that RL13 binds to the Fc of human IgGs on the cell surface and that the internalized complex remains associated with large membranous vesicles containing markers of early endosomes.

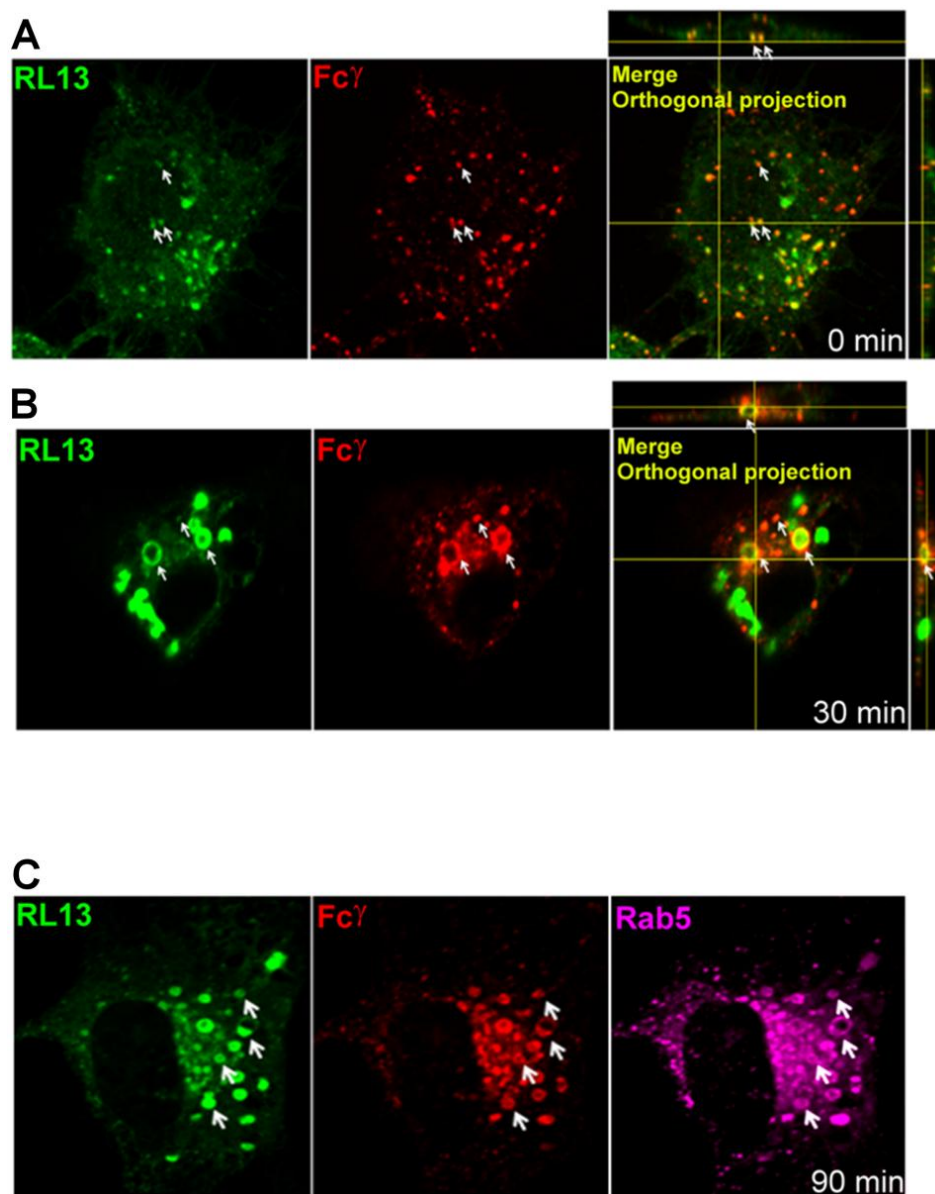


**Figure 5: RL13 binds and internalizes Fc $\gamma$ .**

ARPE-19 epithelial cells were transfected with RL13-YFP (green) and allowed to recover for 48 h. Cells were placed on ice 5 min before adding DyLight 649-conjugated human IgG Fc fragment (red) and incubated on ice for 30 min. Then, cells were washed and **A**: immediately fixed, **B**: shifted to 37°C for 30 min, or **C**: shifted to 37°C for 90 min before proceeding to fixation and confocal analysis. Rab5 (purple) was revealed by specific antibodies after permeabilization of the samples. Examples of co-localization between signals are indicated by white arrows. Orthogonal projections of the optical sections acquired from Z-stack are shown. White arrows indicate examples of co-localized spots. Fluorescent Fc $\gamma$  was absent on the membrane of ARPE-19 cells transfected with empty expression vector used as control and no staining was detected following 30 min switch at 37°C (data not shown).

***Mutation of RL13 sorting motif affects the internalization of Fc $\gamma$*** 

As shown by the *in silico* analysis, the carboxy-terminal domain of RL13 contains a tyrosine-based sorting signal (YxxL<sub>282</sub>) that could be responsible for the internalization of the RL13-Fc $\gamma$  complex. A local multiple sequence alignment of the C-terminal region of RL13 from 15 HCMV strains showed that the YxxL motif was highly conserved (Fig. 6A, residues 279-282). To test the contribution of the cytoplasmic tail, and in particular of the tyrosine motif, to the internalization of the RL13-Fc $\gamma$  complex, a panel of mutants were built (Fig. 6B). Plasmids encoding RL13 with three single amino acid substitution mutants, Y279F, Y279A, T280A, one double substitution mutant Y279A/L282A (indicated as AA), one triple substitution mutant Y279A/R281A/L282A (AAA), and one quadruple substitution mutant with all amino acids of the motif replaced by alanines (AAAA) were produced. Additionally, plasmids encoding a YxxL deletion mutant ( $\Delta$ 279-282), a deletion of the motif and the entire C-terminal ( $\Delta$ 279-294), and a deletion of 12 amino acids immediately C-terminal to the sorting motif ( $\Delta$ 283-294) were generated. 48 h after transfection, internalization of the mutated/deleted proteins was assessed by flow cytometry on HEK293T cells incubated with Fc $\gamma$  at 4°C for 30 min and, after removal of the ligand by extensive washing, shifted to 37°C. The percent of internalized Fc $\gamma$  was calculated from the mean fluorescence intensity of the samples incubated at 37°C for 30 minutes and the samples submitted to the same treatment but kept on ice. As shown in Fig. 6C, the YxxL motif is critical for protein internalization since removing the region downstream did not alter the RL13 Fc $\gamma$  internalization ability while deletion of the motif, both individually or with the C-terminus sequence, strongly reduced the internalization ability of RL13 (Fig. 6C). Substitution of the tyrosine 279 with phenylalanine, an alternative aromatic side chain, did not reduce the ability of RL13 to internalize. In contrast, uptake was reduced by approximately 1/3 when an alanine was placed in this position. Substitution of the adjacent threonine 280 with alanine did not show a difference in internalization

compared to the wild type. However, leucine 282 appeared to play a role as shown by the further internalization reduction of the Y279/L282 double mutant (Fig. 6C). Substitution of multiple residues with alanine reduced internalization to the same extent as complete deletion of the YxxL motif (Fig. 6C).

Taken together these results are consistent with the YxxL<sub>282</sub> motif being necessary for Fc $\gamma$  internalization by RL13 and suggest that an aromatic residue at position 279 is required.



***Fc $\gamma$  binding ability is conserved in the HCMV Merlin strain***

Due to the high variability of the RL13 genes among different HCMV strains [20] we also tested the Merlin RL13 protein (87% aa identity with its TR counterpart) for its Fc $\gamma$  binding ability. *In vitro* synthesized Merlin RL13 gene was cloned in pcDNA3.1(-)/myc-His expression vector and used to transfect HEK293T cells. Intracellular staining was performed as previously described and cells were analyzed through flow cytometry. Both the expression levels (data not shown) and the Fc $\gamma$  binding ability of cells expressing RL13 from Merlin and TR strains were comparable (Fig. 7A). To further confirm the specificity of the binding, both proteins were immunoprecipitated from transfected cell lysates with biotinylated Fc $\gamma$ . Complexes were captured with magnetic streptavidin beads and eluted material was separated by SDS-PAGE and analyzed by immunoblot using anti-tag and anti-human IgG antibodies (Fig. 7B). Both Merlin and TR RL13 proteins were successfully immunoprecipitated from cell lysates. The observed molecular weights of the two proteins in denaturing and reducing conditions appeared to be slightly different: TR RL13 was composed of three major isoforms of around 123 kDa, 111 kDa and 76 to 66 kDa, while Merlin RL13 gave three bands of 116 kDa, 108 kDa and 66 to 52 kDa. These differences in the molecular weight could reflect the different glycosylation profiles, with 7 and 11 predicted N-linked glycosylations for RL13 from Merlin and TR strains, respectively.

These experiments support the conclusion that the Fc $\gamma$ -binding ability of RL13 is conserved in at least two different clinical HCMV isolates.

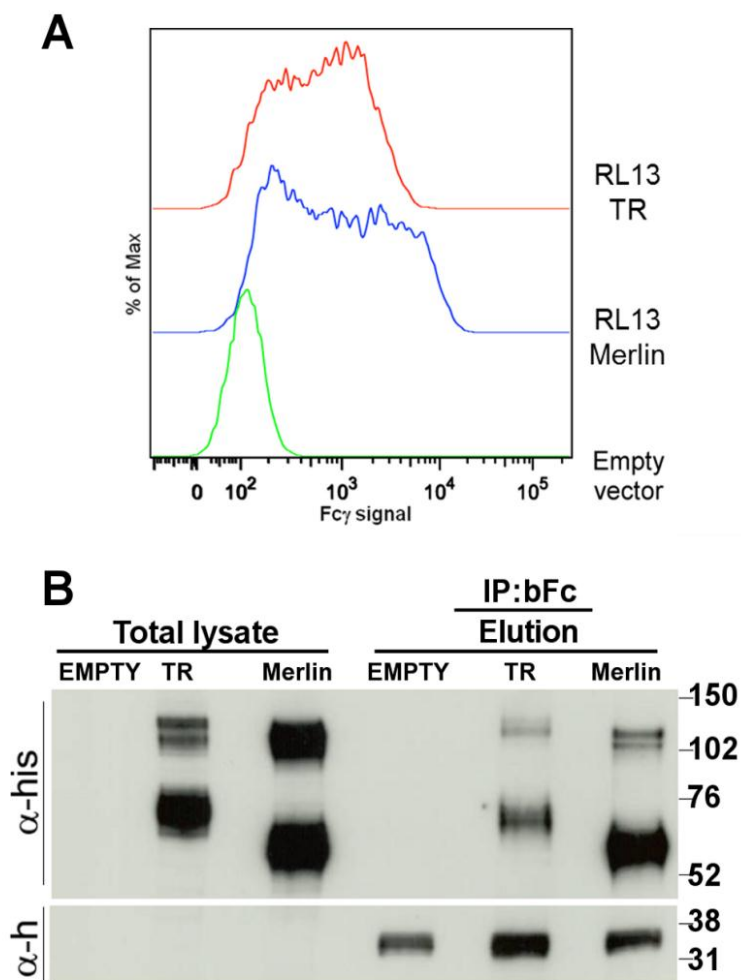


**Figure 7: Fc $\gamma$  binding is a conserved function for recombinant RL13 from Merlin and TR clinical strains.**

**A:** HEK293T cells were transfected with plasmids coding for myc-His tagged RL13 from TR (red), Merlin (blue) strains and empty vector (green). 48 h post-transfection cells were collected, permeabilized and stained with FITC-conjugated mouse anti-myc and 25  $\mu$ g/ml of DyLight 649-conjugated human IgG Fc fragment. 10,000 FITC-positive cells were compared to empty vector transfected cells.

**B:** HEK293T cells were transfected with empty vector or plasmids coding for myc-His tagged RL13 from TR and Merlin strains. 48 h post-transfection cells were collected, lysed and subjected to immunoprecipitation with biotinylated Fc $\gamma$  fragment. Total lysates and elution fractions were subjected to western blot analysis using HRP-conjugated anti-his tag ( $\alpha$ -his) and anti-human IgG ( $\alpha$ -h) antibodies. TR: sample expressing myc-His tagged RL13 from TR strain; Merlin: sample expressing myc-His tagged RL13 from Merlin strain; Empty: empty vector transfected cells.

## DISCUSSION

The low fitness of wild-type RL13-carrying strains cultured *in vitro*, leading to the destruction of the ORF present in the clinical isolates within a few passages [5,6], make functional studies of this protein difficult. To better understand its function, we used synthetic RL13 genes reproducing the sequences of the clinical isolates TR and Merlin. In the absence of an unpassaged reference sample of TR, we cannot say with certainty that the sequence and function of the TR RL13 we used is identical to the originally isolated, naturally occurring virus. However, we do not detect functional differences between RL13 from the TR and Merlin strains. Expression of this recombinant protein in human-derived epithelial cells allowed us to demonstrate that RL13: a) binds Fc from IgG of human (and rabbit) origin; b) preferentially binds to Fc from IgG1 and IgG2 subclasses; c) is at least transiently exposed on the cell surface and is subsequently internalized with (and likely without) bound Fc; d) internalization relies on a YxxL motif and e) its Ig-like extracellular domain is necessary for Fc $\gamma$  binding. Similar analysis of RL13 in human fibroblasts produced identical results (data not shown). Furthermore, we revealed that RL12 also binds IgG1 and IgG2, although we did not study this interaction in detail. Our data does not offer an explanation for why RL13 is so rapidly mutated when clinical isolates of HCMV are grown in cultured cells [5].

Apart from HCMV, viral Fc $\gamma$  binding proteins (vFcBPs) are present on herpes simplex virus type 1 (HSV-1), HSV-2, and varicella zoster virus and on the non-human herpesviruses pseudorabies virus and murine cytomegalovirus [21–25]. The most accepted model to explain how those activities promote immune evasion is the so called “antibody bipolar bridging” in which the neutralizing potential of the IgG Fab domain is counteracted by simultaneous binding of vFcBPs to the Fc domain of the same immunoglobulin molecule [26,27]. The possibility of this mechanism has been supported at a molecular level by Sprague and coworkers [27], who crystallized a portion of HSV gE ectodomain and

gE-gI complex bound to an human IgG Fc fragment. Alternatively, it has been hypothesized that HSV, as well as HCMV vFcBPs, function once expressed on infected cell surface by endocytosis and subsequent degradation of complexes including human IgG and viral antigens [11,27]. Consistent with this hypothesis, we observed that RL13 is able to internalize human IgG Fc fragment from the surface of transfected cells trafficking at early times in Rab5 and EEA1 positive endosomes. The well-recognized YxxL motif is essential for RL13 endocytosis through the aromatic nature of the tyrosine and not its property of phosphate acceptor. As already described for the RID receptor of adenovirus [28], this type of sorting signal does not affect signal transduction pathways. On the other hand, the fact that RL13 is located on the envelope of the virus [6] suggests that antibody bipolar bridging could be an important function of RL13 that would help protect HCMV virions from complement- and antibody-dependent neutralization.

RL13 and RL12 discriminate among human IgG subtypes showing no association with IgG3 and IgG4. To our knowledge, this observation remains the only example of vFcBPs selecting not only among immunoglobulin isotypes but also IgG subtypes. IgG2 represents roughly 25% of human total plasma IgGs in adults and has been traditionally associated with protection from infection with encapsulated bacteria since their immune function is primarily directed against polysaccharide antigens [29]. Recent reports, however, have pointed out a significant association between IgG2 deficiency and severe or even fatal clinical outcome of the pandemic influenza A (H1N1), although IgG2 unbalance has been suggested to be a consequence of cytokine deregulation rather than a predisposing risk factor [30,31]. Due to the low number of studies performed on human IgG2 function related to viral infection, the meaning of such observation remains elusive and needs further analysis. Compared to IgG1, subtype 2 immunoglobulins cannot mediate complement-dependent cytotoxicity or NK-mediated antibody-dependent cellular cytotoxicity (ADCC) but do engage Fc $\gamma$ RIIa receptors and trigger ADCC

mediated by cells of the myeloid lineage [32]. Again, the relative importance of IgG2 subtype in protecting from viral infection just begun to be addressed and it is difficult to evaluate the importance of a viral factor able to counteract such mechanism, if any, but it is noteworthy that HCMV has a latent reservoir in myeloid cells [33]. It is tempting to speculate that a viral IgG2-binding receptor could compete with cellular receptors for binding to cellular antibodies to viral proteins and prevent ADCC. It would be important to determine the affinity of RL13, as well as of the other HCMV Fc $\gamma$  binding proteins, toward IgG2 to evaluate if this protein represents a function more dedicated to a particular IgG subtype.

Atalay and coworkers described the presence of immunoglobulin supergene family (IgSF)-like domains in the products of both RL11 and UL119 genes [11]. We have mapped the RL13 Fc $\gamma$  binding activity to the Ig-like domain in the extracellular region, while the N-terminal proximal region composed of approximately 70 amino acids is not crucial for the binding. Indeed, Sprague *et al.* showed that removing the N-terminal part of the gp68 ectodomain did not impair the Fc $\gamma$  binding [13]. These data are consistent with the presence of an immunoglobulin supergene family (IgSF)-like domains in all the described HCMV Fc binding proteins. Our findings do not rule out the possibility that RL13 could carry out other functions. The best characterized viral Fc binding protein, the gE product of HSV-1, is also involved in cell-to-cell spread or trafficking of viral proteins from neuron body cell into axon independently of its Fc binding capability [34,35]. We are currently investigating other possible roles of RL13 during HCMV pathogenesis.

Our preliminary characterization of transiently transfected RL13 agrees only partially with what was reported by Stanton *et al.* [6]. They found significant differences in cellular localization and apparent SDS-PAGE MW between adenovirus-expressed RL13 and the protein expressed in the context of viral infection. In their report, adenovirus-expressed RL13 showed a lower MW (80 and 55

kDa) compared to the species found in infected cells (100 and 55 kDa) and the protein only co-localized with TGN in the context of infection [6]. The behavior of RL13 observed in this report is more similar to Stanton *et al.*'s data for infected cells, showing a MW above 100 kDa and a sub-cellular co-localization with early endosomes and the TGN. This last observation would be consistent with a default mechanism of internalization similar to what was described for other HCMV envelope proteins [36]. We currently have no explanation for the slight discrepancies between Stanton *et al.* and our report that may be due to the different expression system used or, at least for the confocal analysis, to the protein derived from a different strain. However, characterization of the expressed RL13 remains preliminary and further studies will elucidate this point.

To conclude, we have shown that RL13 encoded by HCMV TR binds the Fc portion of human IgG1 and IgG2 and propose that this protein is used by the virus to circumvent the humoral immune response in the host.

## MATERIALS & METHODS

### *Sequence data, in silico analysis and predictions*

Start to stop open reading frames (ORFs) in the complete genome sequence of the TR strain (Genbank: AC146906.1) were identified using the Getorf program from the EMBOSS suite 5.0.0 [37]. The sequence similarity searching algorithm FASTA 35.4.3 [38]. was exploited to compare the protein sequences of RL13 gene product from the Merlin strain (Genbank: YP\_081461.1) to all the TR ORFs and select homologous ones with BLOSUM50 as substitution matrix and imposing an expectation value (E) upper limit of 1e-05. The putative TR RL13 sequence was searched for specific conserved signatures using InterProScan 4.8 [39] with databases v.34.0. Multiple sequence alignments were performed using the PSI-Coffee mode of T-Coffee v.9.01 [40], comparing the TR RL13 with an additional 14 different RL13 protein sequences (Genbank: YP\_081461.1, AEI84615.1, ACS91939.1, AAR31271.1, AAR31220.1, ACT81850.1, ACT81685.1, ACS92104.1, ACZ79760.1, ACZ79925.1, ADI46773.1, ACZ80255.1, ABV71530.1, ACZ80090.1). Signal peptides and transmembrane regions were predicted by Phobius [41], while secondary structures were predicted using PSIPRED [42]. N-linked and O-linked glycosylation sites were predicted using NetNGlyc 1.0 (<http://www.cbs.dtu.dk/services/NetNGlyc/>) and NetOGlyc 3.1 [43] (<http://www.cbs.dtu.dk/services/NetOGlyc/>) respectively.

### *Cells, plasmids and antibodies*

ARPE-19, MRC-5 and HEK293T cell lines were brought from ATCC and cultured according to the supplier's instructions. DMEM high glucose and DMEM:F12 media (Gibco, Invitrogen) were supplemented with 10% fetal calf serum (FCS) and penicillin streptomycin glutamine (Gibco, Invitrogen). Lipofectamine 2000 (Invitrogen) was used to transfect HEK293T cells while Fugene 6 (Roche) and Nucleofector kit V (Amaxa) were used to transfect ARPE-19 cells as suggested by manufacturer. Human codon-optimized RL10, RL11, RL12, RL13 and gB (UL55) HCMV genes based on the TR strain sequence and RL13 from Merlin strain (NCBI Reference Sequence: YP\_081461.1) were synthesized by Geneart and cloned in plasmid pcDNA3.1(-)/myc-His C (Invitrogen) in frame with C-terminal myc and six histidine tag sequences. Fluorescent fusion proteins were obtained by subcloning a gene of interest upstream of the EYFP sequence in pEYFP-N1 vector (Clontech). Ectodomain and C-terminal tail RL13 mutants were cloned using QuickChange™ Site-directed Mutagenesis kit and instructions therein (Stratagene). Primary antibodies used in this work were mouse anti-His (C-term) and mouse anti-PDI (Invitrogen), mouse anti-Rab5 mouse, anti-GM130, mouse anti-TGN46 and mouse anti-EEA1 (Abcam). Mouse monoclonal antibody against RL13, clone 5H3/B10, was developed by Areta International (Gerezano, Italy). Mice immunization was performed with peptides encompassing the amino acid region 111-246 of TR strain RL13. Secondary antibodies were Alexa Fluor 488-, 568-, and 647-conjugated goat anti-mouse (Invitrogen) and HRP-conjugated secondary antibodies from Perkin Elmer. Chrompure DyLight 649-conjugated rat, rabbit, mouse, goat IgG and human Fc fragment were from Jackson ImmunoResearch, human IgG subclasses from SIGMA, and human IgA, IgE, IgM from Calbiochem.

### *Flow cytometry*

For intracellular staining, HEK293T cells transfected with the plasmids of interest were trypsin detached 48 h post-transfection, incubated 30 min at RT with Live&Dead Aqua (Invitrogen), diluted 1:400 in PBS, fixed and permeabilized with Cytotfix/Cytoperm kit (BD) and stained as instructed by the manufacturer. For cells expressing the myc-tagged proteins, mouse anti-myc-FITC antibody was used at 1:500 dilution. Binding of the Fc portion of the human IgGs (Fc $\gamma$ ) was assessed using DyLight 649-conjugated human IgG Fc fragment or different human immunoglobulin isotypes and human IgG subclasses at different concentrations (5-50  $\mu$ g/ml). Alexa Fluor 647 fluorophore-conjugated secondary antibodies against the above mentioned species were used at 1:200 dilution. For membrane staining, transfected cells were detached with trypsin 48 h post-transfection and incubated for 30 min on ice with DyLight 649-conjugated human Fc $\gamma$ . When needed, cells were subsequently subjected to intracellular staining. A total of  $10^4$  cells were analyzed for each histogram using FACSCanto II (Becton Dickinson, Heidelberg, Germany). For detection of membrane exposed RL13, HEK293T were transiently transfected with vectors coding for YFP or RL13-YFP fusion protein, were incubated with different dilutions of mouse monoclonal 5H3/B10 antibody or mouse IgG1 isotype control (Sigma) for 60 min on ice. As secondary antibody, Alexa Fluor 647-conjugated goat anti-mouse was used for 30 min on ice at 1:200 dilution. Internalization of Fc $\gamma$  in HEK293T cells was quantified through flow cytometry. 48 h post-transfection cells were detached with trypsin and transferred to round bottom 96 well plates for staining. Cells were washed in cold PBS and incubated on ice with human IgG Fc fragment at different concentrations (50, 25, 12.5  $\mu$ g/ml). After 30 min incubation, cells were extensively washed and incubated with warm medium to allow for endocytosis (Fc $\gamma_{37^\circ\text{C}}$ ). Half of the samples were kept on ice for the duration of the experiment (Fc $\gamma_{4^\circ\text{C}}$ ). At the end of the endocytosis, cells were washed with cold medium and Fc $\gamma$  remaining on the surface was stained with Alexa fluor 488 conjugated goat anti-

human antibody. The percentage of internalized Fc $\gamma$  was calculated as:  $(Fc\gamma_{4^{\circ}C} - Fc\gamma_{37^{\circ}C})/Fc\gamma_{4^{\circ}C} \times 100$ .

Values shown are relative based on internalization by RL13 wild type.

### ***Confocal microscopy analysis***

Cells transfected with plasmids of interest were trypsin detached and plated on glass coverslips for 24 h post transfection. For intracellular staining, cells were fixed 48 h post transfection with 3.7% paraformaldehyde, permeabilized with 0.1% Triton X-100 (Sigma), blocked with PBS with 1% BSA and stained at RT by incubating for 1 h with primary antibodies in PBS/1% BSA, washed in PBS, and further incubated with secondary antibodies in PBS/1% BSA for 1 h. The ProLong Gold with DAPI (Invitrogen) was used as mounting solution. For membrane staining, the permeabilization step was omitted and fixation was performed after staining with primary and secondary antibodies for 30 min on ice. For human Fc $\gamma$  internalization, cells expressing RL13-YFP, YFP, or empty vector (controls) were plated on glass coverslips 24h post transfection. 24 h later, cells were washed in cold PBS and incubated at 4°C with 20  $\mu$ g/ml of DyLight 649-conjugated human Fc $\gamma$  for 30 minutes. After extensive washes, temperature was switched to 37°C to allow for internalization. When required, cells were fixed, permeabilized and stained before mounting. The intracellular locations of antibody-tagged or fluorescent fusion proteins were examined under laser illumination in a Zeiss LMS 710 confocal microscope and images were captured using ZEN software (Carl Zeiss).

### ***Immunoprecipitation***

HEK293T cells were transfected with empty vector or myc-His tagged RL13 from TR or Merlin strains. 48 h post-transfection, cells were harvested, washed in cold PBS several times and lysed in

lysis buffer (25 mM Tris-HCl pH 7.4, 150 mM NaCl, 1% glycerol, 1 mM EDTA) containing 1% NP-40 (Roche) and supplemented with complete EDTA-free protease inhibitors (Roche). Supernatants were collected after centrifugation at max speed for 30 min at 4°C in a tabletop centrifuge. 100 µg of lysate was incubated with 2 µg of biotinylated human IgG Fc fragment (Jackson immunoresearch) for 1 h at 4°C, then with 30 µl of Streptavidin Dynabeads (Invitrogen) prewashed in lysis buffer. Precipitation was carried out at 4°C with overnight rotation. Immunocomplexes were collected using magnetic beads, washed 4 times with lysis buffer and eluted by adding 30 µl of LDS-buffer and heating at 96°C for 5 minutes. Lysates were mixed with 100 mM DTT (Sigma) and heated at 96°C for 3 min. Proteins were then separated by SDS-PAGE and blotted on a nitrocellulose membrane. Membranes were blocked in blocking buffer (5% w/v nonfat dry milk in PBS with 0.1% Tween 20). All incubations with antibodies were done at room temperature for 1 h in blocking buffer. Mouse anti-His (Invitrogen) was used at 1:1,000 dilution. Secondary antibodies were diluted 1:10,000 in blocking buffer.

## **ACKNOWLEDGMENTS**

We thank Simona Tavarini, Chiara Sammiceli and Sandra Nuti for their availability and excellent technical support with flow cytometry experiments.

**REFERENCES**

1. Mocarski ES, Shenk T, Pass RF (2007) Cytomegaloviruses. In: Knipe D.M. HPMed, editors. Fields virology. Lippincott Williams & Wilkins. pp. 2701-2772.
2. Britt W (2008) Manifestations of human cytomegalovirus infection: proposed mechanisms of acute and chronic disease. *Current topics in microbiology and immunology* 325: 417-470.
3. Murphy E, Shenk T (2008) Human cytomegalovirus genome. *Current topics in microbiology and immunology* 325: 1-19.
4. Akter P, Cunningham C, McSharry BP, Dolan A, Addison C, et al. (2003) Two novel spliced genes in human cytomegalovirus. *J Gen Virol* 84: 1117-1122.
5. Dargan DJ, Douglas E, Cunningham C, Jamieson F, Stanton RJ, et al. (2010) Sequential mutations associated with adaptation of human cytomegalovirus to growth in cell culture. *J Gen Virol* 91: 1535-1546.
6. Stanton RJ, Baluchova K, Dargan DJ, Cunningham C, Sheehy O, et al. (2010) Reconstruction of the complete human cytomegalovirus genome in a BAC reveals RL13 to be a potent inhibitor of replication. *J Clin Invest* 120: 3191-3208.
7. Powers C, DeFilippis V, Malouli D, Fruh K (2008) Cytomegalovirus immune evasion. *Curr Top Microbiol Immunol* 325: 333-359.
8. Tortorella D, Gewurz BE, Furman MH, Schust DJ, Ploegh HL (2000) Viral subversion of the immune system. *Annu Rev Immunol* 18: 861-926.
9. Hook LM, Friedman HM (2007) Subversion of innate and adaptive immunity: immune evasion from antibody and complement. In *Human Herpesviruses: Biology, Therapy, and Immunoprophylaxis*. Cambridge, UK: Cambridge University Press; Chapter 63.
10. Nimmerjahn F, Ravetch JV (2008) Fcγ receptors as regulators of immune responses. *Nat Rev Immunol* 8: 34-47.
11. Atalay R, Zimmermann A, Wagner M, Borst E, Benz C, et al. (2002) Identification and expression of human cytomegalovirus transcription units coding for two distinct Fcγ receptor homologs. *J Virol* 76: 8596-8608.
12. Lilley BN, Ploegh HL, Tirabassi RS (2001) Human cytomegalovirus open reading frame TRL11/IRL11 encodes an immunoglobulin G Fc-binding protein. *J Virol* 75: 11218-11221.
13. Sprague ER, Reinhard H, Cheung EJ, Farley AH, Trujillo RD, et al. (2008) The human cytomegalovirus Fc receptor gp68 binds the Fc CH2-CH3 interface of immunoglobulin G. *J Virol* 82: 3490-3499.
14. Murphy E, Yu D, Grimwood J, Schmutz J, Dickson M, et al. (2003) Coding potential of laboratory and clinical strains of human cytomegalovirus. *Proc Natl Acad Sci U S A* 100: 14976-14981.

15. Varnum SM, Streblow DN, Monroe ME, Smith P, Auberry KJ, et al. (2004) Identification of proteins in human cytomegalovirus (HCMV) particles: the HCMV proteome. *J Virol* 78: 10960-10966.
16. Davison AJ, Dolan A, Akter P, Addison C, Dargan DJ, et al. (2003) The human cytomegalovirus genome revisited: comparison with the chimpanzee cytomegalovirus genome. *J Gen Virol* 84: 17-28.
17. Sekulin K, Gorzer I, Heiss-Czedik D, Puchhammer-Stockl E (2007) Analysis of the variability of CMV strains in the RL11D domain of the RL11 multigene family. *Virus Genes* 35: 577-583.
18. Bonifacino JS, Traub LM (2003) Signals for sorting of transmembrane proteins to endosomes and lysosomes. *Annu Rev Biochem* 72: 395-447.
19. Letunic I, Doerks T, Bork P (2009) SMART 6: recent updates and new developments. *Nucleic Acids Res* 37: D229-D232.
20. Dolan A, Cunningham C, Hector RD, Hassan-Walker AF, Lee L, et al. (2004) Genetic content of wild-type human cytomegalovirus. *J Gen Virol* 85: 1301-1312.
21. Dubin G, Frank I, Friedman HM (1990) Herpes simplex virus type 1 encodes two Fc receptors which have different binding characteristics for monomeric immunoglobulin G (IgG) and IgG complexes. *J Virol* 64: 2725-2731.
22. Para MF, Goldstein L, Spear PG (1982) Similarities and differences in the Fc-binding glycoprotein (gE) of herpes simplex virus types 1 and 2 and tentative mapping of the viral gene for this glycoprotein. *J Virol* 41: 137-144.
23. Litwin V, Jackson W, Grose C (1992) Receptor properties of two varicella-zoster virus glycoproteins, gpI and gpIV, homologous to herpes simplex virus gE and gI. *J Virol* 66: 3643-3651.
24. Van de Walle GR, Favoreel HW, Nauwynck HJ, Pensaert MB (2003) Antibody-induced internalization of viral glycoproteins and gE-gI Fc receptor activity protect pseudorabies virus-infected monocytes from efficient complement-mediated lysis. *J Gen Virol* 84: 939-948.
25. Thale R, Lucin P, Schneider K, Eggers M, Koszinowski UH (1994) Identification and expression of a murine cytomegalovirus early gene coding for an Fc receptor. *J Virol* 68: 7757-7765.
26. Frank I, Friedman HM (1989) A novel function of the herpes simplex virus type 1 Fc receptor: participation in bipolar bridging of antiviral immunoglobulin G. *J Virol* 63: 4479-4488.
27. Sprague ER, Wang C, Baker D, Bjorkman PJ (2006) Crystal structure of the HSV-1 Fc receptor bound to Fc reveals a mechanism for antibody bipolar bridging. *PLoS Biol* 4: e148.
28. Lichtenstein DL, Krajcsi P, Esteban DJ, Tollefson AE, Wold WS (2002) Adenovirus RIDbeta subunit contains a tyrosine residue that is critical for RID-mediated receptor internalization and inhibition of Fas- and TRAIL-induced apoptosis. *J Virol* 76: 11329-11342.

29. Pan Q, Hammarstrom L (2000) Molecular basis of IgG subclass deficiency. *Immunol Rev* 178: 99-110.
30. Gordon CL, Johnson PD, Permezel M, Holmes NE, Gutteridge G, et al. (2010) Association between severe pandemic 2009 influenza A (H1N1) virus infection and immunoglobulin G(2) subclass deficiency. *Clin Infect Dis* 50: 672-678.
31. Chan JF, To KK, Tse H, Lau CC, Li IW, et al. (2011) The lower serum immunoglobulin G2 level in severe cases than in mild cases of pandemic H1N1 2009 influenza is associated with cytokine dysregulation. *Clin Vaccine Immunol* 18: 305-310.
32. Schneider-Merck T, Lammerts van Bueren JJ, Berger S, Rossen K, Berkel PH, et al. (2010) Human IgG2 antibodies against epidermal growth factor receptor effectively trigger antibody-dependent cellular cytotoxicity but, in contrast to IgG1, only by cells of myeloid lineage. *J Immunol* 184: 512-520.
33. Reeves M, Sinclair J (2008) Aspects of human cytomegalovirus latency and reactivation. *Curr Top Microbiol Immunol* 325: 297-313.
34. Wang F, Tang W, McGraw HM, Bennett J, Enquist LW, et al. (2005) Herpes simplex virus type 1 glycoprotein e is required for axonal localization of capsid, tegument, and membrane glycoproteins. *J Virol* 79: 13362-13372.
35. Weeks BS, Sundaresan P, Nagashunmugam T, Kang E, Friedman HM (1997) The herpes simplex virus-1 glycoprotein E (gE) mediates IgG binding and cell-to-cell spread through distinct gE domains. *Biochem Biophys Res Commun* 235: 31-35.
36. Moorman NJ, Sharon-Friling R, Shenk T, Cristea IM (2010) A targeted spatial-temporal proteomics approach implicates multiple cellular trafficking pathways in human cytomegalovirus virion maturation. *Mol Cell Proteomics* 9: 851-860.
37. Rice P, Longden I, Bleasby A (2000) EMBOSS: the European Molecular Biology Open Software Suite. *Trends Genet* 16: 276-277.
38. Lipman DJ, Pearson WR (1985) Rapid and sensitive protein similarity searches. *Science* 227: 1435-1441.
39. Mulder N, Apweiler R (2007) InterPro and InterProScan: tools for protein sequence classification and comparison. *Methods Mol Biol* 396: 59-70.
40. Taly JF, Magis C, Bussotti G, Chang JM, Di TP, et al. (2011) Using the T-Coffee package to build multiple sequence alignments of protein, RNA, DNA sequences and 3D structures. *Nat Protoc* 6: 1669-1682.
41. Kall L, Krogh A, Sonnhammer EL (2004) A combined transmembrane topology and signal peptide prediction method. *J Mol Biol* 338: 1027-1036.
42. Jones DT (1999) Protein secondary structure prediction based on position-specific scoring matrices. *J Mol Biol* 292: 195-202.

43. Julenius K, Molgaard A, Gupta R, Brunak S (2005) Prediction, conservation analysis, and structural characterization of mammalian mucin-type O-glycosylation sites. *Glycobiology* 15: 153-164.

